



National Library
of Canada

Bibliothèque nationale
du Canada

Canadian Theses Service

Service des thèses canadiennes

Ottawa, Canada
K1A 0N4

NOTICE

The quality of this microform is heavily dependent upon the quality of the original thesis submitted for microfilming. Every effort has been made to ensure the highest quality of reproduction possible.

If pages are missing, contact the university which granted the degree.

Some pages may have indistinct print especially if the original pages were typed with a poor typewriter ribbon or if the university sent us an inferior photocopy.

Previously copyrighted materials (journal articles, published tests, etc.) are not filmed.

Reproduction in full or in part of this microform is governed by the Canadian Copyright Act, R.S.C. 1970, c. C-30.

AVIS

La qualité de cette microforme dépend grandement de la qualité de la thèse soumise au microfilmage. Nous avons tout fait pour assurer une qualité supérieure de reproduction.

S'il manque des pages, veuillez communiquer avec l'université qui a conféré le grade.

La qualité d'impression de certaines pages peut laisser à désirer, surtout si les pages originales ont été dactylographiées à l'aide d'un ruban usé ou si l'université nous a fait parvenir une photocopie de qualité inférieure.

Les documents qui font déjà l'objet d'un droit d'auteur (articles de revue, tests publiés, etc.) ne sont pas microfilmés.

La reproduction, même partielle, de cette microforme est soumise à la Loi canadienne sur le droit d'auteur, SRC 1970, c. C-30.

THE UNIVERSITY OF ALBERTA

The Electrical Double-Layer Sorption Model for Ion Pair Chromatography

By

Hanjiu Liu

A Thesis

Submitted To The Faculty Of Graduate Studies And Research

In Partial Fulfillment Of The Requirements For The Degree

Of Doctor Of Philosophy

Department of Chemistry

Edmonton, Alberta

Fall, 1988

Permission has been granted to the National Library of Canada to microfilm this thesis and to lend or sell copies of the film.

The author (copyright owner) has reserved other publication rights, and neither the thesis nor extensive extracts from it may be printed or otherwise reproduced without his/her written permission.

L'autorisation a été accordée à la Bibliothèque nationale du Canada de microfilmer cette thèse et de prêter ou de vendre des exemplaires du film.

L'auteur (titulaire du droit d'auteur) se réserve les autres droits de publication; ni la thèse ni de longs extraits de celle-ci ne doivent être imprimés ou autrement reproduits sans son autorisation écrite.

ISBN 0-315-45450-4

THE UNIVERSITY OF ALBERTA

RELEASE FORM

NAME OF AUTHOR: Hanjiu Liu

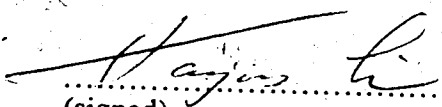
TITLE OF THESIS: The Electrical Double-Layer Sorption Model for Ion Pair
Chromatography

DEGREE FOR WHICH THESIS WAS PRESENTED: Ph.D.

YEAR THIS DEGREE GRANTED: 1988

Permission is hereby granted to THE UNIVERSITY OF ALBERTA LIBRARY to reproduce single copies of this thesis and to lend or sell such copies for private, scholarly or scientific research purposes only.

The author reserves other publication rights, and neither the thesis nor extensive extracts from it may be printed or otherwise reproduced without the author's written permission.


(signed)

PERMANENT ADDRESS:

Jinan, Shandong

China

Date: Oct. 14, 1988

THE UNIVERSITY OF ALBERTA
FACULTY OF GRADUATE STUDIES AND RESEARCH

The undersigned certify that they have read, and recommend to the Faculty of Graduate Studies and Research for acceptance, a thesis entitled **THE ELECTRICAL DOUBLE-LAYER SORPTION MODEL FOR ION PAIR CHROMATOGRAPHY** submitted by **HANJIE LIU** in partial fulfilment of the requirements for the degree of Doctor of Philosophy in Analytical Chemistry.

Fredrick J. Cantwell
F.F. Cantwell, Supervisor

James A. Plambeck
J.A. Plambeck

D.J. Harrison
D.J. Harrison

L.G. Hepler
L.G. Hepler

M.J. Dudas
M.J. Dudas

G.S. Wilson
G.S. Wilson, External Examiner

Date: *Oct. 14, 1988*

This thesis is dedicated to my parents

Abstract

Adsorption isotherms of p-nitrobenzenesulfonate (NBS^-) from an aqueous solution of Na^+NBS^- and of tetra-butylammonium (TBA^+) from an aqueous solution of TBA^+Cl^- onto a chemically bonded octadecylsilyl (ODS) packing were measured as a function of ionic strength, adjusted with NaCl, using a column equilibration technique. The adsorption isotherms of NBS^- onto the ODS packing follow the Langmuir equation and those of TBA^+ follow the Freundlich equation. The effect of ionic strength on the isotherms is quantitatively explained in terms of the Stern-Gouy-Chapman electrical double-layer theory.

It was shown by measuring the surface tension of its solutions as a function of concentration, by the Wilhelmy plate method, that TBA^+Cl^- does not form micelles in solution under the experimental conditions. The completeness of elution of TBA^+ from the ODS packing, in the final step of the column equilibration method, was demonstrated using its brominated derivative ($\text{TBABr}^+\text{Cl}^-$) by determining the "residual" amount on the eluted ODS packing with instrumental neutron activation analysis (INAA).

Then the retention of NBS^- (sample ion) on the ODS packing under typical "ion-pair" conditions, where it is present at "trace" concentration, was studied by measuring its distribution coefficient as a function of the concentration of TBA^+ (pairing-ion) and of ionic strength. The column equilibration system used for the measurement employed two detection systems: an on-line UV detector for NBS^- and an off-line solvent extraction/flow injection analysis (SE/FIA) apparatus for TBA^+ . This feature enabled simultaneous measurement of the sorption isotherms of both NBS^- and TBA^+ . The experimental data are used to demonstrate quantitatively the validity of the electrical double-layer sorption model for ion pair chromatography. According to the model, retention of a sample ion under "ion-pair" conditions is due to two processes: ion exchange in the diffuse part of the

electrical double-layer at the ODS/solution interface and surface adsorption. It is found that for NBS^- with TBA^+ as "pairing-ion", ion exchange makes a significantly greater contribution to retention except at high ionic strength.

Acknowledgement

I would like to sincerely thank Dr. F.F. Cantwell for his guidance, encouragement and patience through the course of this work and for his helpful suggestions in the preparation of this manuscript.

Acknowledgement is also made to S. Angle in the Alberta Research Council for measuring the specific surface area of the ODS packing material, and to Peter Ford in The Slowpoke Facility, University of Alberta and Steven Pitts for their suggestions and instructions in the neutron activation analysis experiment.

Financial support from the University of Alberta is gratefully acknowledged.

Table of Contents

CHAPTER

PAGE

1.	INTRODUCTION	1
2.	EXPERIMENTAL METHODS, PRINCIPLES AND THE ODS PACKING MATERIAL	6
2.1	Chemicals, Reagents and Solvents	6
2.2	The ODS Packing	7
2.3	Column Equilibration Technique for NBS^- alone	13
2.3.1	Principles of the Column Equilibration Technique	13
2.3.2	Apparatus and Column	17
2.3.3	Sample and Eluent Solutions	17
2.3.4	Procedure	19
2.3.5	Void Volume Measurement	20
2.3.5.1	Procedure	20
2.3.5.2	The Gas Chromatography System	20
2.4	Column Equilibration Technique for NBS^- and TBA^+	20
2.4.1	Principle of the Technique	21
2.4.2	Apparatus and Column	24
2.4.3	Sample and Eluent Solutions	24
2.4.4	Procedure	25
2.4.5	Void Volume Measurement	27
2.4.6	Stability of the ODS Packing	27
2.5	Solvent Extraction/Flow Injection Analysis (SE/FIA) for Off-line Determination of TBA^+	28

2.5.1	Principles of SE/FIA	28
2.5.2	Apparatus and Procedure	29
2.5.3	Reagents and Standard Solutions	31
2.6	Surface Tension Measurement with Wilhelmy Balance	31
2.6.1	Principle of the Method	32
2.6.2	Apparatus and Procedure	35
2.7	Instrumental Neutron Activation Analysis (INAA)	36
2.7.1	Principle of INAA	37
2.7.2	Synthesis of TBA^+Br^-	38
2.7.3	Column Equilibration and Elution	39
2.7.4	Preparation of Standards	40
2.7.5	Irradiation and Counting	40
2.8	Other Apparatus	40

3	ADSORPTION OF THE ORGANIC IONS NBS^- AND TBA^+ ONTO ODS PACKING	41
3.1	Introduction	41
3.2	Theory	46
3.2.1	The Electrical Double-Layer at the Interface	46
3.2.2	Adsorption Isotherms	53
3.3	Results and Discussion	56
3.3.1	Adsorption of p-Nitrobenzenesulfonate (NBS^-)	57
3.3.1.1	Adsorption Isotherms of NBS^-	57
3.3.1.2	SGC Behavior of NBS^-	63
3.3.2	Adsorption of Tetrabutylammonium (TBA^+)	72
3.3.2.1	Micelle Formation of TBA^+ in Solution	72
3.3.2.2	Adsorption Isotherms	73

3.3.2.3	Effect of pH on the Adsorption	88
3.3.2.4	SGC Behavior of TBA ⁺	89
3.4	Conclusion	100
4	SORPTION OF NBS ⁻ UNDER "ION-PAIR" CONDITIONS	101
4.1	Introduction	101
4.2	Theory of Electrical Double-Layer Sorption Model	107
4.2.1	Ion-Exchange in the Diffuse Layer	109
4.2.2	Surface Adsorption of S ⁻	111
4.3	Results and Discussions	115
4.3.1	Optimizing Conditions for the Column Equilibration Technique	115
4.3.2	Establishing Trace Conditions for NBS ⁻ on ODS	120
4.3.3	Sorption of NBS ⁻ under "Ion-Pair" Conditions	124
4.4	Conclusion	143
5	FUTURE STUDIES	144
5.1	Mobile Phases with Organic Modifiers	144
5.2	Retention of Large Organic Sample Ions	146
	* * *	
	BIBLIOGRAPHY	148
APPENDIX I	MICROSOFT BASIC PROGRAM FOR CALCULATING THE SURFACE CHARGE DENSITY ON ODS PACKING FROM THE EXPERIMENTALLY MEASURED SURFACE EXCESS OF NBS ⁻	157

APPENDIX II	MICROSOFT BASIC PROGRAM FOR CALCULATING THE SURFACE CHARGE DENSITY ON ODS PACKING FROM THE EXPERIMENTALLY MEASURED SURFACE EXCESS OF TBA^+	160
APPENDIX III	ACTIVITY COEFFICIENT OF NBS^- IN AQUEOUS SOLUTION AT VARIOUS IONIC STRENGTHS	163
APPENDIX IV	ACTIVITY COEFFICIENT OF TBA^+ IN AQUEOUS SOLUTION AT VARIOUS IONIC STRENGTHS	167
APPENDIX V	THE SUBROUTINE PROGRAM (EQN) TO DEFINE THE EQUATION TO BE USED WITH THE LEAST-SQUARE CURVEFITTING (KINET)	171

List of Tables

TABLES	PAGE
2-1 Results of the elemental analysis for TBA^+Br^-	39
3-1 Experimental data of adsorption isotherms of NBS^- onto ODS packing from solution at five different ionic strengths at 25°C	61
3-2 Values of activity coefficient, surface excess of NBS^- and surface charge density on the ODS packing at five different ionic strengths when $a_{\text{NBS}^-} = 2 \times 10^{-4} \text{ M}$	64
3-3 Values of activity coefficient, surface excess of NBS^- and surface charge density on the ODS packing at five different ionic strengths when $a_{\text{NBS}^-} = 4 \times 10^{-4} \text{ M}$	65
3-4 Values of activity coefficient, surface excess of NBS^- and surface charge density on the ODS packing at five different ionic strengths when $a_{\text{NBS}^-} = 6 \times 10^{-4} \text{ M}$	66
3-5 Values of activity coefficient, surface excess of NBS^- and surface charge density on the ODS packing at five different ionic strengths when $a_{\text{NBS}^-} = 8 \times 10^{-4} \text{ M}$	67
3-6 Values of activity coefficient, surface excess of NBS^- and surface charge density on the ODS packing at five different ionic strengths when $a_{\text{NBS}^-} = 10 \times 10^{-4}$	68
3-7 SGC Behavior of NBS^- at the ODS/solution interface	71
3-8 Peak area given by acetaminophen eluted from the ODS column at different times	87
3-9 Bulk activity coefficients of TBA^+ at five different ionic strengths	92
3-10 Values of activity coefficient and surface excess of TBA^+ , and surface charge density on the ODS packing at five different ionic strengths when $a_{\text{TBA}^+} = 2 \times 10^{-3} \text{ M}$	93
3-11 Values of activity coefficient and surface excess of TBA^+ , and surface charge density on the ODS packing at five different ionic strengths when $a_{\text{TBA}^+} = 4 \times 10^{-3} \text{ M}$	94

3-12	Values of activity coefficient and surface excess of TBA^+ , and surface charge density on the ODS packing at five different ionic strengths when $a_{\text{TBA}^+} = 6 \times 10^{-3} \text{ M}$	95
3-13	Values of activity coefficient and surface excess of TBA^+ , and surface charge density on the ODS packing at five different ionic strengths when $a_{\text{TBA}^+} = 10 \times 10^{-3} \text{ M}$	96
3-14	Values of activity coefficient and surface excess of TBA^+ , and surface charge density on the ODS packing at five different ionic strengths when $a_{\text{TBA}^+} = 10 \times 10^{-3} \text{ M}$	97
3-15	SGC behaviors of TBA^+ at the ODS/solution interface.....	99
4-1	Effect of the concentration of TBA^+ in a standard NBS^- solution on the eluted peak area of NBS^-	122
4-2	Experimental data on the sorption of NBS^- in the presence of TBA^+ and on the adsorption isotherms of TBA^+ at five different ionic strengths at 25°C	125
4-3	Experimental and calculated values of distribution coefficients of NBS^- , and experimental values of surface excess of TBA^+ at five different ionic strengths when $a_{\text{TBA}^+} = 2.0 \times 10^{-3} \text{ M}$ and $\Psi_0 = 0.106 \text{ volt}$	129
4-4	Experimental and calculated values of distribution coefficients of NBS^- , and experimental values of surface excess of TBA^+ at five different ionic strengths when $a_{\text{TBA}^+} = 4.0 \times 10^{-3} \text{ M}$ and $\Psi_0 = 0.107 \text{ volt}$	130
4-5	Experimental and calculated values of distribution coefficients of NBS^- , and experimental values of surface excess of TBA^+ at five different ionic strengths when $a_{\text{TBA}^+} = 6.0 \times 10^{-3} \text{ M}$ and $\Psi_0 = 0.125 \text{ volt}$	131
4-6	Experimental and calculated values of distribution coefficients of NBS^- , and experimental values of surface excess of TBA^+ at five different ionic strengths when $a_{\text{TBA}^+} = 8.0 \times 10^{-3} \text{ M}$ and $\Psi_0 = 0.140 \text{ volt}$	132
4-7	Experimental and calculated values of distribution coefficients of NBS^- , and	

	experimental values of surface excess of TBA^+ at five different ionic strengths when $a_{\text{TBA}^+} = 10.0 \times 10^{-3} \text{ M}$ and $\Psi_0 = 0.154$ volt	133
4-8	Experimental and calculated values of distribution coefficients of NBS^- , and experimental values of surface excess of TBA^+ at five different ionic strengths when $a_{\text{TBA}^+} = 12.0 \times 10^{-3} \text{ M}$ and $\Psi_0 = 0.163$ volt	134
4-9	Experimental and calculated values of distribution coefficients of NBS^- , and experimental values of surface excess of TBA^+ at five different ionic strengths when $a_{\text{TBA}^+} = 14.0 \times 10^{-3} \text{ M}$ and $\Psi_0 = 0.169$ volt	135
4-10	Results of the non-linear least-square fitting of the experimental data to equation 4-23a-c	136
A-3a	Activity coefficient of NBS^- at ionic strength above 0.10	164
A-3b	Activity coefficient of NBS^- at ionic strength below 0.10	165
A-4a	Activity coefficient of TBA^+ at ionic strength above 0.10	168
A-4b	Activity coefficient of TBA^+ at ionic strength below 0.10	169

List of Figures

FIGURE	PAGE
1-1 Chromatograms illustrating the effect of the pairing-ion ($\text{C}_8\text{H}_{17}\text{SO}_3^-$) on the separation of protonated catecholamines by reverse-phase chromatography	3
2-1 Synthesis of chemically bonded octadecylsilyl (ODS) phases	11
2-2 Column equilibration technique for measuring adsorption isotherms of a sample component (e.g. NBS^-) onto ODS packing from solution	14
2-3 The column equilibration apparatus used to measure adsorption isotherms of p-nitrobenzenesulfonate (NBS^-) onto the ODS packing from solution	18
2-4 The liquid chromatography system used for simultaneously measuring sorption isotherms of both NBS^- and TBA^+ onto the ODS packing from solution	22
2-5 Column equilibration technique for simultaneously measuring sorption isotherms of TBA^+ and NBS^- onto an ODS packing from solution	23
2-6 The solvent extraction/flow injection analysis (SE/FIA) system for determination of TBA^+	30
2-7 A hypothetical plot of surface tension vs. logarithm of concentration for a micelle-forming surfactant	33
2-8 Schematic illustration of Wilhelmy Plate method for measuring surface tension of solution	34
3-1 The electrical double-layer at the ODS/solution interface due to the adsorption of organic ion P^+ onto the surface from solution	47
3-2 A hypothetical adsorption isotherm	54
3-3 The GC calibration curve of water for the determination of void volume in the system shown in Fig.2-3	58

3-4	Adsorption isotherms of p-nitrobenzenesulfonate (NBS ⁻) onto the ODS packing from aqueous solutions at five different ionic strengths at 25°C	60
3-5	Langmuir plots for the adsorption isotherms of NBS ⁻ onto the ODS packing from aqueous solutions at five different ionic strengths at 25°C	62
3-6	The Stern-Gouy-Chapman plots for the adsorption of NBS ⁻ onto the ODS packing from solutions at five different solution activities of NBS ⁻	70
3-7	Plot of surface tension vs. logarithm of concentration of TBA ⁺ for aqueous solutions with ionic strength of 0.5 and temperature of 25°C	74
3-8	The GC calibration curve of water for the determination of void volume in the system shown in Fig.2-4	76
3-9	Loading curve of TBA ⁺ on the ODS column. The aqueous sample solution contains 5.7×10^{-4} M TBA ⁺ Cl ⁻ with ionic strength of 0.05	76
3-10	Loading curve of TBA ⁺ on the ODS column. The aqueous sample solution contains 2.2×10^{-4} M TBA ⁺ Cl ⁻ with ionic strength of 0.50	77
3-11	The instrumental neutral activation analysis calibration curve of promine at 619keV	80
3-12	The elution curve of TBA ⁺ at the end of the UV detector D	81
3-13	The solvent extraction/flow injection analysis (SE/FIA) calibration curve of TBA ⁺	83
3-14	Adsorption isotherms of TBA ⁺ onto the ODS packing from aqueous solutions at five different ionic strengths at 25°C	84
3-15	Freundlich plots for the adsorption isotherms of TBA ⁺ onto the ODS packing from aqueous solutions at five different ionic strengths at 25°C	86
3-16	The effect of pH on the distribution coefficient of TBA ⁺ onto the ODS packing from aqueous solution	90
3-17	Stern-Gouy-Chapman plots for the adsorption of TBA ⁺ onto the ODS packing from aqueous solutions at five different solution activities	98

4-1	The electrical double-layer sorption model for ion pair chromatography	108
4-2	Loading curve of NBS^- on the ODS column	117
4-3	Typical signals from the UV detector (D) for the determination of the total number of moles of NBS^- in the ODS column ($n_{\text{T,NBS}^-}$)	118
4-4	The column equilibration liquid chromatographic system calibration curve of NBS^- at 266nm	119
4-5	Elution curves of NBS^- and TBA^+ from analytical column C2 for a typical experiment	121
4-6	Sorption isotherms of NBS^- onto the ODS packing from solution in the presence of 0.020M TBA^+ at 25°C	123
4-7	Distribution coefficient of NBS^- (k_s) on the ODS packing vs. the concentration of TBA^+ at five different ionic strengths	125
4-8	Distribution coefficient of NBS^- on the ODS packing vs. ionic strength at $a_{\text{TBA}^+} = 0.004 \text{ M}$	137
4-9	Distribution coefficient of NBS^- on the ODS packing vs. ionic strength at $a_{\text{TBA}^+} = 0.008 \text{ M}$	138
4-10	Distribution coefficient of NBS^- on the ODS packing vs. ionic strength at $a_{\text{TBA}^+} = 0.010 \text{ M}$	139
4-11	Distribution coefficient of NBS^- on the ODS packing vs. ionic strength at $a_{\text{TBA}^+} = 0.014 \text{ M}$	140
A-3	Plot of activity coefficient of NBS^- in aqueous solution vs. ionic strength	166
A-4	Plot of activity coefficient of TBA^+ in aqueous solution vs. ionic strength	170

Chapter 1

Introduction

In the early 1970's a number of workers exploited ion-pair formation as a means of achieving solute retention and separation in both normal-phase and reverse-phase liquid-liquid partition chromatography [1-6]. In liquid-liquid partition chromatography, as in liquid-liquid extraction, both the mobile and stationary phases are composed of bulk immiscible liquids. Under the experimental conditions employed the solute ion was present in the bulk organic phase primarily in the form of an ion-pair formed with the reagent "pairing-ion". This kind of ion-pair partition chromatography was used for separating various ionic compounds including carboxylic acids and aminophenols [2,3], biogenic amines and their metabolites [4], thyroid hormones and sulfa drugs [5], and for isolating nicotinic acid from human serum samples [6].

Because liquid-liquid partition chromatography systems are experimentally difficult to work with, they have been largely replaced in recent years with the so-called bonded phases, in which an organic molecule is covalently bound to a silica-gel surface. As for liquid-liquid partition systems, these bonded phases are referred to as "normal-phase" or "reverse-phase" depending on whether the bound molecule is more or less polar than the mobile phase, respectively. One of the frequently used reverse-phase bonded packings is the octadecylsilyl (ODS or C18) bonded phase in which octadecane is bound to the surface. Based on this early view of bonded-phases as "immobilized liquids", it was natural to refer the separation of ions in the presence of an oppositely charged ion in the mobile phase as "ion pair chromatography" [7]. Ion pair chromatography on bonded phases has been widely used for separating various ionic organic compounds including pharmaceutical molecules and biomolecules, such as amino acids, peptides, proteins, etc in the past decade [8,9,10]. It is usually carried out in the reverse-phase mode. Its operation procedure [11] is the same as that of conventional reverse-phase liquid chromatography on bonded phases

except that the mobile phase contains a "pairing-ion" which is oppositely-charged to the sample ions to be separated. The influence of the pairing-ion on the separation of the sample ions is quite remarkable. This is illustrated by the chromatograms in Fig.1-1 [12]. The separation of some cationic protonated catecholamines on an ODS column is shown in the absence and presence of the anionic pairing-ion, n-octane sulfonate in an aqueous mobile phase. When the mobile phase does not contain any pairing-ions, the sample ions have short retentions on the nonpolar stationary phase and their separation is very poor (see chromatogram A). When the pairing-ion is added to the mobile phase, the retentions of the sample ions increase dramatically and they are separated very nicely on the column (see chromatogram B). This example illustrates what is true in general, that ionizable or very polar compounds are very difficult to separate with reverse-phase columns because of their short retention and severe peak tailing [8,11]. By adding a pairing-ion to the mobile phase, the retention is greatly enhanced and a relatively good separation can usually be achieved.

This kind of chromatography has, at various times, been called ion-pair chromatography [13,14], paired-ion chromatography, surfactant chromatography [14], soap chromatography [15,16], solvent-generated ion-exchange chromatography [17], heteric chromatography [12] and ion-interaction chromatography [18,19]. This technique has become a popular alternative to ion-exchange chromatography for separating mixtures of ionic molecules, especially large biomolecules. Compared with ion-exchange chromatography, ion pair chromatography usually offers a higher separation efficiency and a greater degree of flexibility as far as the eluent (mobile phase) composition is concerned [20].

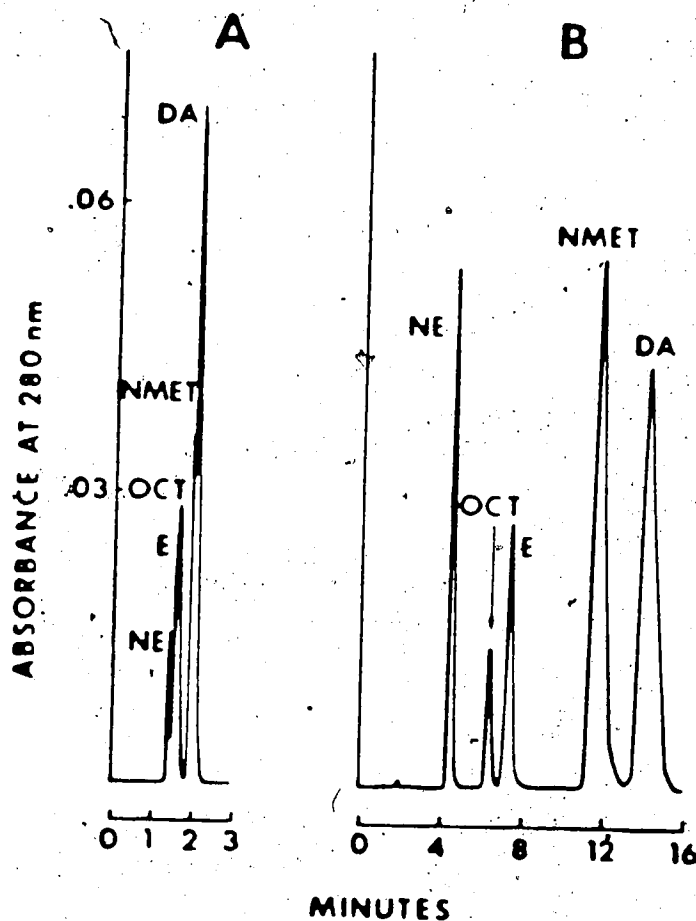


Figure 1-1 Chromatograms illustrating the effect of the pairing-ion ($\text{C}_8\text{H}_{17}\text{SO}_3^-$) on the separation of protonated catecholamines by reverse-phase chromatography.

Column: μm LiChrosorb RP18 (octadecylsilyl bonded phase); mobile phase:

A, 0.05M phosphate aqueous solution, pH = 2.2; B, 0.05M phosphate

and 0.003M octylsulfate aqueous solution, pH = 2.2; flow rate: 2.0 ml/min;

column temperature: 70°C ; inlet pressure: 2200psig.

In spite of the lack of agreement on the physico-chemical process responsible for the retention of ions in ion pair chromatography, the present knowledge, obtained from the work of the past decade, has been able to provide some degree of chromatographic predictability for this technique [21,22] : (1) the retention of a sample ion generally increases with increasing concentration of a pairing-ion in the mobile phase, and sometimes reaches a maximum and decreases with further increase of the concentration; (2) the retention of the sample ion decreases with increasing ionic strength of the mobile phase; (3) the retention of the sample ion decreases dramatically when a pairing-ion bears the same type of charge as the sample ion; (4) the retention of a non-ionic sample decreases with increasing concentration of a charged pairing-ion in a totally aqueous mobile phase.

The goal of the present thesis is to test experimentally the physico-chemical model proposed by Cantwell in which retention in ion-pair chromatography is quantitatively explained on the basis of the properties of the electrical double-layer at the ODS/mobile phase interface. This thesis is divided in the following way:

In Chapter 2 are presented the principles of operations of all the techniques involved in this study, such as the column equilibration technique, solvent extraction/flow injection analysis, Wilhelmy balance, instrumental neutron activation analysis, etc. A detailed description of the experimental procedures for each of the techniques is also given. In addition, the synthesis and properties of the ODS packing used in this study are presented.

In Chapter 3, the adsorption isotherms of an organic cation, tetra-butylammonium (TBA^+), and of an organic anion, p-nitrobenzenesulphonate (NBS^-), onto the ODS packing at five different ionic strengths will be given. Then the effect of ionic strength on the adsorption isotherms will be quantitatively described using the Stern-Gouy-Chapman electrical double-layer theory.

In Chapter 4, the retention of NBS^- (sample ion) under typical "ion-pair" conditions onto an ODS column is presented as a function of the concentration of TBA^+ (pairing-ion) and of ionic strength. The adsorption isotherms of TBA^+ measured at the same conditions are also given. The experimental data are then fitted into the electrical double-layer sorption model. A good agreement between the two is used to indicate the success of the model. In Chapter 5, some possible future work will be discussed.

Chapter 2

Experimental Methods, Principles And The ODS Packing Material

In this chapter are presented the experimental details for all aspects of the research including the column equilibration technique for measuring sorption isotherms, the solvent extraction/flow injection analysis technique for determining tetra-butylammonium (TBA^+) ion, the Wilhelmy balance technique for measuring surface tension of the aqueous solutions of TBA^+Cl^- and the instrumental neutron activation analysis (INAA) technique for determining bromine.

2.1. Chemicals, Reagents and Solvents

p-nitrobenzenesulfonic acid (NBS-acid) was prepared from the practical grade material (Eastman Kodak Co., Rochester, New York) by recrystallizing it from the solvent benzene/ethyl acetate (25:75 v/v). The crystals thus obtained were then vacuum-dried for ~24hr (melting point, $92\sim 93^\circ\text{C}$). A stock solution of $1.250 \times 10^{-3}\text{M}$ was prepared by dissolving 0.1270 grams of the crystals in water in a 500ml volumetric flask.

Tetrabutylammonium chloride (TBA^+Cl^-) (Lot no. D9C, 96%, Eastman Kodak Co., Rochester, New York.) was used without further purification. It is very hygroscopic. A stock solution of TBA^+Cl^- (0.06M) was prepared by dissolving it in water, and was standardized by titration with a standard silver nitrate solution.

Acetaminophen (p-hydroxyacetanilide) was obtained from Matheson, Coleman and Bell (Norwood, Ohio) and used as received.

Sodium Hydroxide (0.1M) solution was prepared by dissolving reagent grade sodium hydroxide in water, and was standardized using primary standard potassium acid phthalate.

Sodium chloride (1.0M) solution was prepared by dissolving reagent grade sodium chloride in water. Its concentration was accurate to within 0.1%.

Acetic acid (0.1M) solution was prepared by dissolving ~ 5g of reagent grade glacial acetic acid in 1000ml of water, and then was standardized using the standard sodium hydroxide solution.

Silver nitrate (0.1M) solution was prepared by dissolving primary standard silver nitrate in water.

Picric acid (BDH Chemicals) solution (0.05M) was prepared by dissolving picric acid in water, and was standardized with the sodium hydroxide solution.

Water used to prepare all the aqueous solutions was obtained by distilling the laboratory distilled water over alkaline permagnate and collecting the middle fraction of the distillate (the first 20% of the distillate was discarded).

Methanol (Anachemia) was reagent grade, and was distilled before use.

Ethanol (BDH Chemicals) was reagent grade, and was distilled before use.

Chloroform (Terochem Labs Ltd.) was reagent grade, and was used as received.

All other chemicals were reagent grade.

2.2. The ODS Packing

Whatman Partisil-10 ODS-3 (batch no.100763, Whatman Inc., Clifton, N.J.) was used as the packing material in this work. This material is considered to be a highly "end-capped" reversed-phase packing.

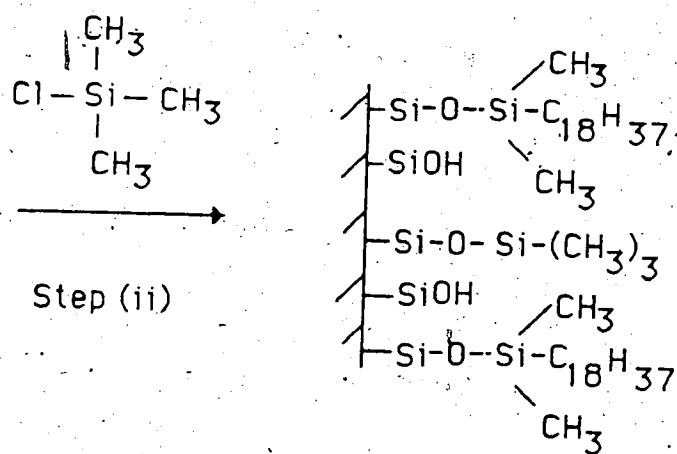
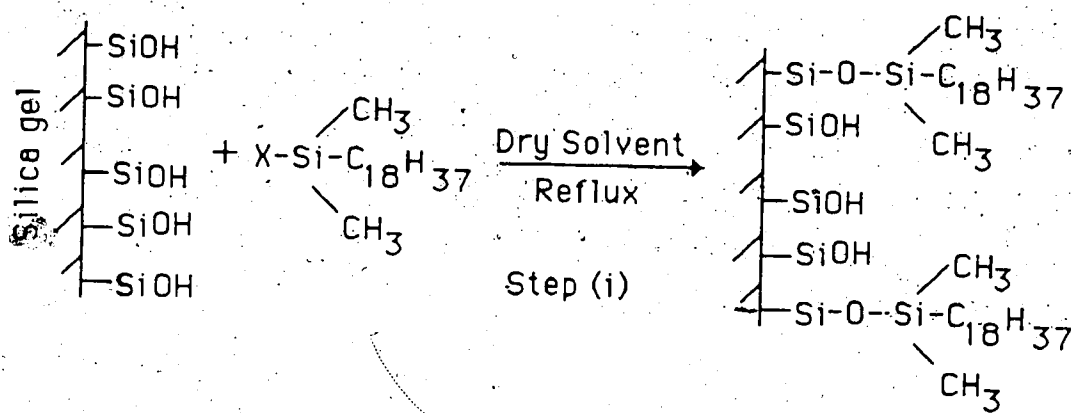
Chemically bonded octadecylsilyl (ODS) microparticles (5 or 10 μm) are by far the most frequently used reversed-phase packing materials in liquid chromatography [23], mainly because of their applicability to diverse separation problems and their high efficiency. The reactions commonly used for synthesizing both monomeric and polymeric ODS [24,25,26] are shown in Fig. 2-1. With a monofunctional silane (e.g. monochloro or monoalkoxysilane), each molecule can react with only one silanol group on the silica surface (see a in Fig. 2.1a). The product thus obtained is called monomeric to indicate that the surface of the silica gel is covered with only a monomolecular layer of the alkyl chains. Monomeric phases can also be prepared by the reaction of silica gel with di- or trifunctional silanes if water is excluded from the reaction (Fig. 2.1b). With water present, a trifunctional reagent can produce a cross linked alkylpolysiloxane layer at the surface (Fig. 3.1c) and such a stationary phase is called "polymeric".

It is generally agreed that the number of accessible silanol groups on the silica surface is about 8 $\mu\text{mol}/\text{m}^2$ (or 4.8 silanols/ nm^2) [24,25,27]. Due to steric constraints, it is believed that less than half [24,28,29] of these silanols can be silanized with the octadecylsilyl which has a relatively long alkyl chain. In order to minimize the unreacted silanols on the surface, the product is usually silanized again with a much smaller silane. Trimethylchlorosilane is commonly used for this purpose. This procedure, as shown in Step (ii) of Fig. 2-1a and Step (iii) of Fig. 2-1b, is usually referred to as "end-capping". Most of the easily accessible silanols could be silanized with this procedure.

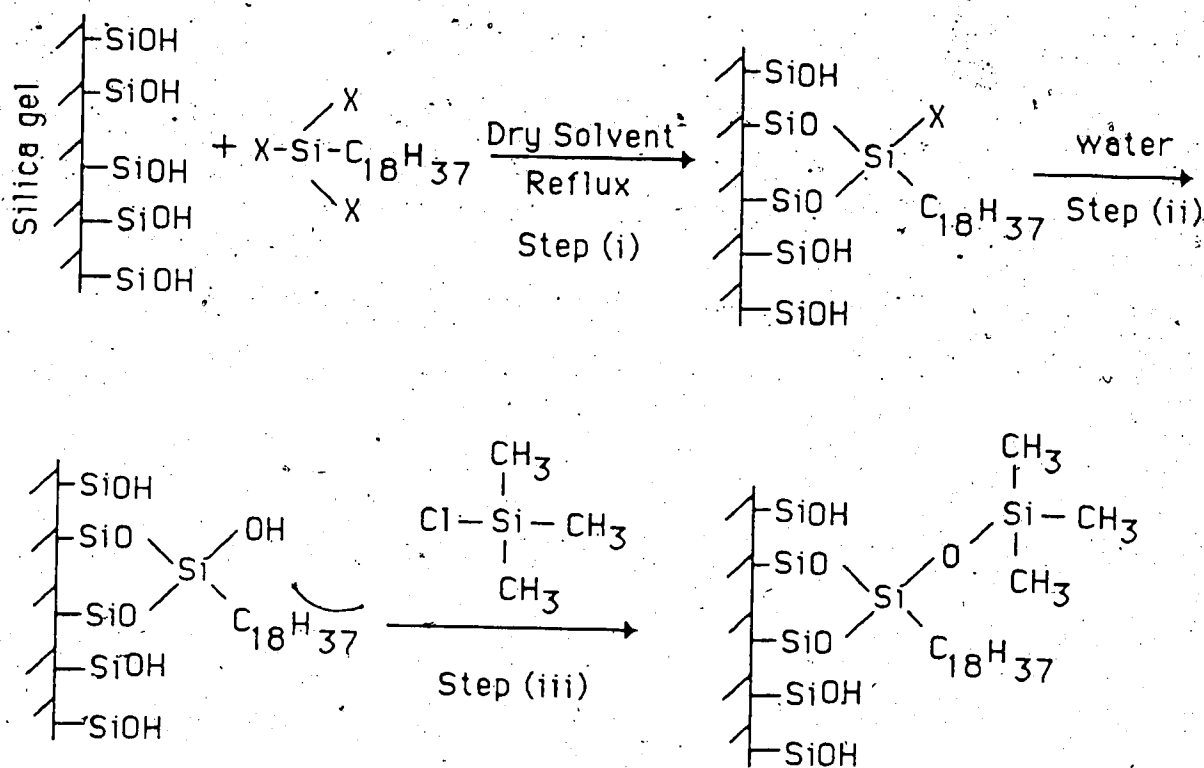
Even after the "endcapping", there may still be some accessible residual silanol groups on the surface [25,26], and their amount depends on the endcapping procedure.

Monomeric Synthesis

a. monofunctional



b. Trifunctional



It is believed that these residual silanol groups are the cause of various problems in chromatography, such as the instability of the packings in aqueous mobile phases and the severe peak-tailing of polar or ionic compounds [30-33]. The effect is usually more significant for basic organic ions, like amino compounds, especially when the mobile phase has a high organic solvent concentration [34,35,36].

The amount of the alkyl chains bonded to the silica is an important parameter frequently used to specify a chemically bonded packing material. It can be expressed in different ways. The two most commonly ways are: (1) Carbon loading: This is the weight percentage of carbon in the packing material, and can be easily obtained from elemental analysis. (2) Surface coverage: This is usually defined as the percentage of the available silanols on the silica gel that have reacted with the silanes. Surface coverage is increased by both the bonding reaction and the "end-capping" silanization. Its value could be different depending on the assumptions involved and measurement techniques [25]. It is generally considered to be desirable to have the surface coverage close to unity for a well "end-capped" bonded stationary phase.

The ODS packing material used in this study was made by bonding a trichlorooctadecylsilane reagent to the Partisil-10 silica under drying conditions, followed by endcapping with trimethylchlorosilane (probably with scheme b in Fig. 2-1). The Partisil-10 silica gel, from which the Partisil-10 ODS-3 packing was made, is irregularly-shaped, porous microparticles with an average diameter of $10\mu\text{m}$ and surface area of approximately $400\text{m}^2/\text{g}$. Its pore size is about 8nm. The final product is a $10\mu\text{m}$ chemically bonded C18 phase with carbon load of approximately 10%. Its surface coverage was estimated by the manufacture to be at least 95% based on the retention of nitrobenzene with n-hexane as the eluent [37]. The specific surface area of the batch of Partisil-10 ODS-3 used in this study has been measured using the BET method to be $309\text{m}^2/\text{g}$ (by S. Angle in the Alberta

Research Council). Whether this packing is truly monomeric or somewhat polymeric is controversial [27,37].

2.3. Column Equilibration Technique for NBS⁻ alone

In this experiment, the sorption of NBS⁻ onto the ODS packing material from aqueous solution was studied by measuring its sorption isotherms at five different ionic strengths, ranging from 0.01 to 0.1. The solution concentration of NBS⁻ ranged from $5 \times 10^{-5} \text{M}$ to $1.5 \times 10^{-3} \text{M}$. The pH of the solutions was adjusted to 5.0, and the temperature was controlled at $25^{\circ}\text{C} \pm 0.5^{\circ}\text{C}$.

2.3.1. Principles of the Column Equilibration Technique

There are many techniques that have been used for measuring sorption isotherms for solid/solution adsorption. These have been extensively discussed by Sorel and Hulshoff [9], by Kipling [38], by Parffit and Rochester [39], by Hux et al [40,41] and by May et al [42]. This discussion will be limited to the column equilibration technique.

Fig. 2-2a shows a column packed with a known weight of the sorbent (i.e. ODS), W_s , through which a solution of the sample component (e.g. Na^+NBS^-), whose concentration is C_m , is being fed. Supposing before the start of the feeding, the column is equilibrated with the solvent not containing the sample component. Then at time 0.0 the sample solution starts to feed into the column. If the sample component is not retained (sorbed) on the sorbent at all, then it will migrate at the same speed as that of the solvent and will emerge from the outlet of the column after one column volume, V_m , of its solution has been fed through. If, on the other hand, the sample component is retained on the sorbent, the front of its zone will migrate at a slower rate than that of the solvent and will emerge from the outlet after a larger volume, V_R , of its solution has been fed through the

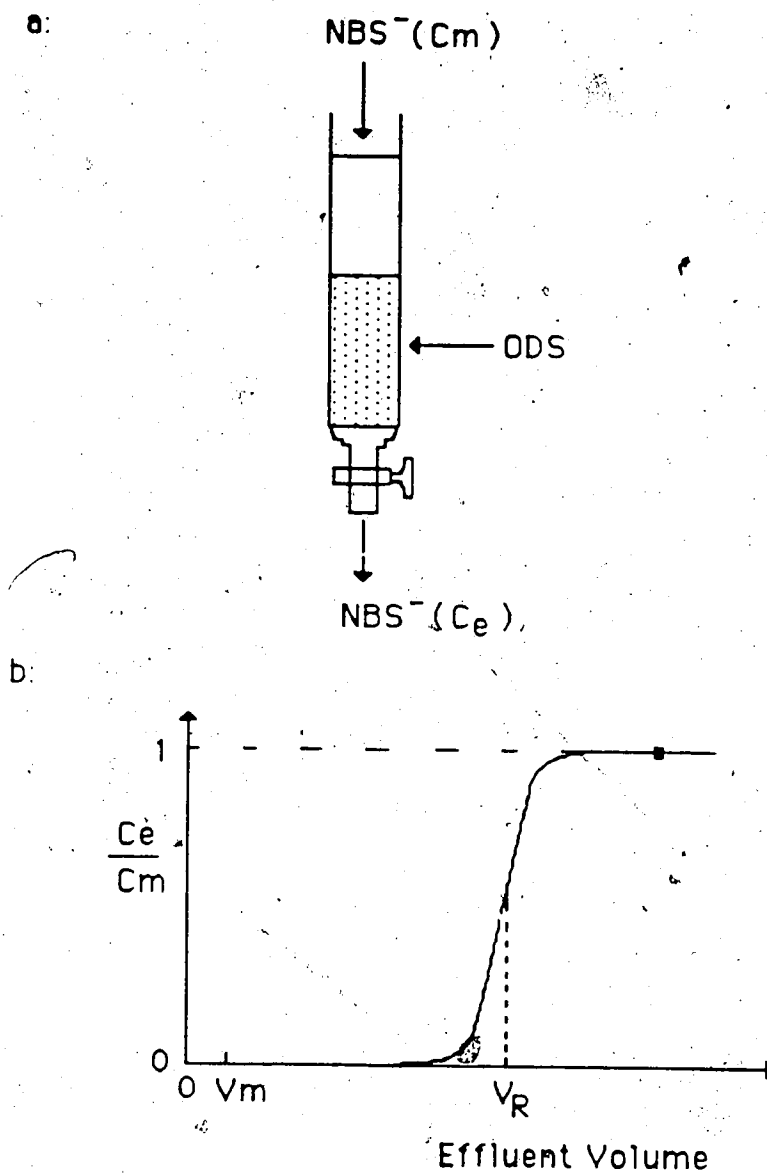


Figure 2-2 Column equilibration technique for measuring adsorption isotherms of a sample component (e.g. NBS^-) onto ODS packing from solution. (a) Showing a column packed with ODS through which a sample solution containing NBS^- is being fed; (b) showing a hypothetical breakthrough curve of NBS^- on the column.

column. V_R is normally referred to as the breakthrough volume of the sample component and is related to its distribution coefficient, K_d , on the sorbent by the equation:

$$V_R = V_m + W_s K_d \quad (2-1)$$

For a given column both W_s and V_m are fixed so that the larger K_d is, the larger will be V_R .

The curve (Fig.2.2b), showing the concentration of sample component in the effluent versus the effluent volume, is referred to as the "breakthrough curve" of the solute on the column. Within experimental error, at larger and larger effluent volumes, the curve approximately approaches a limiting plateau. When the plateau of the breakthrough curve is reached, the concentration of the sample component leaving the column, C_e , is equal to its concentration entering the column, C_m . The sorbent in the column is at equilibrium with the solution, whose concentration is C_m , and complete breakthrough has been achieved.

A better way to measure the approach to equilibrium between the sorbent and the solutions, when the concentration of the sample component in the effluent solution is small and likely to be lost in the baseline noise, is to measure the loading curve [41,42,43] of the sample component. This can be done by the following procedure: (i) pumping a specified volume of the sample solution through the column; (ii) eluting the sorbed sample component with a suitable eluent, collecting the effluent and determining the amount of the sample component, n_T , after each loading operation; (iii) repeating step (i) and (ii) using a larger volume of the sample solution in step (i). The loading curve is a plot of the amount of the sample component sorbed in the column (either peak height or peak area) vs. the volume of the sample solution pumped through the column. The amount of the sample component sorbed in the column usually increases to a limiting plateau, at which point

equilibrium (or complete breakthrough) has been achieved. A typical loading curve is shown later in Fig. 4.2.

The concentration of the compound on the sorbent, C_s (mol/kg) can be calculated by the equation:

$$C_s = \frac{n_T - C_m V_m}{W_s} \quad (2-2)$$

where n_T is the total number of moles of the sample component (e.g. NBS) contained in the column. Various quantitative techniques have been used to determine the amount eluted [44,45,46,47,48]. The void volume, V_m , can be determined by filling the column with water, eluting the column with another solvent and collecting the eluent at the end of the column, and finally quantitatively determining the water content in the collected eluent by a suitable technique [45,49,50].

In the column equilibration technique one is interested in the values of C_s on the complete-breakthrough plateau (i.e. when the packing is at equilibrium with the sample solution). Once C_s at column equilibration is known, the distribution coefficient, K_d , of the compound can then be calculated with equation 3-16 (see Chapter 3). A sorption isotherm for the sample component can be constructed by repeating the operation at several different values of C_m in the sample solution.

In summary, measuring sorption isotherms with the column equilibration technique usually involves four experimental steps: (i) determining the void volume of the column, V_m ; (ii) equilibrating the column by passing enough sample solution through it; (iii) eluting or washing-off the sample component from the column with an eluent, and (iv) determining the amount of the sample component in the collected eluate with a proper quantitative method.

2.3.2 Apparatus and Column

A schematic diagram of the column equilibration apparatus used for NBS⁻ is shown in Fig. 2-3. P1 and P2 are two HPLC pumps (model 501&590, Waters Assoc. Inc., Milford, MA); V is a six-port injection valve (part no. 7010, Rheodyne Inc., CA). The column C₁ is a 2.0cm long x 0.40cm i.d. stainless steel guard column commercially available (part no. 84550, Waters Ass. Inc., Milford, MA). It is dry-packed with 0.1657g of the ODS packing. The column was thermostated in a water bath of $25.0 \pm 0.5^{\circ}\text{C}$. A Cary 118 spectrophotometer (Varian Instruments, Palo Alto, CA) was used for the absorbance measurements.

2.3.3. Sample and Eluent Solutions

Five series of sample solutions were prepared. Each series had a constant ionic strength and contained a range of NBS⁻ concentrations from 0.5×10^{-4} to $15 \times 10^{-4}\text{M}$. The five series were at ionic strengths 0.01, 0.022, 0.034, 0.05 and 0.10. They were prepared by pipetting the stock solution of p-nitrobenzenesulfonic acid into a series of 500ml volumetric flasks, with just enough volumes (less than 7.5ml) of the 0.1M NaOH solution to neutralize the acid into its basic form. Then ~ 0.5ml of the 0.1M acetic acid solution was added to adjust their pH to 5.0, sufficient volume of the 1.0M NaCl solution was added to adjust their ionic strengths to the specific values, and they were diluted to volume with water.

The eluent was prepared by mixing equal volumes of methanol and water.

All solutions were filtered through 0.45 μm pore-sized Nylon-66 filters (catalog no. 38-114, Rainin Instr. Co. Inc., Emeryville, CA) before use.

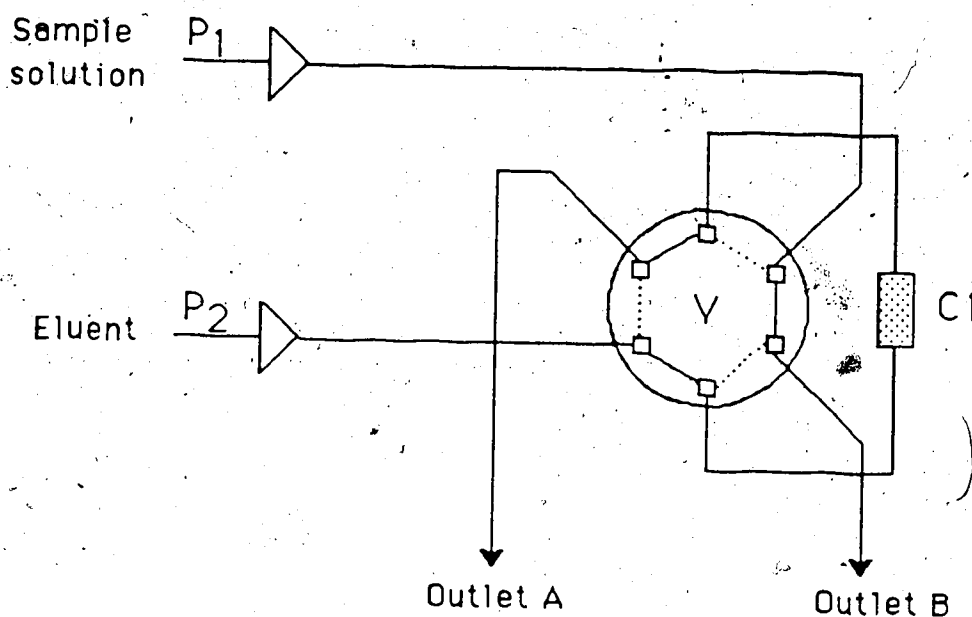


Figure 2-3 The column equilibration apparatus used to measure adsorption isotherms of p-nitrobenzenesulfonate(NBS^-), where P1 and P2 are two HPLC pumps, V is a six-port sample injection valve, and C1 is a column packed with $\sim 170\text{mg}$ of ODS material. The sample solution usually contains NBS^- (concentration ranges from 0.5×10^{-4} to $15 \times 10^{-4} \text{ M}$) with ionic strength ranging from 0.010 to 0.100 and pH 5.0. The eluent is a 1:1 (v/v) mixture of methanol and water containing 0.010M NaCl.

2.3.4 Procedure

With the valve V in the "load" position (the dashed lines), the sample solution was pumped for 5.0 minutes at a flow rate of 2ml/min through column C_1 to waste (outlet B). This is enough to achieve complete breakthrough for NBS^- . Then the valve was switched to the "inject" position (the solid lines). The eluent was pumped for 10.0 minutes at a flow rate of 1ml/min to backflush the column C_1 eluting the NBS^- from the column. The effluent was collected to the mark in a 10ml volumetric flask at the outlet A. The total number of moles of NBS^- , n_{T,NBS^-} , eluted from the column (including that contained in the void spaces) is determined by comparing the absorbance of the collected eluate with a calibration curve of absorbance at 266nm vs. concentration. The absorbance measurement was performed on a spectrophotometer.

The concentration of NBS^- on the ODS packing, C_{S,NBS^-} (mol/kg), can be calculated from equation 2-2 after the void volume, V_m , is measured. The adsorption isotherm of NBS^- at a particular ionic strength is constructed after C_{S,NBS^-} is measured at several different solution concentrations of NBS^- , C_{m,NBS^-} .

Loading curve for NBS^- were studied by pumping the sample solution through the column for various time (3, 4 and 5min) during the equilibration step. The study was done to ensure that 5.0 min was always sufficient to achieve equilibrium. Furthermore, in order to demonstrate that the elution of NBS^- from column C_1 was complete in 10.0min, the elution curve of NBS^- was measured by pumping the eluent through the column for various time (5, 7 and 10min).

2.3.5 Void Volume Measurement

2.3.5.1 Procedure

The void volume, V_m , of the system shown in Fig. 2-3 was measured in the following way: With Y in the "load" position (dashed lines), water was pumped through the column C_1 for 5.0min at a flow rate of 2ml/min. Then V_1 was switched to the "inject" position and ethanol was pumped through the column for 10min at a flow rate of 1ml/min. The effluent was collected in a 10ml volumetric flask. The volume of water in the collected ethanol solution was determined with gas chromatography [45] on the basis of a calibration curve of peak area vs. volume of water. The calibration curve was obtained by injecting 2 μ l of a series of standard solutions of water in ethanol.

2.3.5.2 The Gas Chromatography System

The gas chromatography instrument (Model 3700, Varian, Palo Alto, CA) has a homemade stainless steel column, 2.9 m long x 1.6 mm i.d., which was packed with Porapak Q-S 50/80 mesh (Waters Assoc. Inc., Milford, MA). A thermal conductivity detector was used.

Important instrumental parameters for the measurement are as follows: injector temperature: 200°C; column temperature: 135°C; TCD temperature: 190°C; Helium flow rate: 40ml/min; Filament current: 225mA.

2.4 Column Equilibration Technique for NBS^- and TBA^+

This experiment was intended to study the situation where a "trace" amount of NBS^- is present with a large excess of TBA^+ in the sample solutions at various ionic strengths. These conditions are typical for the so-called "ion-pair" chromatography. Under "trace conditions", the adsorption isotherms of TBA^+ onto the ODS material will not

be affected by the presence of NBS^- in the solution, while the sorption of NBS^- will be changed significantly by the presence of TBA^+ . In the study, the solution concentration of TBA^+ (ranging from 0.002 to 0.05M) and NaCl (ionic strength ranging from 0.05 to 0.5) were varied, and that of NBS^- ($1.488 \times 10^{-6}\text{M}$) was fixed. Using the column equilibration technique, the adsorption isotherms of TBA^+ and the influence of concentration (both in the solution and on the surface of the ODS) of TBA^+ on the sorption of NBS^- at five different ionic strengths were obtained at the same time.

The system used for the measurements is shown in Fig.2-4. Its main feature is that it has two detection systems: one is an on-line UV detector and the other is an off-line solvent extraction /flow injection analysis system. This feature enables it to be used to simultaneously measure the sorption isotherms of both NBS^- and TBA^+ respectively.

The loop L is for the purpose of calibrating the UV detector for NBS^- . The analytical column C_2 is to resolve the NBS^- peak from those of impurities and that of the solvent.

2.4.1. Principle of the Technique

The principle of the technique is schematically illustrated in a simplified system shown in Fig.2-5. The situation is basically the same as that shown in Fig.2-2 except that the sample solution fed into the column contains both components: NBS^- and TBA^+ instead of only NBS^- . The sample solution is passed through the column packed with a known weight of an ODS packing until both of the sample components reach sorption equilibrium with the column. That is, the concentrations of both NBS^- and TBA^+ leaving the column are equal to those entering the column and both of them have achieved complete breakthrough. The breakthrough volumes of NBS^- and TBA^+ are related to their distribution coefficients by equation 2-1. The breakthrough curves are shown in an idealized form in Fig.2-5b. Because TBA^+ has a much smaller K_d than that of NBS^-

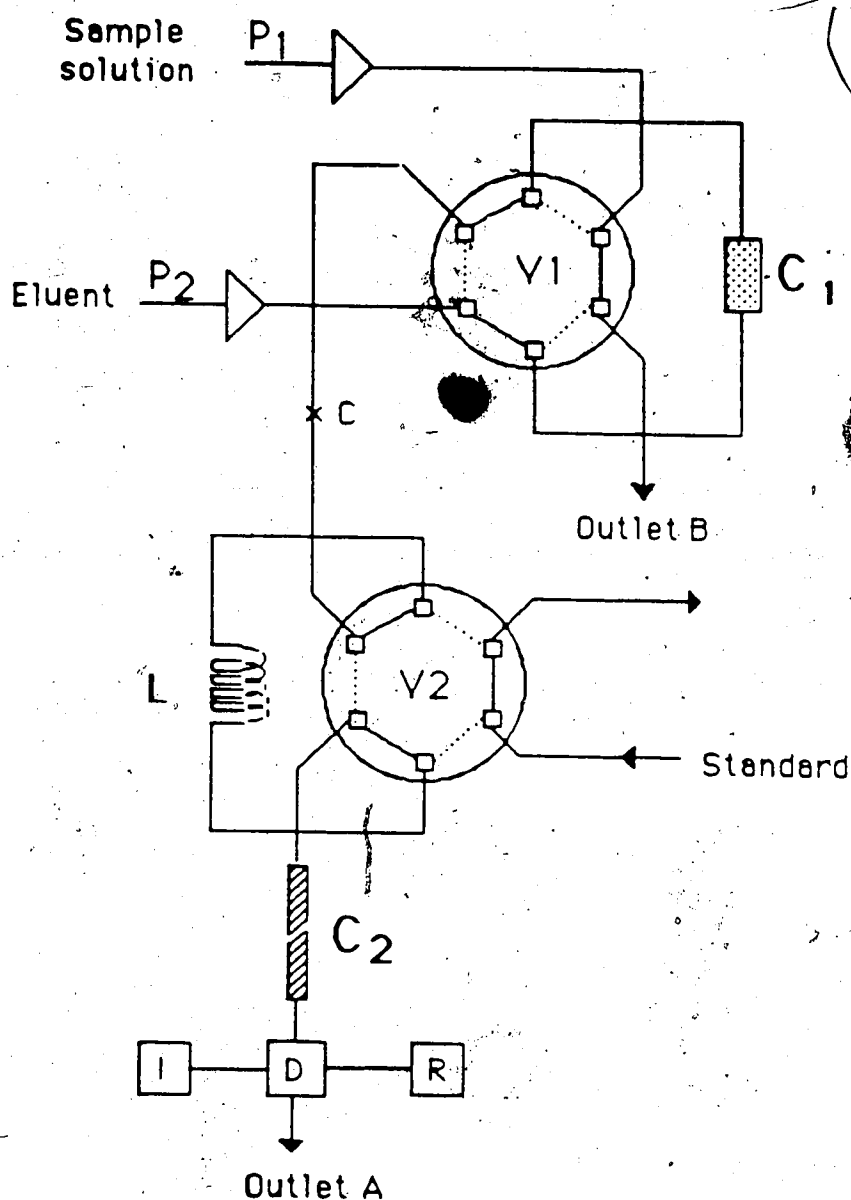


Figure 2-4 The liquid chromatography system used for simultaneously measuring sorption isotherms of both NBS^- and TBA^+ . Where P1 and P2 are two HPLC pumps, V1 and V2 are two six-port sample injection valves, C1 is the column packed with ~ 15mg ODS material, C2 is an analytical column (PRP-1), L is a 2ml loop attached to V2, D is a UV detector, I is an integrator, and R is a recorder. Note, C is the point at which V2 is disconnected from V1 when void volume is to be determined.

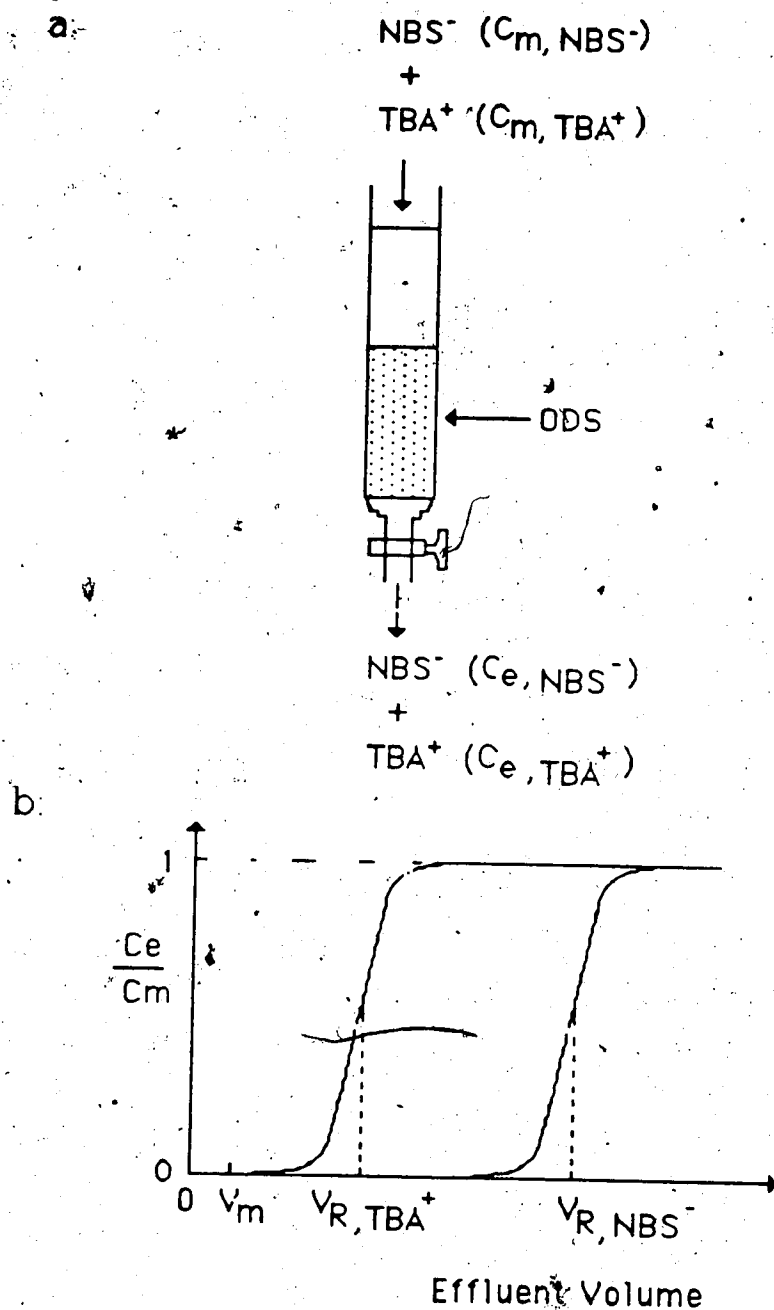


Figure 2-5 Column equilibration technique for simultaneously measuring sorption isotherms of TBA^+ and NBS^- . (a) showing a column packed with ODS packing through which a sample solution containing NBS^- and TBA^+ is being fed; (b) showing the breakthrough curves of TBA^+ and NBS^- on the column.

under the conditions of the experiment, it achieves complete breakthrough first. It should be noted that, in the absence of TBA^+ , NBS^- has a very small breakthrough volume. But under the "ion pair" conditions, in the presence of TBA^+ , NBS^- is much more retained.

After equilibration, NBS^- and TBA^+ are eluted from the column by passing a suitable eluent through and the effluent is collected. The total number of moles of NBS^- eluted from the column, $n_{\text{T,NBS}^-}$, and that of TBA^+ , $n_{\text{T,TBA}^+}$, are then determined. The void volume, V_m , of the column is measured in the same way as described in section 2.3.5. Then the concentrations of the sample components on the sorbent, C_{s,NBS^-} and C_{s,TBA^+} , are calculated with equation 2-2.

2.4.2. Apparatus and Column

P1 and P2 are two HPLC pumps (model 501&590, Waters Assoc. Inc., Milford, MA); V1 is a six-port injection valve (part no. 7010, Rheodyne Inc., CA); V2 is a U6K sample injector (Waters Assoc. Inc., Milford, MA) with a 2ml injection loop; D is a UV spectrophotometric detector (model 481, Lambda-Max, Waters Assoc. Inc.) usually set at 266nm to have a maximum response to NBS^- . I is an integrator (HP3390A, Hewlett-Packard) connected to the detector to give peak area.

The column C_1 is a commercial cartridge (part no. 28690, Chrompack, Netherlands) with a chamber of 2.0mm x 4.6mm id, and usually contains 15.8mg of the ODS packing. It was dry-packed and thermostated in a water bath of $25.0 \pm 0.5^\circ\text{C}$. The analytical column C_2 is a commercial column of PRP-1 (part no. 19425, Hamilton company, Reno, NV).

2.4.3 Sample and Eluent Solutions

Five series of sample solutions were prepared, all containing a fixed concentration of NBS^- ($1.488 \times 10^{-6}\text{M}$), each at a different concentration of TBA^+ in the

range of 0.0017 ~0.02M and each at five different ionic strengths (0.05, 0.07, 0.10, 0.30 and 0.5). All solutions were adjusted to pH 5.0 with ~ 0.5ml of the 0.1M NaOH solution and ~0.5ml of the 0.1M acetic acid solution. Solution preparation involved the following steps: (i) pipetting 12ml of a 6.200×10^{-5} M NBS⁻ acid solution; (ii) pipetting different volumes of the 0.06M TBA⁺Cl⁻ stock solution; (iii) pipetting different volumes of a 5.0M NaCl stock solution; (iv) adjusting pH of these solutions with acetic acid and sodium hydroxide solutions; and (v) adding water to make the final volumes 500ml.

For the experiment of locating "trace conditions" for NBS⁻, two sets of sample solutions were prepared. One set had 0.01942M TBA⁺, various concentrations of NBS⁻ ($0.5 - 2.5 \times 10^{-6}$ M), ionic strength of 0.50 and pH 5.0. The other set of sample solutions had a 0.01942M TBA⁺, various concentrations of NBS⁻ ($0.5 - 2.5 \times 10^{-6}$ M), ionic strength of 0.050 and pH 5.0.

The eluent is a 1:1 (v/v) mixture of methanol and water containing 0.010M NaCl.

All solutions were filtered through 0.45 μ m pore-sized Nylon-66 filters (catalog no. 38-114, Rainin Instr. Co. Inc.) before use.

2.4.4 Procedure

The main objective was to measure distribution coefficients, K_s , of NBS⁻ and isotherms of TBA⁺ using the system shown in Fig.2-4 in combination with the SE/FIA system. With the injection valve V1 in the "load" position (dashed lines), a sample solution containing a known concentration of TBA⁺, C_{m,TBA^+} , and 1.488×10^{-6} M of NBS⁻ at a particular ionic strength adjusted with NaCl was pumped for 65min at a flow rate of 2ml/min through column C₁ to waste (outlet B) using Pump P1. During this time, pump P2 delivered the eluent through valve V1, through an injection valve V2, and then through the analytical column C₂ to the UV detector.

After the 65min equilibration, valve V1 was switched to the "inject" position (solid lines). The eluent was pumped at a flow rate of 1ml/min to backflush column C_1 , eluting TBA^+ and NBS^- from the column C_1 , through V1 and V2, onto the analytical column C_2 where it was separated from the solvent and any impurity peaks before reaching the detector D. The effluent was collected to the mark in a 25ml volumetric flask at the outlet of the detector. The amounts of NBS^- eluted from C_1 (including that in the void spaces) was found by monitoring the effluent with the UV detector at 266nm. The areas of peaks eluted from column C_2 were obtained with the integrator. The total number of moles of NBS^- , n_{T,NBS^-} , eluted was obtained from a calibration plot of peak area of NBS^- vs. number of moles of NBS^- . The calibration was obtained by injecting different volumes (50 ~ 200 μ l) of a NBS^- standard solution using the U6K injector. Actually, two NBS^- standard solutions were prepared in order to cover a wide range of concentrations. One had $2.480 \times 10^{-4} M$ of NBS^- , 0.01933M of TBA^+ and ionic strength of 0.50. The other had $9.920 \times 10^{-4} M$ of NBS^- , 0.01933M of TBA^+ and ionic strength of 0.50. They were prepared in the same way as other sample solutions.

The total number of moles of TBA^+ , n_{T,TBA^+} , was determined through measuring its amount in the collected eluate with the SE/FIA system, which will be discussed in detail in section 2.6.

Loading curves for TBA^+ and NBS^- were studied by pumping different volumes of a sample solution through column C_1 during the equilibration step. The complete breakthrough volume was about 20ml for TBA^+ and 100ml for NBS^- . Therefore, 125ml (i.e. 65min) of sample solutions was always pumped through column C_1 to ensure equilibration. To make sure that the elution of TBA^+ was completed with 25ml of the eluent, the "elution curve" of TBA^+ has been studied. This was done by collecting the effluent continuously at the outlet of the detector D in a series of 2ml-portion, and determining the amount of TBA^+ in each of the portions.

2.4.5 Void Volume Measurement

The total void volume in the system, V_m , (including void of column C_1 , the connecting tubings and valve V1) has been determined in a similar way to that described in section 2.3.5 after disconnecting valve V2 from valve V1 at point C. In this case, however, an internal standard was added to improve measurement precision. The ethanol effluent was collected at the outlet (point C) of V1 in a 10ml volumetric flask, to which 0.10ml of methanol contained in about 1ml ethanol had been added as an internal standard. The calibration curve was obtained by injecting $\sim 3\mu\text{l}$ of a series of standard solutions of water in ethanol, which all contain 0.10ml methanol as an internal standard.

2.4.6 Stability of the ODS Packing

Because high concentration of surfactants, such as TBA^+ , have been observed to decrease the lifetime of ODS packed columns [51], the stability of the packing material contained in the column C_1 was checked periodically by measuring the amount of acetaminophen adsorbed onto the column from its aqueous solution at the concentration of $2.084 \times 10^{-5}\text{M}$. The procedure is the same as that described for NBS^- in section 2.4.4 except that the wavelength of the detector D was set at 244nm to have a maximum response for acetaminophen.

2.5 Solvent Extraction/Flow Injection Analysis

for Off-line Determination of TBA⁺

2.5.1 Principles of SE/FIA

Ion pair solvent extraction has been an extremely important technique for analysis of ionic surfactants [52,53,54]. It usually involves forming an ion pair between the surfactant and a colored ion-pairing reagent in an aqueous solution, and extracting it into a water-immiscible solvent followed by photometric measurement. One such example is the determination of quaternary ammonium ions reported by Schill et al [55]. In their experiment, picrate ion was used to form ion pairs with the quaternary ammonium ions which are extracted into dichloromethane. Determination of the concentration of ion pairs in the organic solvent is done by measuring absorbance at 375nm.

Liquid-liquid solvent extraction was automated into a flow injection analysis configuration by Karlberg and Thelander [56] and by Bergamin et al [57] in 1978. This technique, now usually referred as Solvent Extraction/Flow Injection Analysis (SE/FIA), has been widely used ever since. In a simple ion pair SE/FIA system [58,59], a sample is introduced into a flowing aqueous phase using an injection valve. The aqueous phase usually contains an excess of colored ion-pairing reagent. Then the aqueous phase is merged with a flowing organic phase at a "tee" or other shaped junction to produce alternating small segments of organic and aqueous phases which flow through an extraction coil. The flow of the two streams must be constant and steady, which can be achieved by using a peristaltic, constant pressure, long stroke piston or reciprocating pump. The sample, occupying many aqueous segments, will extract into the adjoining organic segments as it moves along the extraction coil. The two-phase flow will then enter a phase

separator, which allows a portion of the organic phase to enter a flow-through detector. Some property of the sample (i.e. UV absorbance) is monitored by the detector.

The phase separator is the key to the solvent extraction/FIA technique. Porous membrane phase separators, based on the selective permeability to the phase which wets the membrane material, have been shown to have some advantages over other types of separator [58,59] : they are compatible with high flow velocities, and their small internal volume reduces bandbroadening.

Although ion pair SE/FIA has been successfully used as a direct on-line liquid chromatography detector for analyzing ionic surfactants [60,61] , it is used off-line in the presented work.

2.5.2 Apparatus and Procedure

A schematic diagram of the SE/FIA system is shown in Fig.2-6. All the solvents and reagent solution are contained in 2-liter reagent bottles, which are inside four sealed aluminum containers (made by department machine shop). Constant pressure from a nitrogen tank was applied to the four containers to produce solvent flow, which can be stopped by using valve V1 (part no.CAV2031, Laboratory Data Control (LDC), Riviea Beach, FL).

When the system is working, the water flows first through sample injection valve V3 equipped with a 50 μ L loop (Cheminert R-6031 SWP, LDC) before joining the aqueous reagent (picrate solution) stream at a Tee-fitting T1 (part no. CJ-3031, laboratory Data Control, Riviea Beach, FL). The combined aqueous stream then joins the chloroform stream at Tee-fitting T2, and the resulting stream passes through an extraction coil, in which extraction of the ion pairs occurs between the aqueous and the chloroform phases. Then part of the chloroform is separated from the aqueous/chloroform stream using two

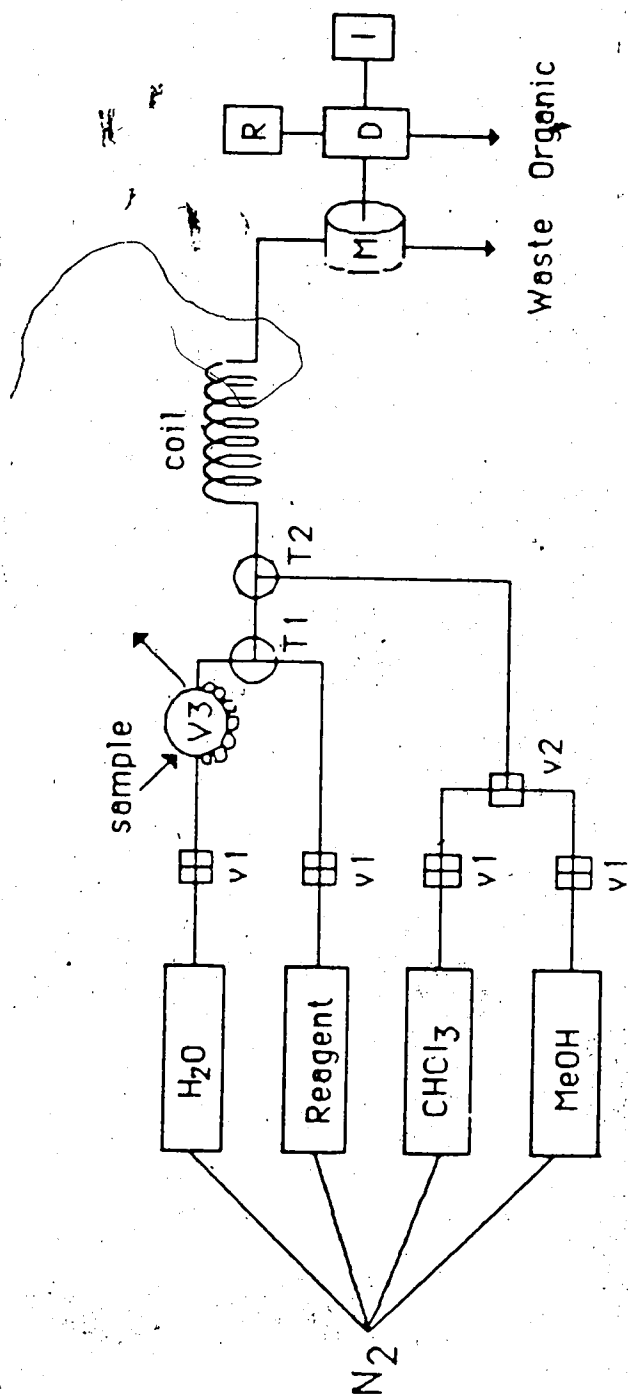


Figure 2-6 The solvent extraction/flow injection analysis system for determination of TBA^+ . Nitrogen gas is for producing constant pressure, $V1$ and $V2$ are three-way valves, $V3$ is the injection valve, M is the membrane phase separator, D is a UV detector (365nm), I is an integrator, and R is a strip chart recorder.

layers of porous Teflon membrane with a pore size of 10-20 μ m (Zitex, part no. E249-122, Chemplast Inc., Wayne, NJ) inside the phase separator M. Finally the chloroform passes through a spectrophotometric detector D (Sp 8200, Spectra-Physics, Santa Clara, CA). Methanol was used to wash out the system at the end of the day.

Important parameters for the assay were as follows: volume of injection loop: 50 μ l; total chloroform flow rate: 1.4ml/min; total aqueous flow rate: 1.1ml/min; chloroform flow rate through the membrane: 0.5ml/min; extraction coil length: 1.5m; wavelength of the UV detector: 365nm; nitrogen pressure: 30psig.

2.5.3 Reagent and Standard Solutions

The reagent solution contained 0.01M sodium picrate. Its pH was adjusted to 5.0 by adding about 0.5ml of acetic acid/acetate buffer and its ionic strength was adjusted to 0.10 with sodium chloride..

A series of standard TBA⁺ solutions were prepared by pipetting different volumes of its stock solution into 50ml volumetric flasks, and adding a mixture of methanol/water(1:1v/v) to the calibration marks. The concentration of these TBA⁺ standards ranges from 1x10⁻⁴M to 1x10⁻³M.

2.6. Surface Tension Measurement with Wilhelmy Balance

Surface tension of aqueous solutions was studied as a function of the concentration of TBA⁺Cl⁻ at a constant ionic strength of 0.50 in order to determine if TBA⁺Cl⁻ forms micelles in the solutions.

2.6.1 Principle of the Method

It is well known that some ionic surfactants and amphipathic surfactants start to form clusters when their concentration is above a certain value in an aqueous solution. These clusters are called micelles, and the threshold concentration at which micellization begins is known as the critical micelle concentration (CMC) of the surfactant. When increasing the concentration of the surfactant, several properties of the solution show a discontinuity at the CMC. The plot of surface tension of the solution vs logarithm of concentration of the surfactant, for example, displays a "break" at the CMC of the surfactant, as shown in Fig.2-7 for a hypothetical case of a micelle-forming surfactant. The CMC value usually decreases with increasing ionic strength [62,63] .

The Wilhelmy plate method is one of the most commonly used methods to measure surface tension of solutions. Fig.2-8 represents a thin vertical plate suspended at a liquid surface from the arm of a tared balance. The manifestation of the surface tension and contact angle in this situation is the entrainment of a meniscus around the perimeter of the suspended plate which is made to just contact the liquid surface. Assuming the apparatus is balanced before the liquid surface is raised to the contact position, the imbalance that occurs on contact is due to the weight of the entrained meniscus. Since the meniscus is held up by the tension on the liquid surface, the weight measured by the apparatus can be analyzed to yield a value for the surface tension γ .

The observed weight, w , of the meniscus must equal the upward force provided by the surface. This upward force equals the vertical component of the surface tension. So at equilibrium

$$w = P \gamma \cos \theta$$

(2-3)

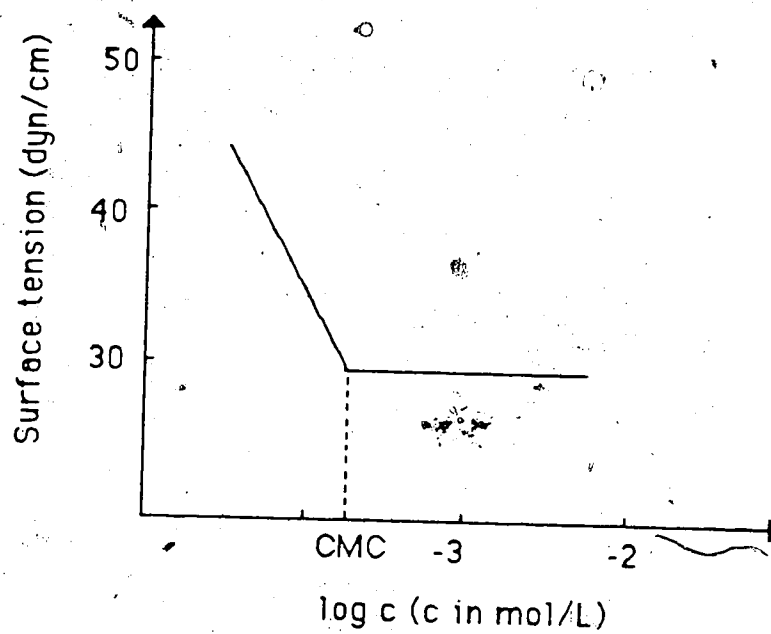


Figure 2-7 A hypothetical plot of surface tension versus logarithm of concentration for a micelle-forming surfactant. Note the "break" at the CMC.

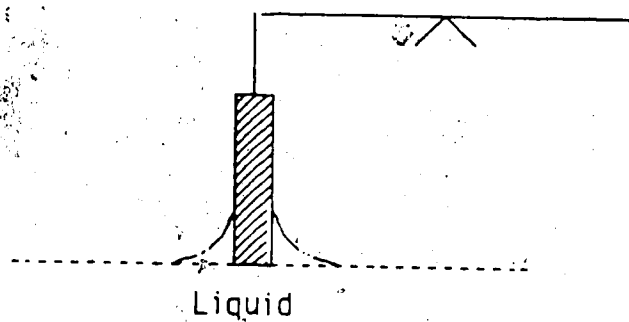


Figure 2-8 Schematic illustration of Wilhelmy Plate method for measuring surface tension of solution.

where θ is the contact angle, P is the perimeter of the plate. For a plate of rectangular cross section having length l and thickness t , then $P = 2(l+t)$. Equation 2-3 can be rearranged as:

$$\gamma = \frac{w}{P \cos \theta}$$

(2-4)

The values of θ is assumed to be constant, independent of solution composition, so that the measured value of w is directly proportional to γ . The proportionality constant $(P \cos \theta)^{-1}$ is obtained by measuring γ of pure water, which is known to be 71.97 dyn/cm at 25°C [64]. A plot of surface tension vs. concentration of TBA^+Cl^- can be obtained by measuring γ at several different concentrations of TBA^+Cl^- .

2.6.2 Apparatus and Procedure.

The balance used in the study is a Cahn R-100 Electrobalance (Cahn Instrument Inc., CA). The plate is made from platinum with dimension of 2.593cm long x 0.0109cm thick. Its height is irrelevant.

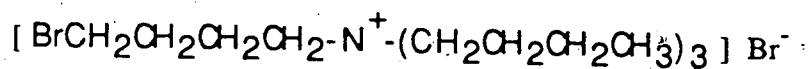
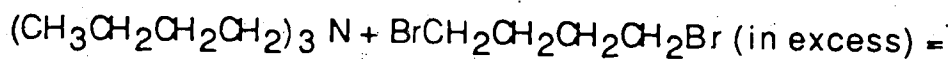
A series of aqueous solutions of TBA^+Cl^- , covering the concentration range of 0.0001- 0.02M at an ionic strength of 0.5 adjusted with NaCl, were prepared in 50ml volumetric flasks. They were poured into a series of Petri dishes (diameter 10cm) for the measurements.

The platinum plate was adjusted to just touch the surface of the solution, the weight difference of the plate after and before the touching was recorded by a recorder. The plate was heated in a Bunsen burner flame for a minute or so and cooled to room temperature before each measurement in order to remove any grease. The balance was calibrated with pure water.

2.7 Instrumental Neutron Activation Analysis (INAA)

It has been suggested that when large organic ions, such as TBA^+ , are present in the mobile phase for a silica-based bonded column, "even when no more hetaeron can be detected in the eluate, this is not always a guarantee that all of the hetaeron has been removed from the column packing" [9]. Several authors have pointed out the difficulties of quantitatively washing-off the strongly adsorbed pairing-ions [65-69]. Dreux and co-workers [69] reported that surfactants (pairing-ions) can be irreversibly adsorbed onto their C18 columns. Knox et al [65] reported that lauryl sulphate could not be washed off completely from the packing material with pure methanol or isopropanol. Van Der Houwen and co-workers [46] showed that pairing-ions sorbed by an ion-exchange process to the residual silanols on the ODS surface could not be removed by eluent containing no suitable electrolytes. Tomlinson et al [68] used solutions containing strongly adsorbed anions to remove alkylbenzyltrimethylammonium compounds from the column.

In order to make sure that the elution of TBA^+ from column C₁₈ (Fig.2-5) is complete within 25ml of the eluent in the experiment described in 2.4.4, the amount of "residual" TBA^+ on the ODS packing after the elution was determined with the technique of instrumental neutron activation analysis (INAA). To take advantage of the extremely high sensitivity of INAA for bromine, an analogue of TBA^+ was synthesized in the following way [70]:



This ion (TBABr^+) was used as a substitute for TBA^+ in the experiment. Since it is even more strongly sorbed than TBA^+ onto the ODS packing material it is reasonable to assume that if TBABr^+ is completely eluted then TBA^+ will also be completely eluted.

2.7.1 Principle of INAA

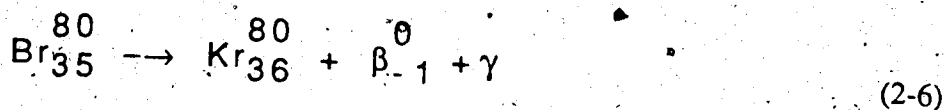
Neutron activation analysis is one of the radiochemical methods of analysis for elements [71]. In this technique a nonradioactive sample is bombarded with neutrons which induce radioactivity for some elements of the sample, then the radiation emitted from the sample is measured. The most important advantage of the technique is its high sensitivity to certain elements.

When a nucleus of an atom is bombarded with a neutron, the incoming neutron can be absorbed by the target nucleus, forming a new nuclide with the same atomic number as the parent nuclide, but one unit higher in mass number. For example:



An amount of energy equal to the binding energy of the neutron in that nucleus plus the kinetic energy of the incoming neutron is then available to raise the product nucleus to an excited state. There are two major ways in which the nucleus in excited state can release this excess energy: (1) it may radiate γ -rays, or (2) it may emit one or more nuclear particles (β -ray, protons, etc). If sufficient energy is available, then both of them can take place.

One example is



The half life of the reaction is 17.6 minutes. One important feature of such reactions is that the γ -ray spectrum is unique for every different reaction, and can be used as a fingerprint in an analysis.

In a typical neutron activation analysis experiment, the flux density (usually $10^{11} - 10^{13} \text{ n/cm}^2\text{-sec}$) of neutrons (usually thermal neutrons) from a nuclear reactor is held constant. The samples and standards are exposed to the neutron flux for a known length of time. They are then allowed to "cool" for a definite length of time so that short-lived interfering isotopes decay away. They are counted for a fixed length of time and at the appropriate energy with a γ -ray spectrometer. The total counts are directly proportional to the amount of the element present in the sample. The analysis of an element is accomplished through comparing the total counts of the sample with a calibration plot of total counts vs. amount of the element, which is obtained from the standards at the same energy and for the same length of time.

2.7.2 Synthesis of $\text{TBABr}^+\text{Br}^-$

A quantity of 2 grams of tri-n-butylamine was mixed with 8 grams of 1,4-dibromobutane and 2ml methanol. This mixture was refluxed for 48 hours (the color changes from yellowish to dark brown). The methanol was evaporated using a rotatory evaporator. It left a dark brown viscous oil. To this oil was added 5ml of n-hexane. The mixture was warmed to $\sim 60^\circ\text{C}$ and ethyl ether was added dropwise with swirling until the oil dissolved. This solution was held at -5°C for about 2 days, after which time light yellowish crystals had formed. The crystals were again dissolved in the mixed solvent for a 2nd recrystallization. The resulting white crystalline material was vacuum-dried for 24 hours. Yield of the reaction was $\sim 40\%$. Its elemental analysis is given in Table 2-1.

Table 2-1 Result of the elemental analysis for TBA^+Br^-

Element	Actual Content %	Theoretical Content %
N	3.12	3.49
C	49.9	47.9
H	8.57	8.73
Br	38.5	39.9

The Fast Atom Bombardment mass spectrum of the material clearly shows the peak of TBA^+Br^- at 321 m/e.

2.7.3 Column Equilibration and Elution.

In this experiment, the on-line detector system (shown in Fig.2-5) was disconnected from the valve V1 at the point C. All the apparatus is the same as that described in section 2.4.2. The equilibration and elution procedures were the same as that described in section 2.4.4.

The sample solution has $2.88 \times 10^{-3} \text{ M}$ TBA^+Br^- , and an ionic strength of 0.05 adjusted with NaCl. A blank solution was prepared to have $2.88 \times 10^{-3} \text{ M}$ TBA^+Br^- and an ionic strength of 0.05. The purpose of the blank solution is to ensure that the inorganic Br^- anion is eluted completely from the column so that any Br detected by INAA is due to that in TBA^+Br^- . The eluent is the same as that used in section 2.4.3.

The ODS packing in the column (~ 15mg) was then transferred into a polyethylene vial and dried at the room temperature for a day. The vial was then sealed and ready for INAA. Obviously, a fresh ~ 15mg packing of the ODS was used for each experiment. The weight of ODS was measured accurately for each column.

2.7.4 Preparation of Standards

Standards for the analysis were prepared from an aqueous solution of NH_4Br . To a series of polyethylene vials containing 10-13mg of the ODS, different volumes of the standard solution were pipetted. To make the ODS wettable to the aqueous solution, 2 or 3 drops of methanol were added to the vials after adding the aqueous solution. The ODS material in the vials was then allowed to dry for a day in the air. Finally all the vials were sealed.

2.7.5 Irradiation and Counting

The Irradiation and counting operations were carried out at the SLOWPOKE II reactor facility of University of Alberta. All Samples and standards were irradiated for 5.00 minutes at a flux of $\sim 10^{12}$ n/cm².sec. and then allowed to cool for 2.00 minutes. The 619 kev γ -ray peak for ^{80}Br ($t_{1/2} = 17.7$ minutes) was then counted for 5.00 minutes.

2.8 Other Apparatus

pH measurements were made with a Fisher Accumt Model 525 Digital pH meter. Chemicals were weighed with a Fisher Gram-ATIC balance. A Haake circulating thermostat Model R20 was used to provide a constant temperature of $25.0 \pm 0.5^\circ\text{C}$ for both the sample solutions and the column packed with the ODS packing material. The Fisher Recordall Series 5000 stripchart recorder was used to record the signals.

Chapter 3

Adsorption Of The Organic Ions NBS^- And TBA^+ Onto ODS Packing

3.1. Introduction

It is possible to separate ionic organic compounds by conventional reverse-phase chromatography with chemically bonded ODS stationary phase [12,72,73] but it is rarely done. The separation is mostly carried out today with ion-pair reverse-phase chromatography. In either case, the adsorption of organic ions, either the sample ion or the pairing-ion, from the mobile phase onto the stationary phase is involved. It is of both theoretical interest and practical importance to study and understand the adsorption of an organic ion onto the stationary phase from solution.

Adsorption of organic solutes (either neutral or ionized) onto various solid surfaces from solution (mainly aqueous), in general, has been a subject of wide study for quite a long time because of its major technological and commercial importance. Both its theoretical and experimental aspects are well established [38,39,74]. For nonpolar adsorbents, such as the graphitized carbons or a copolymer such as the Hamilton PRP-1, it is generally believed that the main "attractive" forces between the solute molecule and the surface are dispersion forces [39,74]. Because these "attractive" forces are relatively weak, solvent-solute interactions, solvent-solvent interactions and solvent structure (entropy) effects can account for a significant amount of the energy associated with adsorption of solutes from aqueous solution onto nonpolar adsorbents.

The adsorption of organic solutes onto chemically bonded phases, such as the octadecylsilyl (ODS), from various solvent systems is a more recent and rather limited subject of study [25,27,21]. It is well known that organic ions can be sorbed onto the

chemically bonded ODS packing. But there are quite different views about the origin of the "sorption". Some workers [75,76,77] considered it as a partitioning process between the bonded hydrocarbonous "liquid layer" and the bulk solution. Others [78,79,80] suggested that it is a solid/liquid adsorption process. Scott and Kucera [81,82] argued that, when the mobile phase is an aqueous/organic solvent mixture such as water/methanol, it is a partitioning process between the bulk solution and a layer of organic solvent over the surface of the nonpolar sorbent. Horvath and Melander [72,12,83] proposed that, whatever process occurring at the interface, the sorption is essentially due to the "hydrophobic and/or solvophobic effect" from the bulk solution. This is often referred to as the solvophobic theory.

The solvophobic theory has been the most popular theory used to describe the sorption of solutes onto the chemically bonded phases from polar solutions, and has been reviewed in detail [25]. It treats the adsorbent (e.g. ODS packing) as a "passive acceptor" rather than an "active attractor" for the solutes. The surface of the ODS packing is considered to be covered with alkyl chains, so the only attractive forces between an organic ion and the surface are dispersion forces. These forces are considered to be very weak compared with the "hydrophobic effect" from aqueous solution. The "hydrophobic effect" originates from a net "repulsion" between water and the bonded nonpolar hydrocarbonaceous chains as well as the nonpolar moiety of the organic ion. The tendency of water to reduce the nonpolar surface area of the organic ions in contact with it is mainly responsible for the sorption.

The sorption process has been quantitatively described with the "solvophobic theory" by considering different free energies associated with the solute-sorbent, solvent-solute and solvent-sorbent interactions. After combining all the free energy contributions, the following equation has been derived:

$$\ln K_S = \frac{1}{RT} [\Delta A(N\gamma + a) + NA_s\gamma(k^e - 1) + W - \frac{\Delta Z}{\epsilon}] + \ln \frac{RT}{P_0V} \quad (3-1)$$

where K_S is the distribution coefficient of the organic solute; W and a are solvent-dependent parameters (measurable); R = gas constant; T = temperature; ΔA = change in exposed surface area of ligand (the bonded chain) and the organic ion before and after the sorption; N = Avogadro's number; γ = surface tension of the solution; A_s = surface area of the solvent molecule; k^e = correction factor adjusting surface tension from macroscopic to molecular level; ϵ = dielectric constant of the solvent; ΔZ = term of electrostatic interaction in the solution; $\ln(RT/P_0V)$ = free volume change term. The main parameters in the equation are surface tension (γ) and change in contact area term (ΔA).

The "solvophobic theory" is, by and large, quite successful in explaining the sorption behavior of nonionic solutes onto the chemically bonded phases, especially from neat-aqueous solutions [25,72,12,84,85]. For example, the linear relationship between $\ln K_S$ and the chain length of organic solutes (homologous series plots) can be easily explained with equation 3-1. However, it cannot account for the adsorption behavior of certain compounds, such as the extremely long retentions and the excessive peak tailing of amine compounds specially in organic-rich mobile phases [30,31,32] and the increase of the amount of quaternary ammonium ions adsorbed onto ODS phases with increasing pH of the solutions [44,45,86]. The failure was believed to be caused by its neglect of the accessible residual silanol groups on the chemically bonded surface. Therefore, Horvath and co-workers [34,35] added another term to the equation to account for all the possible interactions (ion-exchange or H-bonding) between the accessible residual silanols and the solute molecules. The significance of these "silanophilic" interaction has been suggested to depend on (i) the surface coverage of the ODS packing [87]; (ii) pH of the solutions [46]; (iii) nature of the solvent [34,35,36]; and (iv) nature of the solutes [30,31,32].

The effect of the concentration of inert salts on the sorption of ions onto reverse-phase packing materials is of particular interest here. Horvath and co-workers [12] reported that the amount of organic ions adsorbed onto an ODS phase from solution decreases first and then increases with increasing ionic strength of the solutions, and the adsorption reaches a minimum when ionic strength equals approximately 0.3. They explained that the first decrease was due to the decrease in electrostatic interaction (ΔZ in equation 3-1) in solution while the increase was due to the increase in surface tension (γ) when ionic strength increases in the solutions. However, the decrease they observed was very likely caused by the silanophilic interaction between the organic ions and the accessible residual silanols on the ODS surface and the solvophobic-silanophilic theory is generally less suitable for explaining the sorption of ions onto ODS packing than for nonionics.

The extent of adsorption of organic ions onto a nonpolar sorbent usually increases with increasing concentration of inert electrolytes or ionic strength in the solutions. Pietrzyk and Chu [88,89] suggested that "ion-pairing" might account for this increase. It was also suggested that "salting-out" might be responsible for the phenomena [90]. Rudzinski et al [84,85] and others [91,92] explained that the increase is due to the decrease in "Donnan expulsion" in the pores of the ODS packing when ionic strength increases. It was suggested that organic ions can be excluded from the pores of the ODS packing at low ionic strength presumably because of the existence of electrical charges on the surface. The charges may arise from either ionization of the residual silanol groups on the ODS surface or adsorption of the "first few molecules" of the organic ion. Bidlingmeyer et al [93] suggested that the increase is caused by the decreasing charge repulsion between the adsorbed organic ions on the surface when ionic strength increases. Cantwell and Puon [94] have quantitatively explained this increase in terms of the Stern-Gouy-Chapman electrical double-layer theory. The organic ion can be adsorbed onto the hydrophobic

surface and creates a net charge on the surface. This net surface charge is balanced by an excess of its inorganic counterion in the adjacent solution. It was assumed that the surface potential created by the adsorbed ion is a constant when the solution activity of the ion is fixed. So when ionic strength is increased by adding more inert electrolyte (e.g. NaCl) to the solution while maintaining the solution activity of the organic ions constant, the number of the counterions in the diffuse layer will increase. Consequently, more of the organic ion must be adsorbed onto the surface in order to keep the electroneutrality in the double-layer region.

Ever since the concept of electrical double-layer theory was introduced into the field, it has been widely cited in the literature for explaining retention of ions in reverse-phase chromatography [20,46,50,18,65, 94-113]. The electrical nature of the ODS/eluent interface has been examined by Knox and co-workers [65] through measuring the zeta potential on the ODS particles onto which octylsulphate ions have been adsorbed. Weber et al [98] reported a method for estimating values of the surface potential on an ODS stationary phase, onto which organic ions (e.g. tetrabutylammonium) have been adsorbed, by comparing retention capacity factors of certain solutes on the column. Deelder and co-worker [50] found that the adsorption of alkylsulphonates onto ODS packing from solution could be quantitatively described by the electrical double-layer theory. Based on the electrical double-layer theory, Stahlberg [111] recently derived some theoretical equations for describing the sorption isotherm of organic ions onto nonpolar packing materials from solution. Pietrzyk et al [100,102,105] supported the concept of the electrical double-layer by showing a linear relationship between the inverse of the capacity factor of organic ions onto reverse-phase stationary phases and the reciprocal of the square root of ionic strength of the mobile phase, which was predicted by the electrical double-layer model.

In the present study, adsorption of an organic ion (either a cation or an anion) onto an ODS packing material from aqueous solution was studied by measuring its sorption

isotherms as a function of ionic strength using the column equilibration technique. The influence of ionic strength on the sorption isotherms was then explained quantitatively in terms of the Stern-Gouy-Chapman electrical double-layer theory.

3.2 Theory

3.2.1 The Electrical Double-Layer at the Interface

As discussed before, organic ions can be sorbed onto the surface of chemically bonded ODS phase. While it is not at all critical to the approach taken in this thesis whether the process is "partitioning" or "adsorption", the close association of a solute molecule with the ODS/solution interface will be called "adsorption" in order to distinguish this kind of sorption process from "ion exchange" which is discussed in Chapter 4. Since the surface of a well "end-capped" ODS is basically nonpolar, it is assumed that there is no coulombic (electrical) interaction between the surface and the adsorbed organic ions. In other words, there are not significant amounts of accessible residual silanol groups on the ODS surface. The description of the electrical double-layer presented in this section is largely taken from references 94 by Cantwell and Puon, and from references 95 and 96 by Cantwell.

Fig.3-1 shows the interfacial region between the surface of an ODS packing and a solution which contains an organic ion (P^+), present as the Cl^- salt, and an indifferent electrolyte (e.g. $NaCl$). Since the pores size ($\sim 80\text{\AA}$) in the ODS particle are much larger than that of small organic ions, such as tetrabutylammonium, it is assumed that the surface inside the pores is flat. The adsorbed P^+ ions are assumed to all be in the same plane, regardless of whether that plane lies at the outer boundary of, or within, the chemically bonded alkyl layer. The adsorbed organic ion, usually referred to as the potential

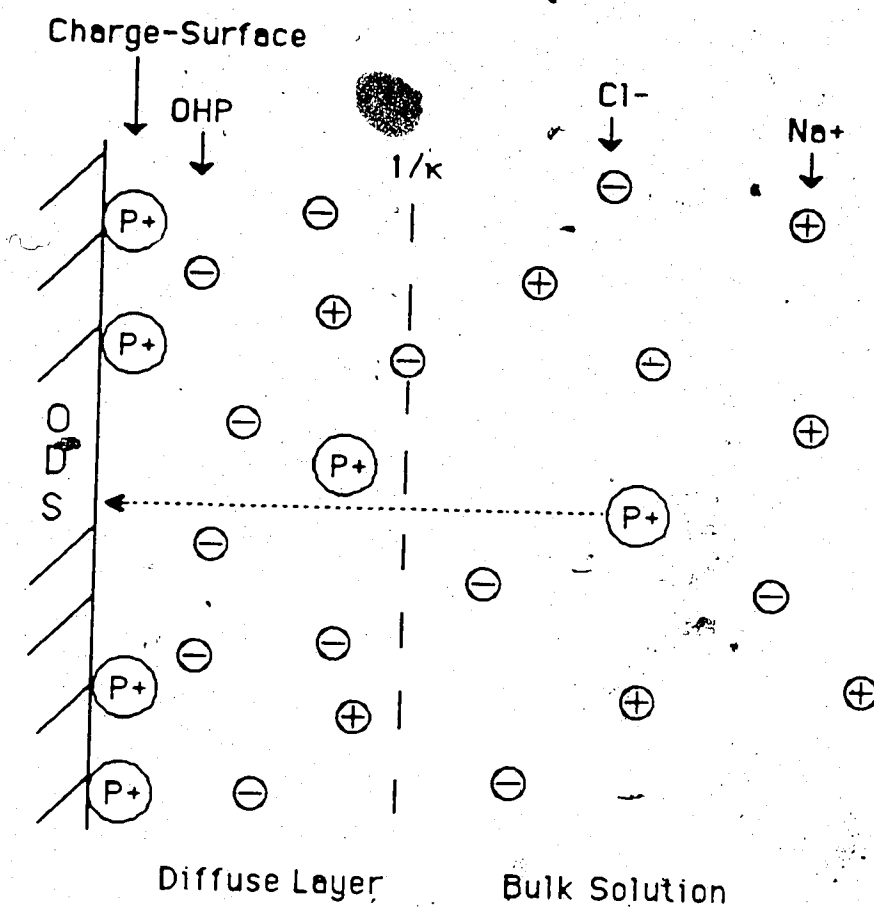


Figure 3-1 The electrical double-layer at the ODS/solution interface due to the adsorption of organic ion P^+ onto the surface of chemically bonded ODS packing from solution.

determining ion in electrochemistry, is responsible for the electrical potential difference, Ψ_0 , between the surface and the bulk solution. Since overall electrical neutrality must be maintained, the net charge on the surface created by the adsorbed ions must be balanced by an exactly equal net charge of opposite sign on the solution side. This is usually referred to as the electrical double-layer. The distribution of the neutralizing ions (e.g. Cl^- , usually called counterions) in the solution side can be described by the Stern-Gouy-Chapman (SGC) theory [114,115].

The relationship between the activity of the potential determining ion in the bulk solution, a_{P^+} , and the surface potential, Ψ_0 , is given by the Nernst equation [149, 164]

$$\Psi_0 = k + \frac{RT}{Z_+ F} \ln a_{P^+} \quad (3-2)$$

where R is the ideal gas constant ($8.314 \text{ C} \cdot \text{V} \cdot \text{mol}^{-1} \text{ K}^{-1}$); F is the Faraday constant ($96,487 \text{ C eq}^{-1}$); T is the absolute temperature; Z_+ is the charge number on the P^+ and k is a constant. In the present treatment it is not necessary that equation 3-2 be valid, but only that, regardless of their functional relationship, Ψ_0 is constant at constant a_{P^+} .

The charges of the adsorbed ions are considered to be smeared out on the surface, with a plane passing through them identified as the charge-surface. The surface charge density, σ_0 , is given in unit of coulombs per cm^2 . It is assumed that the counterion (e.g. Cl^-) is not "specifically adsorbed" to the charge-surface, and can only approach the charge-surface to within about a hydrated ionic radius. This plane of closest approach of the counterions is called the Outer Helmholtz Plane (OHP).

The electrical double-layer at the interface can be divided into two parts, the compact part and the diffuse part. The compact part extends from the charge-surface to the OHP. Its thickness, d , in a given system of adsorbent and an inert electrolyte, is

essentially a constant. The compact layer is considered to be an electrical capacitor with constant thickness and constant specific capacitance, C_1 :

$$C_1 = \frac{\sigma_0}{\Psi_0 - \Psi_{OHP}} \quad (3-3)$$

The charge-surface acts as one plate (potential Ψ_0) of the capacitor and the OHP (potential Ψ_{OHP}) as the other. The decay of the electrical potential across the compact layer is linear.

The diffuse part of the double-layer includes the OHP and extends from it to the bulk solution. The diffuse layer can also be treated as a capacitor, with the OHP as one plate and a hypothetical plane located in the diffuse layer at a distance of $1/\kappa$ from the OHP as the other. $1/\kappa$ is the distance at which the electrical potential has the value of $\frac{\Psi_{OHP}}{e}$ (where $e =$

2.787), and it can be considered as the thickness of the diffuse layer. In this layer the potential decays nearly exponentially. The value of $1/\kappa$ varies with ionic strength in the bulk solution. It decreases with increasing ionic strength of the bulk solution. That is, increasing ionic strength of the bulk solution causes compression of the diffuse layer.

The concentration of a species i in the interfacial region is expressed as its surface excess, Γ_i , which is the number of moles of i per square centimeter of surface and/or its adjoining layer in the solution, which are in excess of the moles of the same species contained in an "equivalent volume" of bulk solution. An equivalent volume of bulk solution is defined as containing the same total moles of charge of all species as there are in 1 cm^2 of the interface being considered. Obviously concentration of the counterion (e.g. Cl^-) is higher in the diffuse layer than in the bulk, and that of the co-ion (e.g. Na^+) is lower in the diffuse layer than in the bulk.

Based on the SGC theory it is possible to derive the following equation

$$\frac{1}{\sigma_o} = \frac{1}{C_1 \Psi_o} + \frac{1}{2.28 \times 10^{-4} c^{1/2} \Psi_o \left[\left(\frac{Z F \Psi_{OHP}}{2 RT} \right)^{-1} \sinh \left(\frac{Z F \Psi_{OHP}}{2 RT} \right) \right]} \quad (3-4)$$

where $Z=1$ and c is the ionic strength in the bulk solution.

The increase of adsorption of an organic ion onto a nonpolar sorbent increases with increasing ionic strength of the bulk solution as can be easily explained by the theory. At a fixed activity of the organic ion in the solution, Ψ_o and C_1 are constant. The correction

term, $\left(\frac{Z F \Psi_{OHP}}{2 RT} \right)^{-1} \sinh \left(\frac{Z F \Psi_{OHP}}{2 RT} \right)$, is relatively constant under the condition. It

is obvious, from equation 3-4, that σ_o increases with increasing c .

Equation 3-4 predicts a simple straight line plot of

$$\frac{1}{\sigma_o} \text{ vs. } \frac{1}{c^{1/2} \left[\left(\frac{Z F \Psi_{OHP}}{2 RT} \right)^{-1} \sinh \left(\frac{Z F \Psi_{OHP}}{2 RT} \right) \right]} \quad (3-5)$$

under such conditions where Ψ_o is constant (achieved by fixing the activity of P^+ in bulk solution). Also, if this plot is repeated at several different Ψ_o , then the ratio of the intercept to the slope should be the same for each plot and should have the value of $2.28 \times 10^{-4} / C_1$. From the slopes and intercepts of these plots, it is possible to evaluate both Ψ_o and the capacitance of the compact layer C_1 with the following relations.

$$\Psi_o (\text{volt}) = \frac{1}{2.28 \times 10^{-4} \times \text{slope}} \quad (3-6)$$

$$C_1 \text{ (F/cm}^2\text{)} = \frac{1}{\Psi_0 \times \text{intercept}}$$

(3.7)

In the present study the surface excess, Γ_{P^+} , of adsorbed organic ions at various bulk concentration of P^+ are measured as a function of ionic strength (c) using the column equilibration technique. Applying equation 3-4 to such experimental data is not straightforward since the surface charge density σ_0 does not have a simple relation with the experimental measured surface excess Γ_{P^+} . The charge density σ_0 arises from only those P^+ which are adsorbed on the surface, while the experimentally measured Γ_{P^+} includes all of the P^+ in the double-layer region, both those adsorbed on the surface and, in a negative sense, those which have been expelled from the diffuse layer. Let $\Gamma_{P^+}^{AD}$ stand for only the surface excess of P^+ due to that adsorbed on the surface. The charge density σ_0 is then directly proportional to $\Gamma_{P^+}^{AD}$.

$$\sigma_0 = Z_+ F \Gamma_{P^+}^{AD}$$

(3-8)

The distinction between $\Gamma_{P^+}^{AD}$ and Γ_{P^+} is from the fact that the positive charge on the surface is balanced by some combination of both a positive surface excess of counterions (Cl⁻) in the diffuse layer Γ_{-}^{DL} , and a negative surface excess (i.e. deficiency) of positively charged co-ions, Na⁺ and P^+ , in the diffuse layer Γ_{+}^{DL} . So Γ_{P^+} is really the sum of $\Gamma_{P^+}^{AD}$ plus a negative-valued $\Gamma_{P^+}^{DL}$. To calculate σ_0 from Γ_{P^+} , the following iterative process is needed:

(i) as a first approximation assume:

$$\Gamma_{P^+}^{AD} = \Gamma_{P^+}$$

(3-9)

(ii) then calculate charge density by the equation:

$$\sigma_0 = Z_+ F \Gamma_{P^+}$$

(3-10)

(iii) for symmetrical Z:Z type electrolytes (e.g. P^+Cl^- or Na^+Cl^-) the value of Ψ_{OHP} can now be evaluated from the equation

$$\sinh\left(\frac{ZF\Psi_{OHP}}{2RT}\right) = 8.53 \times 10^4 \sigma_0 c^{-1/2}$$

(3-11)

where Z is the absolute value of the charge number.

(iv) the ratio of surface excess of the positive ions (Na^+ and P^+) to that of the negative ions (Cl^-) in the diffuse layer (at $25^\circ C$) is calculated from the equation

$$\frac{\Gamma_+^{DL}}{\Gamma_-^{DL}} = \frac{\exp(-19.47\Psi_{OHP}) - 1}{\exp(19.47\Psi_{OHP}) - 1}$$

(3-12)

(v) a better estimate of the charge density is obtained from the equation

$$\sigma_0 = Z_+ F \Gamma_{P^+} \left[\frac{\alpha - R}{\alpha - R(1-\alpha)} \right]$$

(3-13)

where

$$\alpha = \frac{[P^+]}{c}$$

(3-14)

$$R = \alpha \frac{\Gamma_+^{DL}}{\Gamma_-^{DL}}$$

(3-15)

The new estimate of σ_0 from equation 3-13 is used iteratively in steps (iii) to (v) until a constant value of σ_0 is obtained. Then Ψ_{OHP} can be calculated from equation 3-11. A simple computer program has been developed to do these calculations (see Appendix I and II).

Although the above equations are illustrated for cations, they are also valid for anions with appropriate sign changes.

3.2.2 The Adsorption Isotherms

Experimental data for adsorption of solutes onto solid adsorbent from solution is usually presented in the form of an adsorption isotherm [39,74]. It is a plot of the concentration of the compound on the solid, C_s (mol/kg), vs. the concentration in the solution, C_m (mol/L), under equilibrium conditions at a constant temperature. A typical adsorption isotherm is shown in Fig.3-2. At any point on the isotherm, the distribution coefficient of the solute is defined as

$$K_S = \frac{C_s \text{ (mol/kg)}}{C_m \text{ (mol/L)}}$$

(3-16)

Adsorption isotherms can have a variety of shapes depending largely on the adsorption mechanisms and experimental conditions. A general treatment and classification

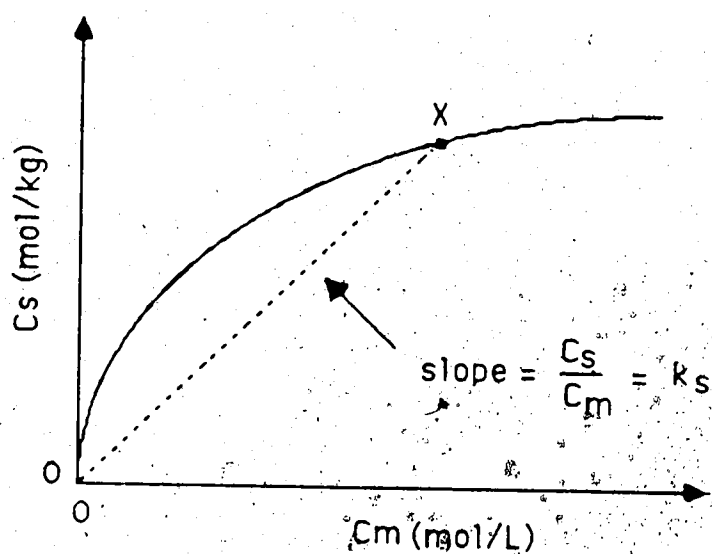


Figure 3-2 A hypothetical adsorption isotherm (the curved line). The distribution coefficient (k_s) at any point X is the ratio of C_s/C_m .

of adsorption isotherms has been given by Giles et al [148] and others [38,39,74]. The main classification is based on the initial shape of the isotherms. Of the four main classes of isotherms, the L-type and the H-type isotherms have commonly been observed for the adsorption of ionized compounds onto the ODS packing.

An important example of L-type isotherm is the Langmuir isotherm. In the Langmuir isotherm C_s initially increases nearly linearly with C_m then increases at a decreasing rate and eventually approaches a limiting plateau. It is described by the Langmuir equation:

$$\frac{1}{C_s} = \frac{1}{K C_{s,\max} C_m} + \frac{1}{C_{s,\max}} \quad (3-17)$$

where K is a constant, and $C_{s,\max}$ is the maximum adsorption capacity of the adsorbent. Plots of $\frac{1}{C_s}$ vs. $\frac{1}{C_m}$ yield straight lines. A number of workers [44,45,81,116,117]

have found that the adsorption isotherms of organic ions onto ODS packing materials follow this equation. The physical basis of the equation is the assumption that the solute molecules are adsorbed onto a limited number of active sites on the surface of the adsorbent, with the same adsorption energy, and eventually form a monolayer. However, often for solid/liquid adsorption, the above meanings cannot be assigned to the terms of the Langmuir equation and it must be considered a more-or-less empirical fit of the data [39].

H(high affinity)-type isotherms result from extremely strong adsorption of solutes onto some of the active sites of the adsorbent. The Freundlich equation is frequently used to describe this type of isotherm.

$$C_s = a C_m^b$$

(3-18)

where a and $b(<1)$ are constant. The Freundlich equation originates from a consideration of the heterogeneity of the surface when applied to the adsorption of vapors on solid sorbents [38,74]. This type of adsorption isotherm has also frequently been observed for adsorption onto reverse-phase packing material of relative large (e.g. long chain) organic ions from organic-lean solutions [107,118,49,93,67].

3.3 Results and Discussion

In this section, the adsorption isotherms of NBS^- and TBA^+ from aqueous solutions onto the ODS packing at five different ionic strengths, measured with the column equilibration technique, will be presented. Then the effect of ionic strength on the adsorption isotherms will be quantitatively described using the SGC theory. Since TBA^+ is more strongly adsorbed onto the ODS packing than NBS^- is, the column used for the measurements of TBA^+ contains only about 15mg of the ODS packing while that used for NBS^- contains 170mg. Both the equilibration and elution steps on the columns have been studied by measuring loading and elution curves, respectively. Completeness of elution of TBA^+ adsorbed on the ODS was investigated by determining the "residual" amount of TBA^+ on the ODS packing after elution, using the INAA technique. The silanophilic interaction between TBA^+ and the residual silanol groups on the ODS material has also been studied by measuring its adsorption isotherms at different values of pH. In order to determine if TBA^+ forms micelles in the ranges of concentration and ionic strength employed, surface tensions of its solutions have been measured with the Wilhelmy plate method.

3.3.1. Adsorption of p-Nitrobenzenesulfonate (NBS^-)

3.3.1.1. Adsorption Isotherms of NBS^-

Adsorption isotherms were measured as described in section 2.3. Each point on the isotherm was calculated via equation 2-2, which requires a knowledge of the void volume V_m . In the measurement of V_m , water is first pumped through the column until equilibrium between the two is reached. Verification of equilibrium involves pumping increasing volumes of water (i.e. 4ml, 6ml and 8ml) through the column C_1 before eluting with ethanol. The following values of V_m were found: $(218.6 \pm 3.0) \mu\text{l}$ for 4ml, $(213.4 \pm 3.7) \mu\text{l}$ for 6ml and $(218.2 \pm 4.7) \mu\text{l}$ for 8ml (all at 95% confidence level), showing that equilibrium was achieved when less than 4ml water was pumped through the column. To be on the safe side 10.0ml was used in all the subsequent experiments.

The void volume for the system shown in Fig. 2-3 was measured to be $(211.9 \pm 4.2) \mu\text{l}$ (at 95% confidence level). The GC calibration curve used for the water determinations is given in Fig. 3-3.

Equilibration of the ODS column with the sample solution of NBS^- has been verified by pumping increasing volumes (i.e. 6ml, 8ml and 10ml) of the sample solution, which contained $1.009 \times 10^{-4} \text{ M}$ of NBS^- with ionic strength of 0.100, through the column before switching to the elution step, and subsequently determining the number of moles of NBS^- in the column. It was found that the total number of moles of NBS^- ($n_{\text{T},\text{NBS}^-}$) was: $(1.64 \pm 0.02) \times 10^{-8}$ for 6ml, $(1.66 \pm 0.02) \times 10^{-8}$ for 8ml and $(1.65 \pm 0.02) \times 10^{-8}$ for 10ml, showing that equilibrium was reached in less than 6ml. 10ml was used for all the subsequent experiments.

The completeness of elution of NBS^- from the column was verified by first loading the column using 10ml of the NBS^- solution and then eluting with either 4ml, 6ml or 8ml

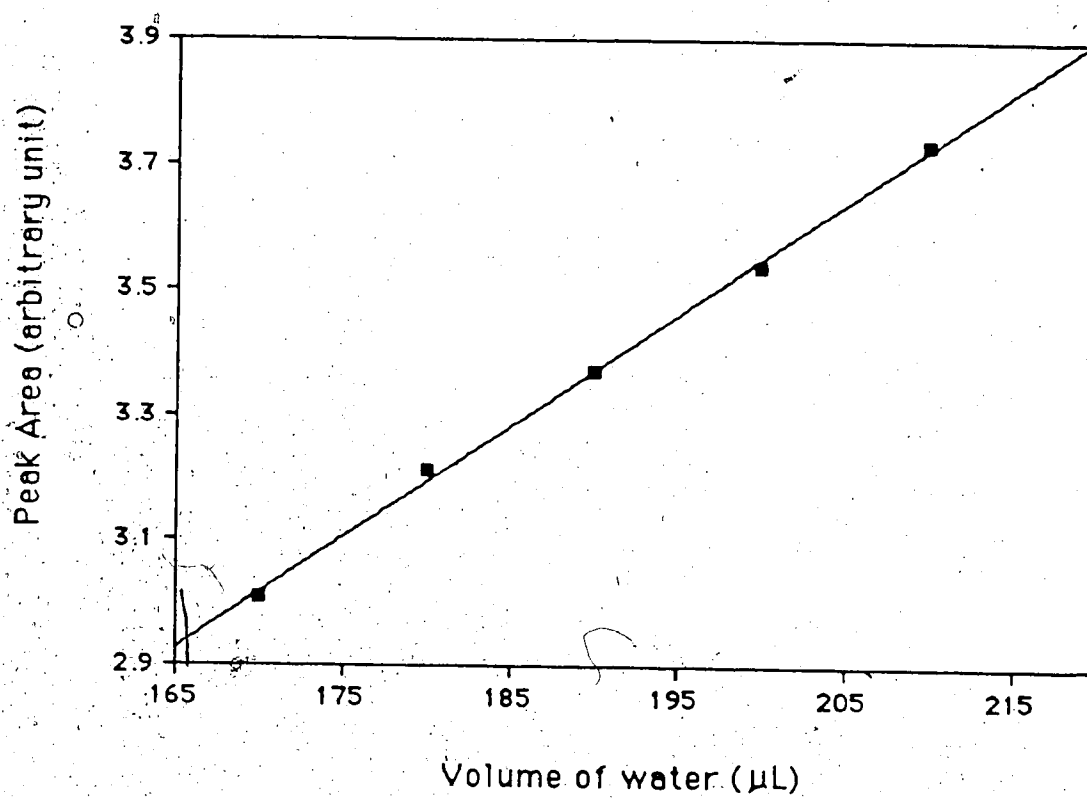


Figure 3-3 The GC calibration curve of water for the determination of void volume in the system shown in Fig.2-3. (see section 2.3.5 for experimental details)

of the eluent. The amount of NBS^- in the collected eluent was quantified by measuring the absorbance of the solution at 266 nm. It was found less than 6ml was enough. In the subsequent experiments, 10ml was always used. A calibration curve of absorbance vs. concentration (mol/L) of NBS^- has been done. It has a slope $(1.006 \pm 0.003) \times 10^4$ and an intercept of $(0.003 \pm 0.003) \times 10^4$.

The adsorption isotherms of NBS^- at five different ionic strengths are presented in Fig.3-4, and the data are given in Table 3-1. Surface excess, Γ_{NBS^-} (moles/cm²), instead of surface concentration is used in these plots for convenience of the calculation. The surface excess, Γ_{NBS^-} , can be calculated from the surface concentration, C_s , by the equation

$$\Gamma_{\text{NBS}^-} (\text{mol/cm}^2) = \frac{C_s (\text{mol/kg})}{A_{sp} (\text{cm}^2/\text{kg})} \quad (3-19)$$

where $A_{sp} = 3.09 \times 10^9 \text{ cm}^2/\text{kg}$.

It was found that the experimental data fit the Langmuir equation

$$\frac{1}{\Gamma_{\text{NBS}^-}} = \frac{1}{K C_{m,\text{NBS}^-} \Gamma_{\text{NBS}^-, \max}} + \frac{1}{\Gamma_{\text{NBS}^-, \max}} \quad (3-20)$$

where K is a constant, $\Gamma_{\text{NBS}^-, \max}$ is the constant corresponding to the maximum surface excess (monolayer coverage) of NBS^- on the surface and C_{m,NBS^-} is the solution concentration (mole/L) of NBS^- .

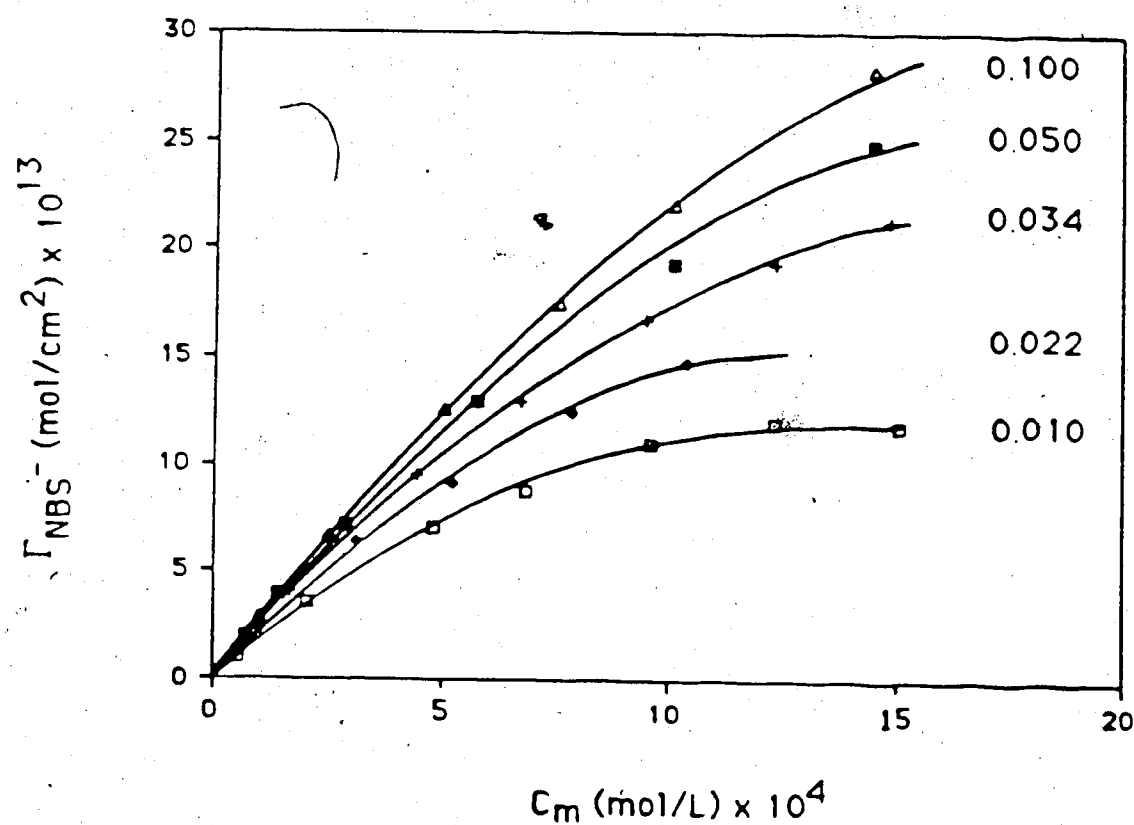


Figure 3-4 Adsorption isotherms of p-nitrobenzenesulfonate (NBS⁻) on chemically bonded ODS packing from aqueous solutions at various ionic strength and at 25°C.

Table 3-1 Experimental data of adsorption isotherms of NBS^- onto S packing from aqueous solution at five different ionic strengths at 25°C

c	C_m (M) $\times 10^4$	$n_{\text{T},\text{NBS}^-}$ $\text{mol} \times 10^7$	$C_{\text{s},\text{NBS}^-}$ (mol/kg) $\times 10^4$	$\Gamma_{\text{s},\text{NBS}^-}$ (mol/cm ²) $\times 10^{13}$
0.010	0.5142	0.594 ± 0.022	2.93 ± 0.14	0.948 ± 0.045
0.010	2.057	2.27 ± 0.11	11.1 ± 0.60	3.59 ± 0.19
0.010	4.800	4.58 ± 0.09	21.5 ± 0.71	6.96 ± 0.23
0.010	6.857	5.91 ± 0.03	26.9 ± 0.74	8.71 ± 0.24
0.010	9.600	7.68 ± 0.07	34.1 ± 1.0	11.0 ± 0.32
0.010	12.34	8.70 ± 0.05	36.7 ± 1.2	11.9 ± 0.39
0.010	15.09	9.23 ± 0.15	36.4 ± 1.7	11.8 ± 0.55
0.022	1.046	1.41 ± 0.027	7.20 ± 0.19	2.33 ± 0.06
0.022	3.136	3.91 ± 0.02	19.6 ± 0.32	6.34 ± 0.10
0.022	5.227	5.79 ± 0.08	28.2 ± 0.67	9.13 ± 0.21
0.022	7.841	8.00 ± 0.07	38.3 ± 0.91	12.4 ± 0.29
0.022	10.42	9.78 ± 0.23	45.7 ± 1.2	14.8 ± 0.39
0.034	0.5592	0.810 ± 0.06	4.24 ± 0.36	1.37 ± 0.12
0.034	1.678	2.467 ± 0.037	12.7 ± 0.27	4.11 ± 0.09
0.034	4.474	5.78 ± 0.047	29.1 ± 0.50	9.42 ± 0.16
0.034	6.710	8.03 ± 0.07	39.9 ± 0.75	12.9 ± 0.24
0.034	9.506	10.5 ± 0.09	51.5 ± 1.0	16.7 ± 0.32
0.034	12.30	12.5 ± 0.06	59.5 ± 1.2	19.3 ± 0.38
0.034	14.83	14.1 ± 0.10	65.8 ± 1.4	21.3 ± 0.45
0.050	0.7225	1.16 ± 0.13	6.10 ± 0.79	1.97 ± 0.26
0.050	1.445	2.30 ± 0.10	12.0 ± 0.64	3.88 ± 0.21
0.050	2.890	4.28 ± 0.058	22.1 ± 0.44	7.15 ± 0.14
0.050	5.780	7.80 ± 0.10	39.7 ± 0.81	12.9 ± 0.26
0.050	10.12	12.0 ± 0.13	59.7 ± 1.2	19.3 ± 0.39
0.050	14.45	15.8 ± 0.05	76.6 ± 1.4	24.8 ± 0.45
0.100	0.5043	0.820 ± 0.075	4.30 ± 0.45	1.39 ± 0.15
0.100	1.009	1.65 ± 0.02	8.65 ± 0.17	2.80 ± 0.06
0.100	2.521	3.94 ± 0.13	20.6 ± 0.84	6.67 ± 0.27
0.100	5.043	7.56 ± 0.11	38.6 ± 0.83	12.5 ± 0.27
0.100	7.565	10.58 ± 0.22	54.2 ± 1.5	17.5 ± 0.48
0.100	10.09	13.4 ± 0.3	68.0 ± 0.96	22.0 ± 0.31
0.100	14.45	17.6 ± 0.39	87.5 ± 2.7	28.3 ± 0.87

* Uncertainties are standard deviations from triplicate measurements.

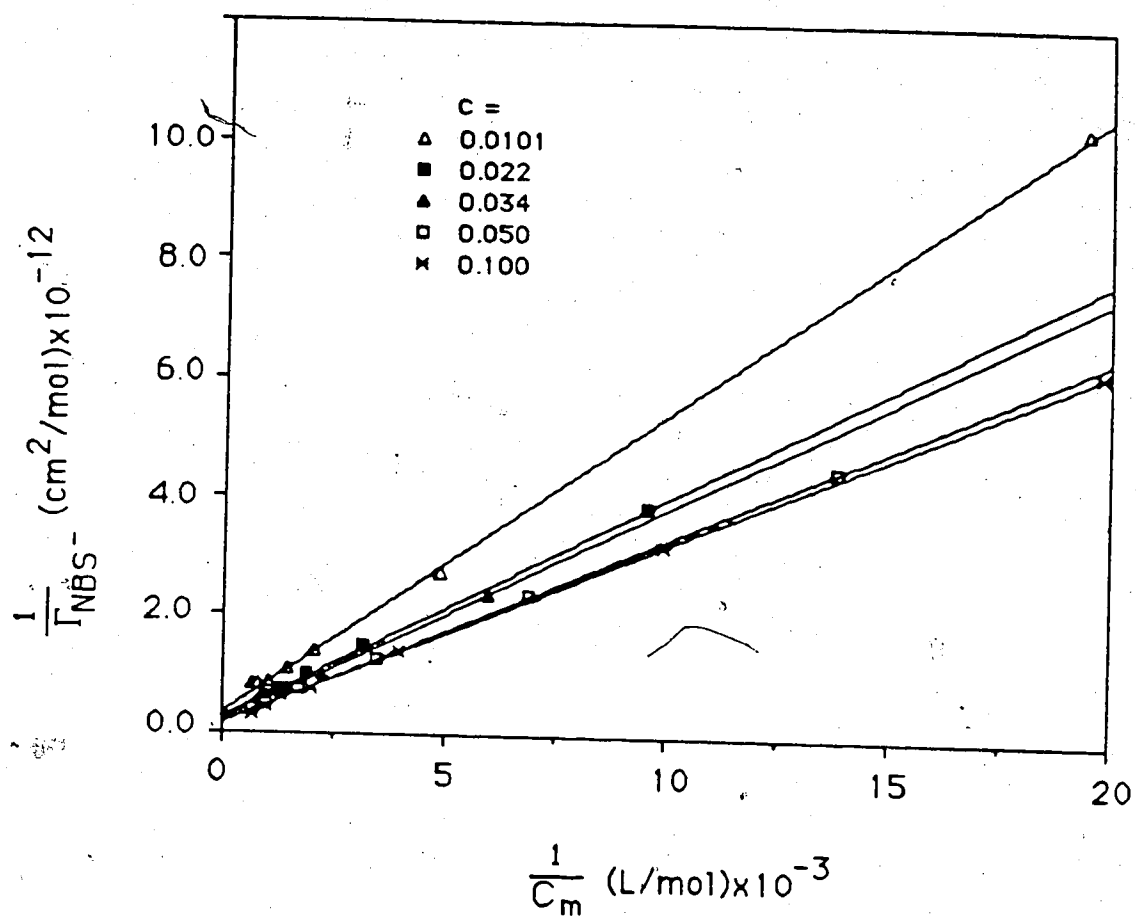


Figure 3-5 Langmuir plots for the adsorption isotherms of NBS^- onto chemically bonded ODS packing from aqueous solution at various ionic strengths at 25°C .

The Langmuir plots are shown in Fig.3-5. The y-axis intercepts for all the curves are roughly the same, which indicates that the value of $\Gamma_{\text{NBS}^-}^{\text{max}}$ is approximately the same for the five different ionic strengths. This intercept value of $(2.26 \pm 0.10) \times 10^{11} \text{ cm}^2/\text{mole}$ corresponds to a area of approximately 37 nm^2 for each NBS^- molecule when the ODS surface is covered with a monolayer of NBS^- . This area is much larger than that of the cross section of NBS^- molecule, which is approximately 0.9 nm^2 [74]. In contrast, Cantwell and Puon [94] found that the area per molecule occupied in a monolayer of the organic cation diphenylguanidinium, which shows Langmuir behavior, is equal to its cross sectional area on a styrene-divinylbenzene copolymer adsorbent, Amberlite XAD-2. It is not possible to say whether the difference between the areas occupied by NBS^- on an ODS packing and by diphenylguanidinium on XAD-2 reflects a general difference between the two packings or whether it reflects a difference between the two adsorbed species because relatively few studies of monolayer coverage have been performed on these packings.

3.3.1.2. SGC Behavior of NBS^-

It is obvious from Fig.3-4 that the extent of adsorption of NBS^- onto the ODS packing increases with increasing ionic strength (or the concentration of the electrolyte NaCl). The effect can be quantitatively explained using equation 3-4 as follows: First, the solution activity coefficients of NBS^- were used to convert the molar concentration (the x-axis in Fig.3-4) into activities. The solution activity coefficients of NBS^- at the five different ionic strengths are obtained from the extended Debye-Huckel equation [120] by taking its ionic size parameter to be $3.5 \times 10^{-8} \text{ cm}$ (for explanation, see Appendix III), and are given in Tables 3-2 to 3-6.

Next, at a fixed value of activity of NBS^- , a_{NBS^-} , the corresponding surface excess, Γ_{NBS^-} , for each of the five ionic strengths (c) was obtained by reading from the adsorption isotherms in Fig.3-4. The values of Γ_{NBS^-} at the five different c for a_{NBS^-}

Table 3-2 Values of activity coefficient, surface excess of NBS^- and surface charge density on the Oxide due to the adsorption of NBS^- at five different ionic strengths when $a_{\text{NBS}^-} = 2 \times 10^{-4} \text{ M}$

c	γ_{NBS^-}	Γ_{NBS^-} (mol/cm ²) $\times 10^{13}$	$-\sigma_0$ (coul/cm ²) $\times 10^8$
0.010	0.900	3.82	3.69
0.022	0.868	4.76	4.59
0.034	0.840	5.48	5.29
0.050	0.810	6.13	5.92
0.100	0.759	6.57	6.34

Table 3-3. Values of activity coefficient, surface excess of NBS^- and surface charge density on the ODS packing due to the adsorption of NBS^- at five different ionic strengths when $a_{\text{NBS}^-} = 4 \times 10^{-4} \text{ M}$.

c	γ_{NBS^-}	Γ_{NBS^-} (mol/cm^2) $\times 10^{13}$	$-\sigma_0$ (coul/cm^2) $\times 10^8$
0.010	0.900	6.82	6.58
0.022	0.868	8.38	8.09
0.034	0.840	9.80	9.46
0.050	0.810	10.8	10.4
0.100	0.759	12.4	12.0

Table 3-4 Values of activity coefficient, surface excess of NBS^- and surface charge density on the ODS packing due to the adsorption of NBS^- at five different ionic strengths when $\lambda_{\text{NBS}^-} = 6 \times 10^{-4} \text{ M}$

c	γ_{NBS^-}	Γ_{NBS^-} (mol/cm ²) $\times 10^{13}$	$-\sigma_0$ (coul/cm ²) $\times 10^8$
0.010	0.900	8.93	8.62
0.022	0.868	11.3	10.9
0.034	0.840	13.5	13.1
0.050	0.810	14.8	14.3
0.100	0.759	17.5	16.9

Table 3-5 Values of activity coefficient, surface excess of NBS^- and surface charge density on the ODS packing due to the adsorption of NBS^- at five different ionic strengths when $a_{\text{NBS}^-} = 8 \times 10^{-4} \text{ M}$

c	γ_{NBS^-}	Γ_{NBS^-} (mol/cm ²) $\times 10^{13}$	$-\sigma_o$ (coul/cm ²) $\times 10^8$
0.010	0.900	10.5	10.2
0.022	0.868	13.7	13.2
0.034	0.840	16.4	15.7
0.050	0.810	18.6	17.9
0.100	0.759	21.8	21.0

Table 3-6 Values of activity coefficient, surface excess of NBS^- and surface charge density on the ODS packing due to the adsorption of NBS^- at five different ionic strengths when $a_{\text{NBS}^-} = 10 \times 10^{-4} \text{M}$

	γ_{NBS^-}	Γ_{NBS^-} (mol/cm ²) $\times 10^{13}$	$-\sigma_o$ (coul/cm ²) $\times 10^8$
0.010	0.900	11.5	11.1
0.022	0.868	15.6	15.0
0.034	0.840	18.7	18.0
0.050	0.810	21.9	21.1
0.100	0.759	25.4	24.5

$=2 \times 10^{-4}$ are listed in the 3rd columns of Table 3-2. The processes are repeated for each of four additional values of a_{NBS^-} and the results are given in Table 3-3 through 3-6.

The value of the charge density σ_0 was then calculated for each pair of Γ_{NBS^-} and c by the iterative calculations discussed in section 3.2.1 (see Appendix I). The results are given in the 4th columns of Table 3-2 to 3-6.

Since the surface excesses of NBS^- on the ODS packing are relatively small (less than one NBS^- molecule per 60 nm^2), the surface charge densities are small.

Consequently, the surface potential Ψ_0 and the potentials at the OHP are small (only a few millivolts). So the correction term

$$\left[\left(\frac{ZF\Psi_{\text{OHP}}}{2RT} \right)^{-1} \sinh \left(\frac{ZF\Psi_{\text{OHP}}}{2RT} \right) \right]^{-1}$$

turns out to be always equal to 1.00. Under these conditions equation 3-4 predicts that the plot of σ_0 vs. $c^{-1/2}$ is linear when a_{NBS^-} is fixed at a specific value. The plots of σ_0 vs. $c^{-1/2}$ at five different values of a_{NBS^-} are presented in Fig. 3-6. The lines are least-square fits of the experimental points. The linearity of the curves is obvious, which is consistent with the prediction of the SGC theory, and suggests that Ψ_0 and C_1 are constant at a fixed value of a_{NBS^-} , independent of c . Values of (intercept/slope), Ψ_0 and C_1 , along with their standard deviations calculated from the slopes and intercepts of the curves shown in Fig. 3-6, are listed in Table 3-7. It can be seen that C_1 is not strictly constant, but rather increases somewhat with increasing a_{NBS^-} . This can be seen by intercomparing the individual values of C_1 in the light of their standard deviations using statistical test such as the t-test or an analysis of variance [145]. The increase in C_1 value presumably reflects a decrease in the thickness of the compact part of the double-layer or an increase in its

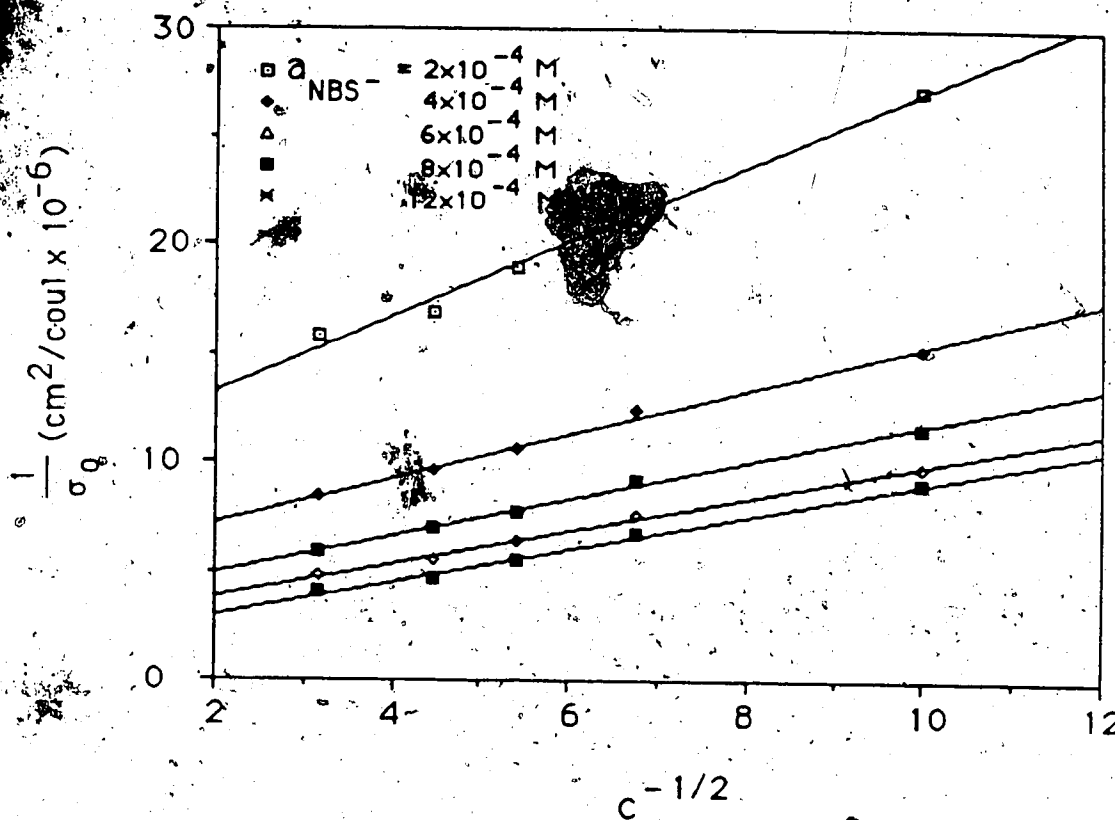


Figure 3-6 The Stern-Gouy-Chapman plots for the sorption of NBS^- onto chemically bonded ODS packing from solution at five different solution activities of NBS^-

Table 3-7 SGC behavior of NBS^- at the ODS/solution interface.

a_{NBS^-} (mol/L) $\times 10^4$	intercept* slope	$-\Psi_0$ (mV)	C1* ($\mu\text{F}/\text{cm}^2$)
2.00	5.68 ± 0.74	2.54 ± 0.15	40.1 ± 5.1
4.00	5.00 ± 0.91	4.34 ± 0.05	44.3 ± 3.7
6.00	3.85 ± 0.43	5.20 ± 0.04	59.2 ± 5.7
8.00	3.21 ± 0.36	5.88 ± 0.03	71.2 ± 7.0
10.0	2.15 ± 0.44	5.93 ± 0.05	106 ± 20
		mean	$64 \pm 10^{**}$ $\pm 23^{***}$

* the \pm values of the individual entries are their standard deviations based on the linear regression of the plots in Fig. 3-6.

** the \pm value for the mean of C1 is a "pooled" standard deviation [145] calculated from the individual standard deviations of the entries.

*** the \pm value for the mean of C1 is obtained in the conventional manner, i.e.

$$\left[\frac{\sum (x_i - \bar{x})^2}{(n-1)} \right]^{1/2}, \text{ from the individual entries of C1.}$$

dielectric constant. Nevertheless, the change in C_1 is not large and, for some purpose, C_1 can be taken as a constant of $64 \mu\text{F}/\text{cm}^2$.

The thickness of the compact layer could be evaluated from the average value of C_1 , assuming the dielectric constant ϵ to be that of pure water, with the equation

$$d = \frac{\epsilon}{4 C_1 \pi} \quad (2-21)$$

A value of $8.6 \times 10^{-8} \text{ cm}$, or 8.6 \AA is obtained. In comparison, the radius of a hydrated sodium ion (Na^+) is 4.8 \AA [120]. This discrepancy might be due to the fact that ϵ of water in the compact part of the double-layer is smaller than that of bulk water (163).

3.3.2. Adsorption of Tetrabutylammonium (TBA^+)

3.3.2.1. Micelle Formation of TBA^+ in the Sample Solutions

Various techniques have been used in an attempt to determine if TBA^+ forms micelles and, if so, the value of its critical micelle concentration (CMC). Most studies have been done with TBA^+Br^- with no added inert electrolytes. Two investigators concluded that TBA^+Br^- forms micelles. Using a dye spectral change method one found a CMC of 0.04M [122], and using solubility of benzene in the aqueous solution, the other found a CMC of 1.0M [122,123]. Other investigators, using surface tension measurements, found no evidence of micelle formation for TBA^+Br^- [124,125]. In a study of TBA^+Cl^- in the absence of added inert electrolytes, no evidence for micelle formation was found up to 0.05M using surface tension measurements [125]. The absence of micelle formation for TBA^+ salts has been predicted on the basis of the spherical shape [119].

The tendency to form micelles is influenced not only by the nature of the counterion (e.g. Cl^- or Br^-) but also by the ionic strength of the solution [63]. Since micelle formation by TBA^+Cl^- will have a profound effect both on the adsorption of TBA^+ ion and on the sorption of NBS^- in the presence of a large excess of TBA^+ , it is important to know if micelles are formed under the experimental conditions used in the present study, i.e. TBA^+ from 0.002M to 0.05M in aqueous solution of ionic strength from 0.05 to 0.50.

The plot of surface tension vs. log C_m of TBA^+ at ionic strength of 0.50 is given in Fig.3-7. The smooth decrease of surface tension with increasing concentration of TBA^+ in the solution and the absence of a "break" in the plot (compare with Fig.2-7) indicates that there is no micelle formation occurring in this concentration range at ionic strength of 0.50. In aqueous solutions, the value of CMC for a surfactant usually increases with decreasing ionic strength in the solution [63]. So micellization of TBA^+ is not expected to occur within the concentration range at any ionic strength lower than 0.5.

3.3.2.2 Adsorption Isotherms

The adsorption isotherm measurements for TBA^+ were carried out in the presence of a "trace" concentration ($1.488 \times 10^{-6} \text{M}$) of NBS^- in its solution. As discussed later, this causes no detectable difference in the adsorption of TBA^+ compared to that observed in solution of TBA^+ with no NBS^- present.

The determination of void volume in the instrument used for studying TBA^+ (see Fig.2-4) involves disconnecting valve V2 from valve V1 at the point C and equilibrating column C_1 with water. The equilibration was verified by pumping increasing volumes of water through the column. The following void volumes were found: $(64.36 \pm 0.75) \mu\text{l}$ for 10ml; $(63.56 \pm 0.40) \mu\text{l}$ for 20ml and $(65.55 \pm 0.96) \mu\text{l}$ for 40ml (all at 95% confidence level), showing that equilibrium was achieved in less than 10ml. To be on the safe-side, 20ml (i.e. 10min pumping time) was used. The GC calibration curve for the determination

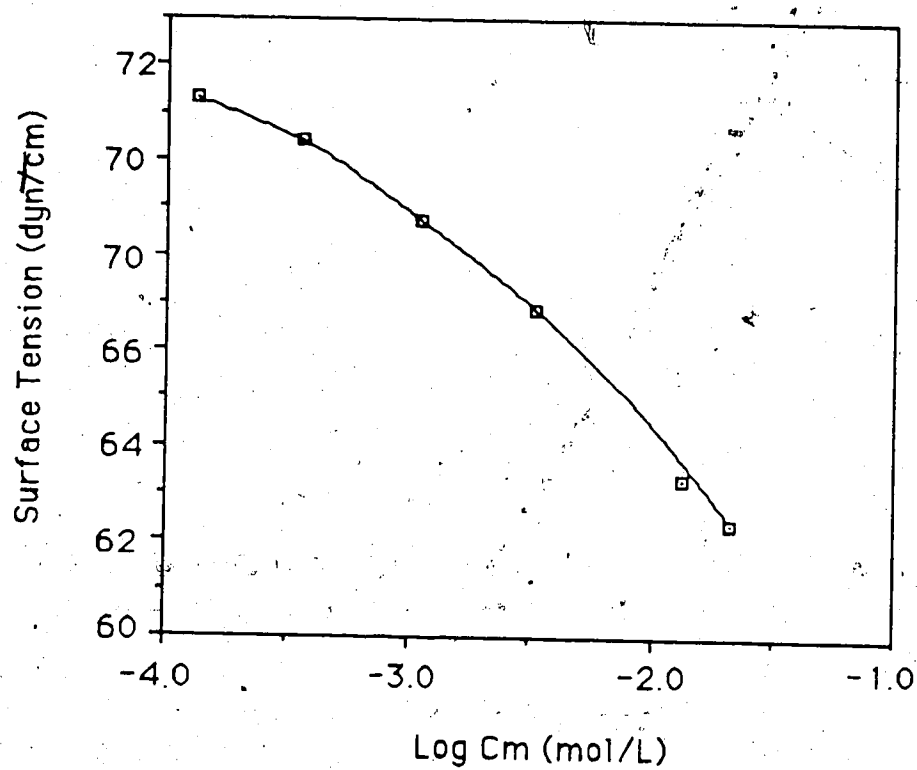


Figure 3-7 Plot of surface tension γ (dyn/cm) vs. logarithm of concentration of TBA^+ (mol/L) for aqueous solutions with ionic strength of 0.5 at $25^\circ C$.

of water is shown in Fig.3-8. The void volume was found to be $(65.21 \pm 1.18) \mu\text{l}$ at 95% confidence level.

Equilibration of column C_1 with the sample solution was verified by measuring the loading curve of TBA^+ . Two such curves, measured at different ionic strengths are shown in Fig.3-9 and 3-10, in which the amount (normalized) of TBA^+ in column C_1 is plotted against the volume of the sample solution passed through the column. Fig.3-9 shows the equilibration process when the aqueous sample solution contains $5.7 \times 10^{-4} \text{ M}$ TBA^+ with ionic strength of 0.05, while Figure 3-10 shows that when the aqueous sample solution contains $2.2 \times 10^{-4} \text{ M}$ TBA^+ with ionic strength of 0.50. It is evident that in both cases the column was equilibrated with the aqueous sample solution when less than 40ml was passed through it. The equilibration volume used for all subsequent measurements is 125ml.

In the elution step, it is important that all the TBA^+ adsorbed onto the ODS packing in column C_1 is completely eluted with the eluent (50% methanol/water (v/v) with 0.01M NaCl). In this study the completeness of the elution has been carefully verified by: (i) measuring the elution curve of TBA^+ at the end of column C_1 , and (ii) determining, with INAA, the amount of the "residual" TBA^+ left on the ODS column after the elution. The elution curve of TBA^+ was measured by continuously collecting the eluate in 2ml portions at the point C (see Fig.2-4), and subsequently determining the amount of TBA^+ in each fraction. Elution of TBA^+ was complete in the first 2ml of eluent passed through the column. In the actual measurements, 25ml of eluent was always passed through the column in the elution step.

The maximum amount of the "residual" TBA^+ left on the ODS packing was estimated using its derivative TBABr^+ with an instrumental neutron activation analysis technique. The use of $\text{TBABr}^+\text{Cl}^-$ in place of TBA^+Cl^- for the study is justified by the

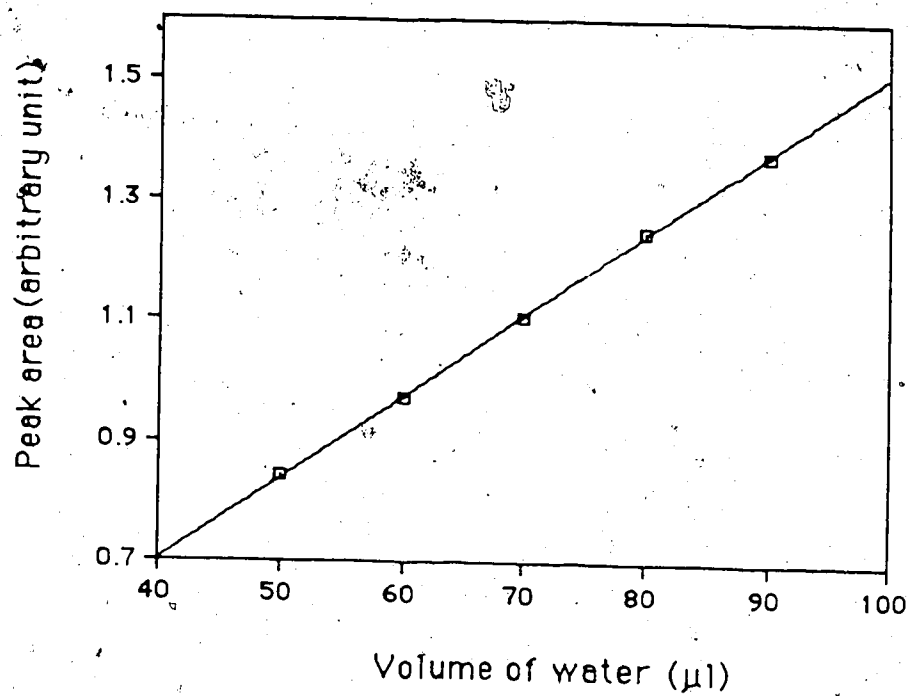


Figure 3-8 The GC calibration curve of water for the determination of void volume in the system shown in Fig.2-5. (see section 2.4.5 for experimental details).

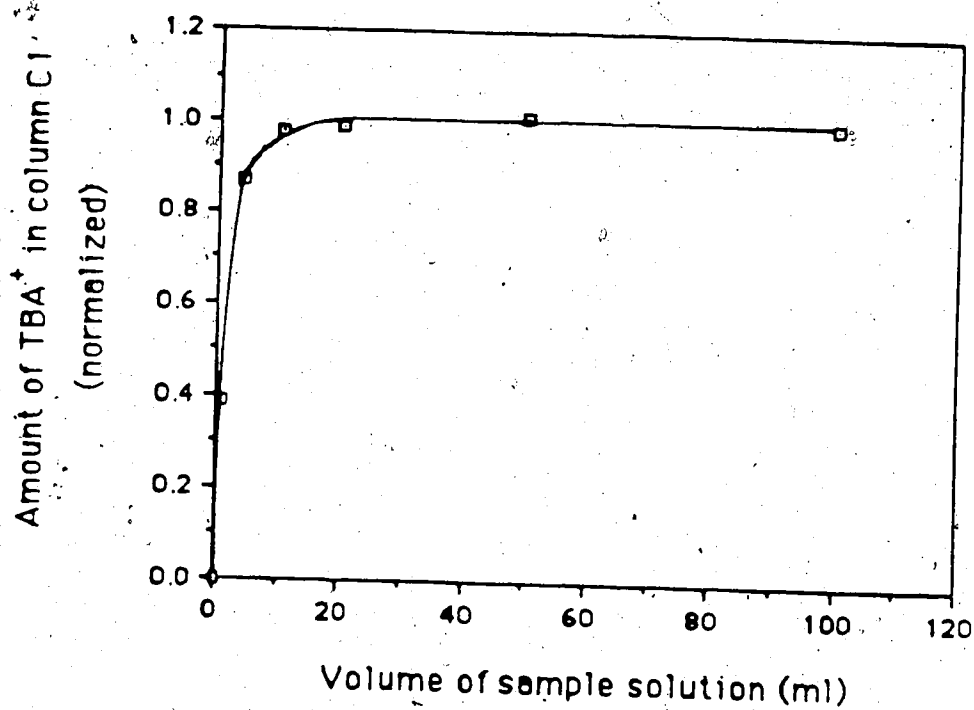


Figure 3-9 Loading curve of TBA⁺ on column C1 (contains ~15mg ODS packing).

The aqueous sample solution contains 5.7×10^{-4} M TBA⁺Cl⁻ with ionic strength of 0.05.

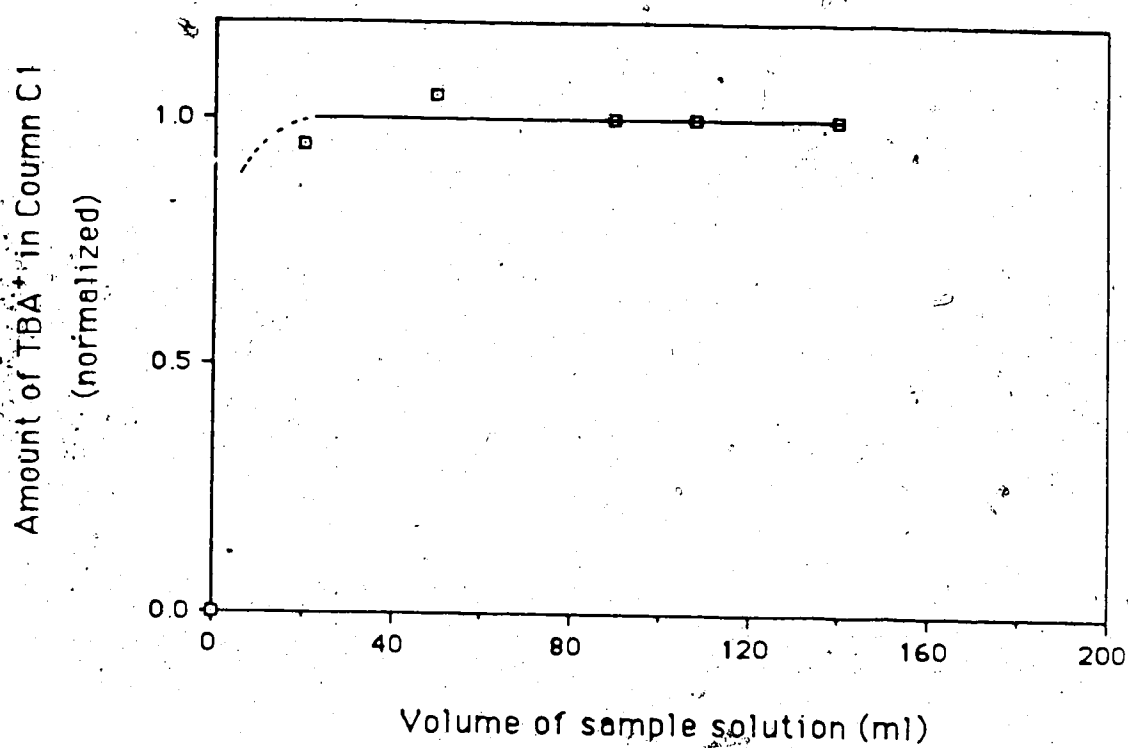


Figure 3-10. Loading curve of TBA⁺ on column C1 (~15mg ODS material). The aqueous sample solution contains 2.2×10^{-4} M TBA⁺ with ionic strength of 0.50.

observation that the distribution coefficient for TBA^+Cl^- of (343 ± 13) L/kg is larger than that for TBA^+Cl^- of (267 ± 21) L/kg at an ionic strength of 0.50 and quaternary ammonium chloride sample concentration of 2.51×10^{-4} M. The residual concentration of TBA^+ was found to be $(1.93 \pm 8.3) \times 10^{-8}$ mol/g ODS (95% confidence limits) after eluting with 25ml of the eluent. The calibration curve of the neutron activation analysis for bromine at 619keV is presented in Fig.3-11. In the present study, the minimum concentration of TBA^+ on the ODS packing in any experiment is approximately 8×10^{-5} mol/g ODS (see the adsorption isotherms of TBA^+ in Fig.3-14). Comparing the two numbers, it is obvious that more than 99.9% of the adsorbed TBA^+ would be eluted in the elution step.

In the actual experiment of measuring the adsorption isotherms of TBA^+ , the eluent from column C_1 must also pass through valve V1, injection valve V2, analytical column C_2 and the UV detector D (see Fig.2-5) before being collected for determination. Thus, in studying the completeness of elution of TBA^+ by measuring its elution curve, the eluate was collected in fraction at the outlet of the UV detector D in Fig.2-4. The elution curve is given in Fig.3-12, which shows that all the TBA^+ was completely eluted with less than 20ml of the eluent. Therefore, 25ml of the eluate was collected in all the subsequent measurements.

The amount of TBA^+ in the collected eluate was quantified using the SE/FIA system. With a 50 μ l sample injection loop, the volume of the collected eluate necessary to rinse and fill the sample loop for a quantitative determination is less than 1mL. The minimum injected concentration of TBA^+ for its detection with the system is $\sim 1.0 \times 10^{-6}$ M based on a TBA^+ signal that is 2 times the peak-peak baseline noise. This kind of sensitivity makes it possible to use a very small amount (~ 15 mg) of the ODS material in column C_1 for the isotherm measurements. The breakthrough volume for TBA^+ on column C_1 was greatly reduced, compared to that reported for strongly adsorbed organic

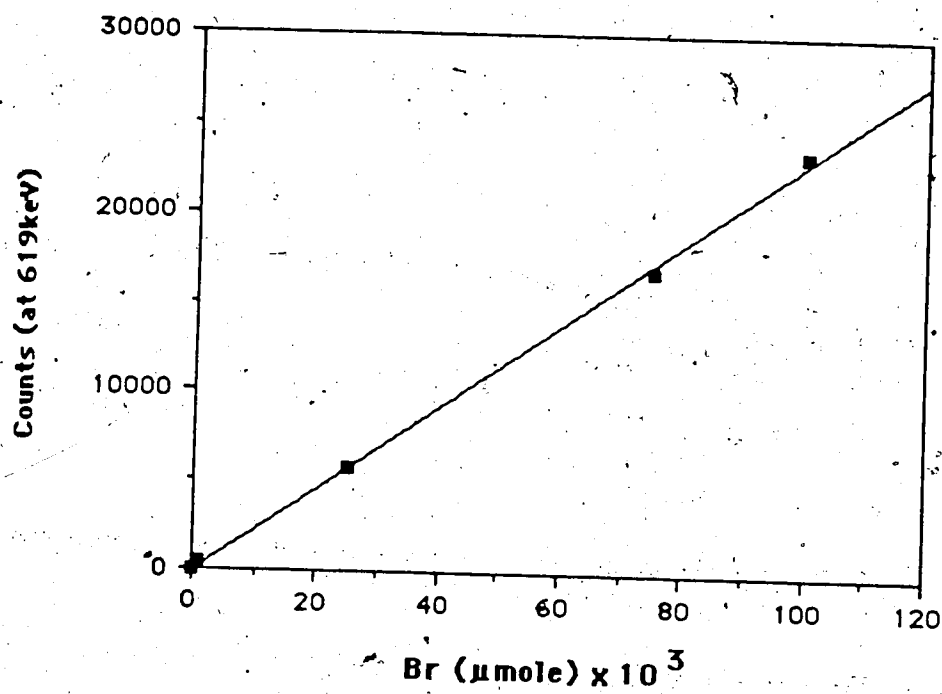


Figure 3-11 The instrumental neutron activation analysis calibration curve of bromine at 619keV.

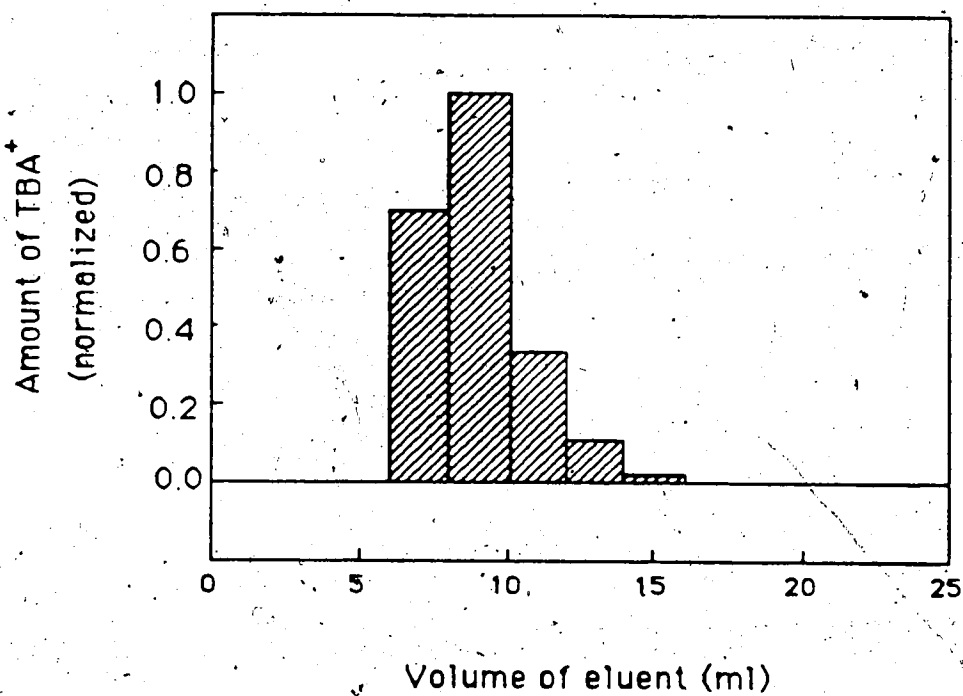


Figure 3-12 The elution curve of TBA⁺ at the end of the UV detector D (see Fig. 2-5).

Flow rate of the eluent: 1.0ml/min.

ions in the literature [16], as a result of the small amount of ODS packing used in the column.

The SE/FIA system was calibrated with a series of standard TBA^+ solutions. The calibration curves are plotted in Fig. 3-13. It is obvious that either peak height or peak area can be used to quantify TBA^+ with the system. In the present study peak height was used for convenience. The effect of picrate concentration in the reagent solution on the calibration curve has been investigated. It was found that the calibration curve is essentially identical when the picrate concentration changed from 0.005M to 0.010M. In the subsequent experiments 0.005M was always used.

Adsorption isotherms of TBA^+ from its aqueous solutions onto the ODS packing at five different ionic strengths are shown in Fig. 3-14. Surface excess Γ_{TBA^+} (mol/cm^2) is used instead of surface concentration C_s in the plot for the convenience of calculation. The adsorption data for TBA^+ are presented in Table 4-2 in Chapter 4, along with the data for sorption of NBS^- under "trace conditions". As discussed later, the isotherms of TBA^+ do not follow the Langmuir equation and may not approach a limiting value. At a solution concentration of 0.02 M TBA^+ , which is near the highest value used in the studies, the surface area occupied per molecule of TBA^+ is found to range from 2.6 nm^2 to 3.5 nm^2 over the range of ionic strength studied. Assuming that TBA^+ is a spherical molecule, the projected surface area per molecule is about 0.5 nm^2 .

The adsorption isotherms of TBA^+ onto ODS packing have been measured by other workers. Del Rey et al [107] reported that the adsorption isotherms of TBA^+ onto ODS packing from a solution of water:acetonitrile(9:1) follow the Freundlich equation. In contrast, Schill and co-workers [44,45] found that the isotherms of TBA^+ onto ODS from solutions of water:acetonitrile (75:25) follow the Langmuir equation. Huang and Taylor [47] measured its isotherms without controlling ionic strength of the solution. Vigh and

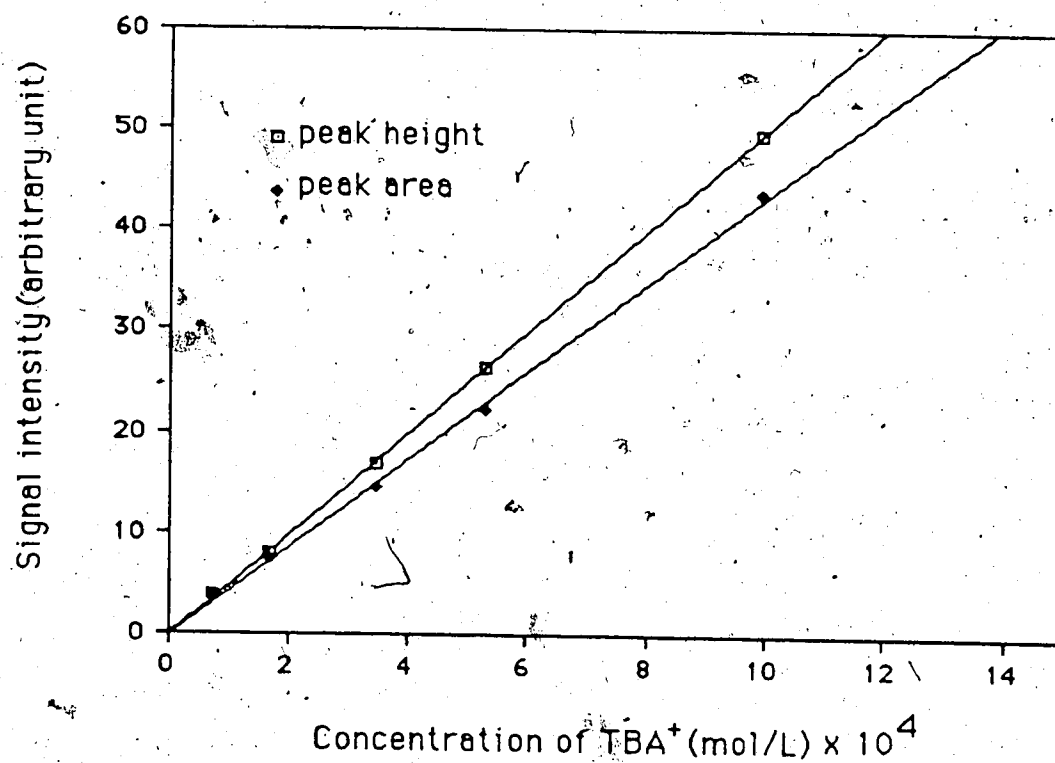


Figure 3-13 The solvent extraction/flow injection analysis (SE/FIA) calibration curve of TBA⁺.

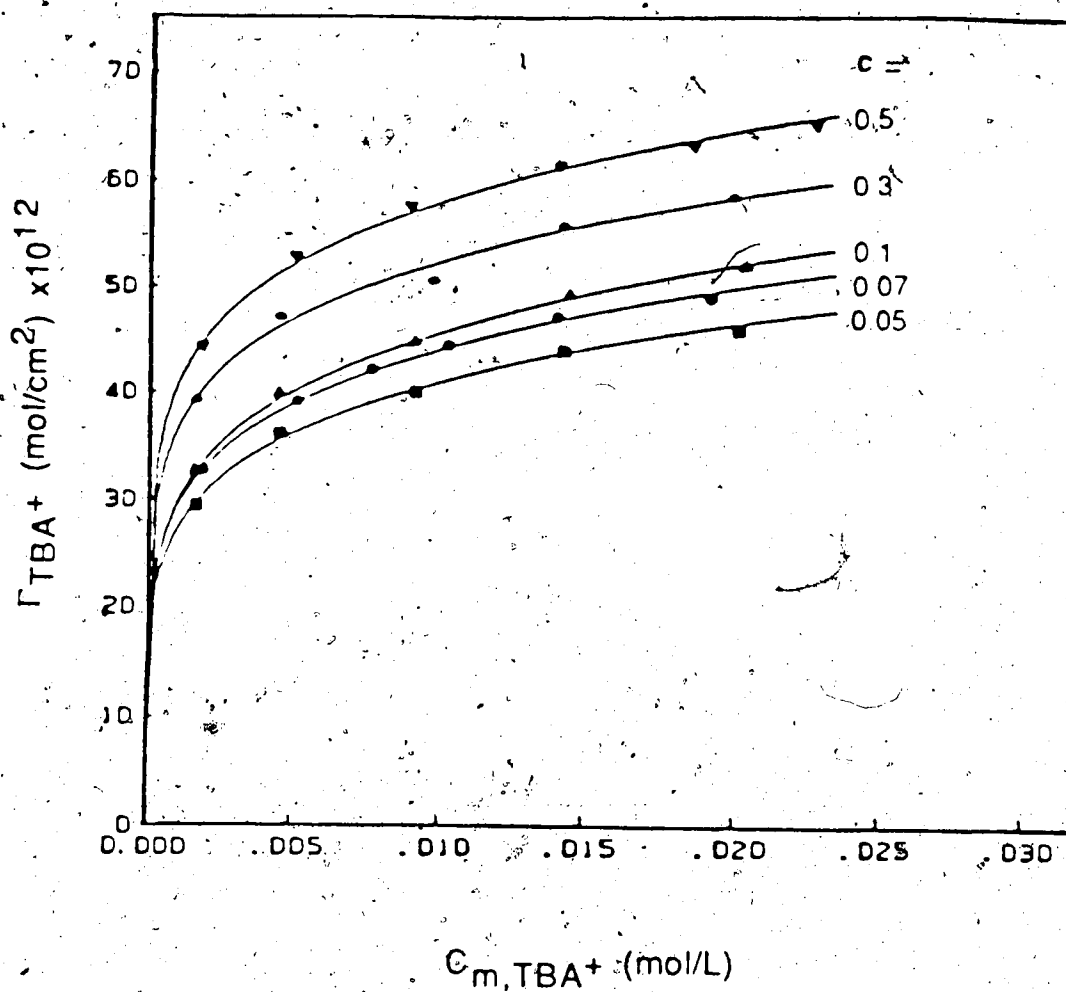


Figure 3-14 Adsorption isotherms of tetrabutylammonium (TBA⁺) onto chemically bonded ODS packing from aqueous solutions at five different ionic strengths at 25°C

co-workers[121] studied the isotherms over quite a wide range of concentrations. Both reported that the isotherms follow neither Freundlich nor Langmuir equations. Evidently, isotherm shape depends on experimental conditions.

It was found that the adsorption isotherm data fit the Freundlich equation:

$$\Gamma_{TBA^+} = a \cdot C_{m,TBA^+}^b \quad (3-22)$$

where a and b ($b < 1$) are constants. The Freundlich plots for these isotherms are presented in Fig.3-15, as plots of negative logarithm of the surface excess Γ_{TBA^+} (mol/cm²) vs. negative logarithm of the solution concentration (mole/L).

The effect of the presence of "trace" concentration of NBS⁻ ion in the sample solution on the adsorption isotherms of TBA⁺ has been investigated by measuring the total number of moles of TBA⁺ on the ODS column C₁ as a function of the concentration of NBS⁻ in the sample solution having 0.01957M TBA⁺ and ionic strength of 0.50. The following values were found: $(4.471 \pm 0.02) \times 10^{-6}$ mol TBA⁺ in the absence of NBS⁻, $(4.482 \pm 0.040) \times 10^{-6}$ mol in the presence of 1.488×10^{-6} M NBS⁻ and $(4.437 \pm 0.040) \times 10^{-6}$ mol for the presence of 2.480×10^{-6} M NBS⁻. Obviously, the presence of the "trace" amount of NBS⁻ ion has no effect on the sorption isotherm of TBA⁺.

The stability of the ODS packing in the column was checked periodically by equilibrating the column with a 2.084×10^{-4} M aqueous solution of acetaminophen, eluting the column with the eluent and measuring the peak area given by acetaminophen. The peak areas obtained at different times are listed in Table 3-8.

Since the standard deviation of the peak area around the mean value of 4.97 is less than 5% and random, there is no indication that the ODS packing changed during the whole period of the measurement.

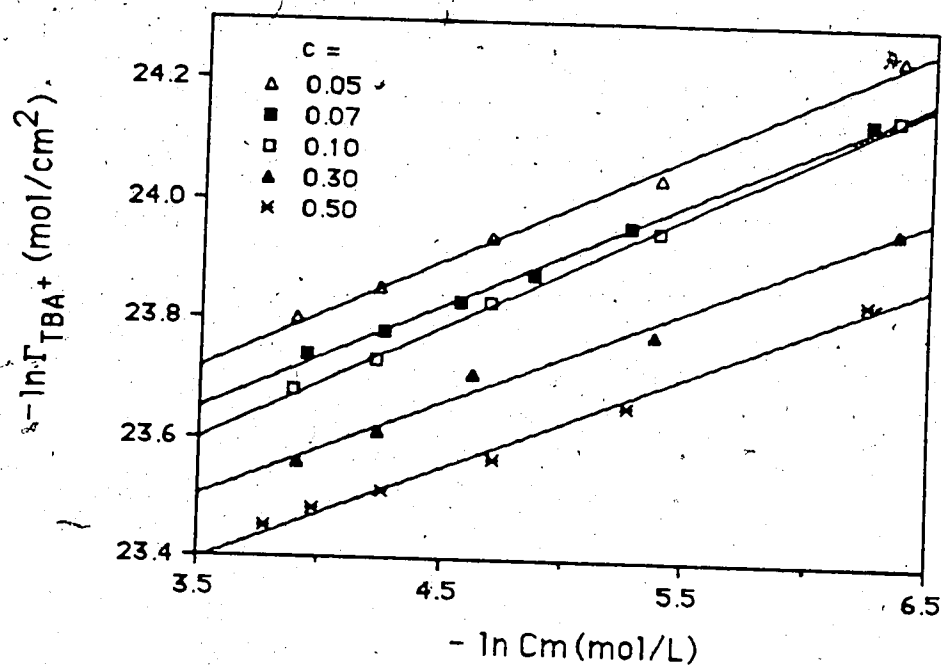


Figure 3-15 Freundlich plots for the adsorption isotherms of TBA⁺ onto ODS packing from aqueous solutions at five different ionic strength c .

Table 3-8 Peak area given by acetaminophen eluted from the ODS column at different times in 1986.

Time (dates)	July 29	Sept. 13	Oct.1	Oct.8	Oct.16	Nov. 7
Peak Area * (arbitrary unit)	4.91±0.05	5.26±0.03	4.91±0.04	4.91±0.02	4.87±0.02	5.06±0.02
Average	4.97 ± 0.03					

* Uncertainties are standard deviations from duplicate measurements.

3.3.2.3 Effect of pH on the Adsorption

Gelijkens and De Leenheer [86] obtained a linear correlation between the amount of TBA^+ adsorbed onto a C18 stationary phase and pH of the mobile phase (5% methanol in aqueous eluent, pH range 3 to 8). van der Houwen and co-workers [46] reported that the amount of TBA^+ adsorbed onto their C18 column increases with increasing pH of the mobile phase (methanol/water 1:1, pH range 5.8 to 8.8). They suggested that the adsorption is partly due to an ion-exchange process between TBA^+ and the residual silanol groups on the ODS surface. At a higher pH value, the ion-exchange process is favored by the increasing numbers of dissociated silanol groups on the surface, consequently more TBA^+ is sorbed. Schill et al [44,45] also reported that the amount of TBA^+ adsorbed onto ODS increases with increasing pH of the solution. It was explained [31,44,45, 87,122] by assuming that the ODS surface has two kinds of sorption-sites with different binding abilities and capacities, and the capacity of one of the sorption-sites increases with increasing pH.

For silica gel, it is generally agreed that the total ionizable silanol groups on the surface is in the range $5.5 \sim 5.8 \text{ nm}^{-2}$ [162]. It is well known that the number of ionized silanol groups (SiO^-) increases with increasing pH of the solution. The number of ionized silanols (SiO^-) per square nanometer, at a given pH in the solution, can be calculated from the empirical equation:

$$\log [\text{SiO}^- (\text{nm}^{-2})] = 5.2 \log (\text{pH}) - 4.78 \quad (3-23)$$

Assuming that the equation is still valid for the "residual" silanol groups on the chemically bonded ODS packing and the ODS packing has a surface coverage of 95% with the alkyl groups, it is possible to calculate the number of ionized silanols (SiO^-) on the ODS surface ($A_{\text{sp}} = 3.09 \times 10^9 \text{ cm}^2/\text{kg}$). The ionized silanol groups (SiO^-) is about $1.5 \times 10^{-6} \text{ mol/g}$

ODS for pH 5.0 which was always used in the experiments. The minimum concentration of TBA^+ on the ODS packing in any experiment of the present work is approximately 8×10^{-5} mol/g ODS (see the adsorption isotherms of TBA^+ in Fig 3-14). Therefore, the sorption of TBA^+ onto the ODS packing by an ion-exchange process with the "residual" silanol groups is not expected to be significant comparing to the adsorption onto the surface by other processes (e.g. dispersion forces and/or hydrophobic interaction).

In this study, the number of moles of TBA^+ adsorbed onto the ODS packing was measured against pH (range 4.2 to 6.4) of the solution at a fixed concentration of TBA^+ ($=2.880 \times 10^{-3}$ M) and a fixed ionic strength of 0.10. The result is plotted in Figure 3-16. A constant value for the distribution coefficient of TBA^+ has been observed over the pH range of 4.2 to 6.4. It can be shown that the number of ionized silanol groups on the ODS surface increases about 9 times (from 7.4×10^{-7} mol/g to 6.6×10^{-6} mol/g) when the pH increases from 4.2 to 6.4 in aqueous solution [162]. The fact that the distribution coefficient is constant within this pH range implies that the sorption of TBA^+ onto the highly end-capped Partisil-10 ODS-3 by ion exchange with the silanolate groups is negligible compared to the adsorption onto the surface by dispersion and/or hydrophobic interaction. This result is consistent with the highly end-capped character of the ODS packing, as discussed above.

3.3.2.4 SGC Behavior of TBA^+

The description of the adsorption behavior of TBA^+ onto the ODS packing at various ionic strength in terms of the SGC theory is similar to that for NBS^- as discussed in section 3.3.1.2. The solution activity coefficient of TBA^+ was used to convert its solution concentration (x-axis) in Fig 3-14 into activity. Its aqueous activity coefficients at high ionic strength (>0.1) have been measured by Lindenbaum [122], and those at low ionic strength can be calculated from the extended Debye-Huckel equations [120] by

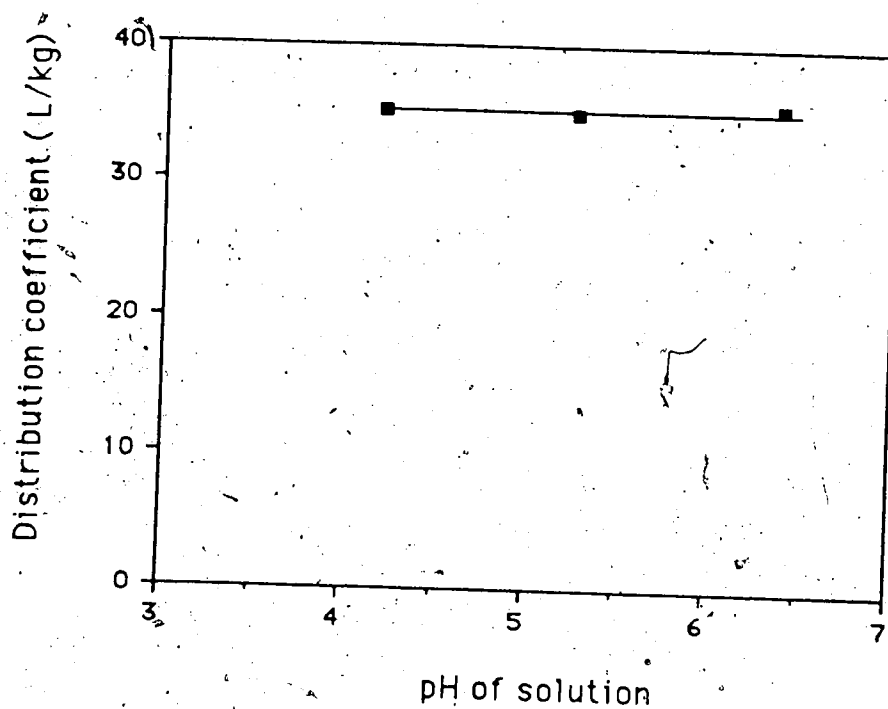


Figure 3-16 The effect of pH on the distribution coefficient of TBA⁺, the sample solution contains $2.881 \times 10^{-3} \text{ M TBA}^+$ with ionic strength = 0.10.

assuming its ionic parameter to be 3.0×10^{-8} cm (for explanation see Appendix IV). The values of activity coefficients at various ionic strengths are given in Table 3-9.

At a fixed activity of TBA^+ (a_{TBA^+}), the surface excess (Γ_{TBA^+}) corresponding to each of the five ionic strengths was obtained by reading from the adsorption isotherms in Fig. 3-14. This process was repeated for several different values of a_{TBA^+} . Then each of the surface excesses (Γ_{TBA^+}) was converted into charge density σ_0 by the iterative process described in the theory part (see section 3.2.1 and Appendix II). The values of Γ_{TBA^+} and σ_0 at various c , each at different a_{TBA^+} , are listed the 2nd and 3rd columns in Tables 3-10 to 3-14. The plots of $1/\sigma_0$ vs.

$c^{-1/2} \left[\left(\frac{ZF\Psi_{\text{OHP}}}{2RT} \right)^{-1} \sinh \left(\frac{ZF\Psi_{\text{OHP}}}{2RT} \right) \right]^{-1}$ are presented in Fig. 3-17. The values of

the correction term $\left[\left(\frac{ZF\Psi_{\text{OHP}}}{2RT} \right)^{-1} \sinh \left(\frac{ZF\Psi_{\text{OHP}}}{2RT} \right) \right]^{-1}$ under different conditions are

listed in the 4th column of Tables 3-10 to 3-14. The lines are linear least-square fits of the experimental points. The values of (intercept/slope), Ψ_0 and C_1 can be calculated from the reciprocals of the slopes and intercepts of the curves, and are given in Table 3-15. At the 99% confidence level using the t-test, the values of C_1 are constants, independent of a_{TBA^+} and c . This is in agreement with the prediction of the SGC theory.

The thickness of the compact layer could be evaluated from the average value of C_1 , assuming the dielectric constant ϵ to be that of pure water, with equation 3-21. A value of 10.3×10^{-8} cm, or 10.3 \AA is obtained. In comparison, the radius of a hydrated chloride ion (the counterion) is 3.7 \AA [120]. This discrepancy might be due to the fact that ϵ of water in the compact part of the double-layer is smaller than that of bulk water (163).

Table 3-9 Bulk activity coefficients of TBA^+ at five different ionic strengths

c	0.050	0.070	0.100	0.300	0.500
γ_{TBA^+}	0.805	0.780	0.755	0.670	0.637

Table 3-10 Values of activity coefficient and surface excess of TBA^+ , and surface charge density on the ODS packing due to the adsorption of TBA^+ at five different ionic strengths when $a_{\text{TBA}^+} = 2 \times 10^{-4} \text{ M}$

c	Γ_{TBA^+} (mol/cm ²) $\times 10^{12}$	σ_o (coul/cm ²) $\times 10^6$	U^*
0.050	32.5	3.17	0.845
0.070	35.0	3.41	0.864
0.100	36.3	3.53	0.890
0.300	43.9	4.25	0.938
0.500	48.9	4.73	0.953

where $U^* = \left[\left(\frac{ZF\Psi_{\text{OP}}}{2RT} \right)^{-1} \sinh \left(\frac{ZF\Psi_{\text{OP}}}{2RT} \right) \right]^{-1}$

Table 3-11 Values of activity coefficient and surface excess of TBA^+ , and surface charge density on the ODS packing due to the adsorption of TBA^+ at five different ionic strengths when $a_{\text{TBA}^+} = 4 \times 10^{-4} \text{ M}$

c	Γ_{TBA^+} (mol/cm ²) $\times 10^{12}$	σ_o (coul/cm ²) $\times 10^6$	U^*
0.050	34.3	3.40	0.830
0.070	39.3	3.87	0.839
0.100	40.9	4.01	0.867
0.300	48.9	4.75	0.926
0.500	54.4	5.28	0.943

where $U^* = \left[\left(\frac{ZF\Psi_{OP}}{2RT} \right)^{-1} \sinh \left(\frac{ZF\Psi_{OP}}{2RT} \right) \right]^{-1}$

Table 3-12 Values of activity coefficient and surface excess of TBA^+ , and surface charge density on the ODS packing due to the adsorption of TBA^+ at five different ionic strengths when $a_{\text{TBA}^+} = 6 \times 10^{-4} \text{ M}$

c	Γ_{TBA^+} (mol/cm ²) $\times 10^{12}$	σ_0 (coul/cm ²) $\times 10^6$	U^*
0.050	38.0	3.80	0.805
0.070	42.4	4.20	0.820
0.100	44.0	4.34	0.852
0.300	52.1	5.08	0.917
0.500	58.0	5.63	0.936

where $U^* = \left[\left(\frac{ZF\Psi_{\text{OHP}}}{2RT} \right)^{-1} \sinh \left(\frac{ZF\Psi_{\text{OHP}}}{2RT} \right) \right]^{-1}$

Table 3-13 Values of activity coefficient and surface excess of TBA^+ , and surface charge density on the ODS packing due to the adsorption of TBA^+ at five different ionic strengths when $a_{\text{TBA}^+} = 10 \times 10^{-4} \text{ M}$

c	Γ_{TBA^+} (mol/cm ²) $\times 10^{12}$	σ_0 (coul/cm ²) $\times 10^6$	U^*
0.050	43.0	4.39	0.769
0.070	46.2	4.66	0.796
0.100	48.3	4.82	0.829
0.300	56.2	5.51	0.906
0.500	62.5	6.09	0.927

where $U^* = \left[\left(\frac{ZF\Psi_{\text{OP}}}{2RT} \right)^{-1} \sinh \left(\frac{ZF\Psi_{\text{OP}}}{2RT} \right) \right]^{-1}$

Table 3-14 Values of activity coefficient and surface excess of TBA^+ , and surface charge density on the ODS packing due to the adsorption of TBA^+ at five different ionic strengths when $a_{\text{TBA}^+} = 14 \times 10^{-4} \text{ M}$

c	Γ_{TBA^+} (mol/cm ²) $\times 10^{12}$	σ_0 (coul/cm ²) $\times 10^6$	U^*
0.050	45.0	4.68	0.753
0.070	48.5	4.97	0.781
0.100	51.1	5.17	0.814
0.300	58.6	5.78	0.899
0.500	65.2	6.38	0.921

where $U^* = \left[\left(\frac{ZF\Psi_{\text{OHP}}}{2RT} \right)^{-1} \sinh \left(\frac{ZF\Psi_{\text{OHP}}}{2RT} \right) \right]^{-1}$

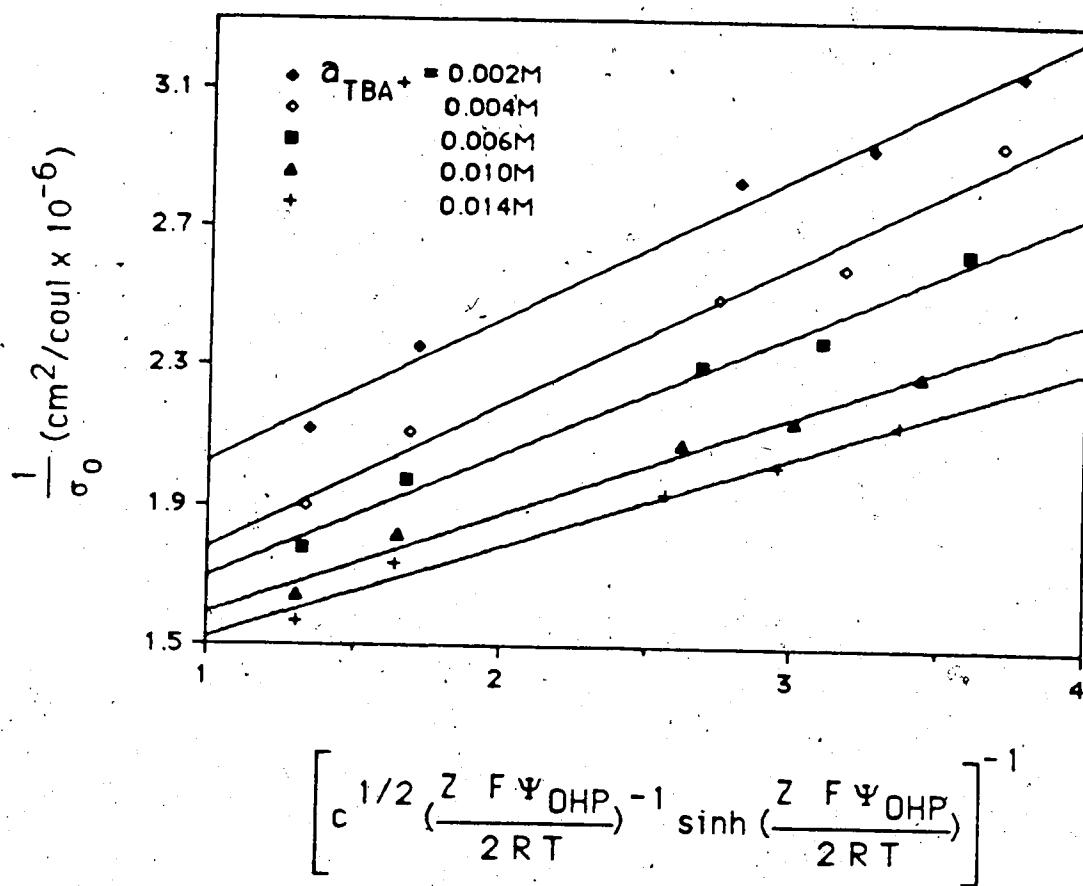


Figure 3-17 Stern-Gouy-Chapman plots for the sorption of TBA^+ onto ODS from aqueous solutions at its five different solution activities.

Table 3-15 SGC behavior of TBA⁺ at the ODS/solution interface *.

a _{TBA⁺} (M)	intercept slope	Ψ ₀ (mV)	C ₁ (μF/cm ²)
0.002	3.85 ± 0.60	106 ± 13	58.9 ± 8.6
0.004	3.35 ± 0.66	107 ± 17	68.0 ± 12.6
0.006	3.85 ± 0.60	125 ± 16	59.9 ± 9.5
0.010	4.55 ± 0.83	154 ± 20	49.8 ± 7.2
0.014	4.76 ± 0.68	169 ± 21	46.7 ± 7.0
		mean	56.7 ± 9.3 **

* Uncertainties are standard deviations.

** Uncertainty is a "pooled" standard deviation.

3.4 Conclusion

The adsorption isotherms of an organic ion (both a cation and an anion) onto the ODS/solution interface have been measured. The effect of ionic strength on the isotherms can be interpreted in terms of the electrical double-layer at the interface and can be quantitatively described with the Stern-Gouy-Chapman theory. Under the experimental conditions, the adsorption of TBA^+ onto the ODS packing is mainly due to processes such as dispersion forces and hydrophobic interaction rather than ion exchange between TBA^+ and the residual silanol groups on the surface.

Chapter 4

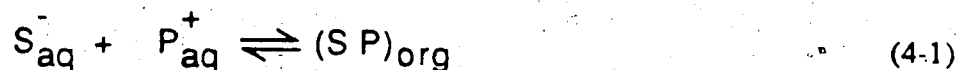
Sorption Of NBS⁻ Under "Ion-Pair" Conditions

4.1. Introduction

Although ion pair chromatography has enjoyed widespread use, the physico-chemical model which explains the retention of sample ions (S⁻) in the presence of a "pairing-ion" (P⁺) is still controversial. There is a vast amount of literature on this subject, but only those models commonly referred to will be reviewed here.

Ion-pair models

In the very early stages of the technique, Schill et al [2,3], Karger et al [4,5] and other workers [6,7] believed that its principle of operation is the same as that of ion-pair liquid/liquid extraction. The process can be expressed by an equilibrium

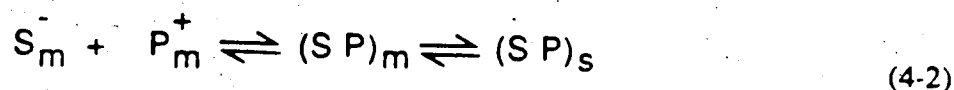


in which the subscript aq indicates the ions in the (aqueous) mobile phase and org indicates the ion-pair in or on the (organic) stationary phase. It was suggested that the ion-pair is not formed in the aqueous mobile phase but rather is formed in or on the surface.

Schill and co-workers [44,45,126] extended the model to include the sorption of all other possible ion-pairs not only between S⁻ and P⁺ but also between them and all other ions (e.g. Na⁺, Cl⁻, buffer, etc) present in the mobile phase. All these ion-pairs are assumed to compete for a limited number of sorption-sites on the surface. It is further

assumed that there are two kinds of sorption sites present on the surface of ODS stationary phase, and each has its own binding ability and capacity.

Horvath et al [12] and Tomlinson et al [14,68,153] also proposed models based on ion-pair formation. However, in their models the ion-pair between the sample ion (S^-) and the pairing-ion (P^+) is formed in the mobile phase, and this neutral complex is then sorbed onto the stationary phase. The process can be represented by the equilibria



where the subscript m indicates the mobile phase and s indicates the stationary phase.

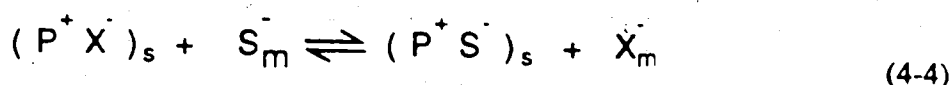
Since their model could not satisfactorily explain all aspects of their experimental data, Melander and Horvath [159,160] then extended it to a more complicated "dynamic complex exchange model". In this model, they still insisted that an ion-pair is formed between S^- and P^+ in the mobile phase. The ion-pair is then sorbed onto the stationary phase surface which is covered with P^+ , and interacts reversibly with the adsorbed P^+ to form a new ternary complex consisting of one S^- ion and two P^+ ions. Quantitative equations were derived for the capacity factor of S^- by considering all the equilibria involved.

In their present form, the two major "ion-pair" model [160,161] both involve many simultaneous equilibria. When fitting experimental data to their model the resulting equation have between 4 and 5 constants which are treated as "adjustable parameters". This weakens the claims of validity for such models.

"Dynamic" Ion-Exchange Models

Knox et al [15,16,65,118] were the first to suggest that possibly ion pair chromatography "operates rather like ion-exchange". This concept was then further amplified by Kissinger [127], Kraak et al [17,128,129], Deelder et al [49,50,130] and

other workers [121,131-134]. Speaking of a system in which the pairing-ion is a sulfonate and the sample is a cation, Peter Kissinger [127] stated that "a sulfonate ion-pair reagent may be thought of as a modifier used to convert a C18 column into a strong cation exchanger column with properties not unlike those of chemically bonded alkyl sulfonates". This model is now often referred to as the "dynamic" ion-exchange model. For the present case in which the pairing-ion is a cation P^+ , the model can be expressed by the equilibria



where X^- could be Cl^- or other inorganic anions. According to this model, the retention of the sample ion is merely the result of an ion-exchange process.

Kraak et al [128,129] derived an expression for k' of S^- based on the "dynamic" ion-exchange model. The expression predicts that k' has a linear relationship with $C_{s,P^+}/C_m$, where C_{s,P^+} is the concentration of P^+ on the stationary phase and C_m is the concentration of X^- . This linear relationship was also experimentally observed by Vigh et al [121,131-134]. Deelder et al [49,50,130] found that the plot of k' vs. $C_{s,P^+}/C_m$ is not linear. They suggested that the nonlinearity might be due to the change of the ion exchange equilibrium constant for equation 4-4 with increasing C_{s,P^+} . The "dynamic" ion-exchange model correctly predicts the increase in sample retention with increasing concentration of pairing-ion and with decreasing ionic strength, and it often correctly predicts the retention order of sample ions in general; that is, their retention order is predicted to be the same as that observed with a conventional bonded ion-exchanger packing. The observed foldover of a plot of k' for S^- with increasing P^+ in the mobile phase was successfully explained by Deelder et al [50] using the "dynamic" ion-exchange model. These successes of the model in explaining sorption behavior are responsible for the continued growth in popularity of

the model in the recent years. However, there are limitations to the model. For example, Bidlingmeyer et al [18] pointed out that the observed retention order of certain compounds is not correctly predicted.

Hung and Taylor [47,48] extended the basic "dynamic" ion-exchange model to include the contribution to the retention from the partition of the sample ion onto the surface of the stationary phase. They suggested that the retention of S^- originates from two separate mechanisms. One is the ion-exchange process, the other involves desolvation of S^- and its "partition" on the C18 phase. The contribution from the desolvation process may be appreciable if S^- is hydrophobic. In this model, Hung and Taylor do not take into account the influence of the electrical potential on the C18 surface, which is coated with P^+ ions, in the partitioning of the S^- ion.

Ion-Interaction Models

Bidlingmeyer et al [18,135,136] proposed an ion-interaction model. According to this model, P^+ in the mobile phase can be adsorbed onto the surface of the stationary phase. These adsorbed P^+ ions form a charged primary ion layer on the reversed-phase surface. The oppositely-charged ions (e.g. Cl^-) form a secondary layer just beyond the primary layer. Both layers are in dynamic equilibrium with the mobile phase. The sample ion S^- can be retained on the surface by competing with Cl^- for a position in the secondary layer. If S^- has an "adsorbophilic" functional group, it will tend to be pulled (or pushed) from the secondary layer to the primary layer, where its alkyl chain will be found "on" the surface of the stationary phase. This has the net effect of cancelling one of the charges of P^+ in the primary layer. So another P^+ from the mobile phase must be adsorbed onto the first layer in order to restore electrostatic equilibrium on the surface. The net result is that a pair of ions (i.e. S^- and P^+) has been adsorbed onto the stationary phase. This model is more general than the previous two, but there are no quantitative equations given.

Furthermore, the proposed model is formally analogous to the "ion-pair" model in which the ion pair is formed on the surface.

Since the ion-interaction model could not quantitatively explain some observed effects, like the foldover of the plot of k' for S^- with increasing concentration of P^+ , Deming et al [22,137] proposed a quantitative, thermodynamic model based on the assumption that simple Langmuir adsorption of P^+ at the stationary phase-mobile phase interface is one of the major factors governing the retention of S^- . In this model, P^+ can affect the retention of S^- in two ways: by changing the interfacial tension and by ionic interaction with S^- on the adsorbed phase.

Electrical Double-layer Sorption Model

Almost at the same time of the appearance of the ion-interaction model in the literature, Cantwell and Puon [94] introduced the concept of electrical double-layer into the subject. It was suggested that large organic ion (P^+) can be adsorbed onto the surface of a reversed-phase sorbent to create a net surface charge which is balanced by the presence of an excess of its counterions (e.g. Cl^-) in the diffuse layer. The electrical double-layer at the sorbent/liquid interface can be quantitatively described by the Stern-Gouy-Chapman (SGC) theory. In two subsequent papers, Cantwell et al [41,138] further developed the electrical double-layer sorption model. In order to have a better control of the surface charge, a known amount of either quaternary ammonium or sulphonate groups was covalently bound to the sorbent instead of creating the surface charge by "dynamically" adsorbing these ions. It was found that two processes are responsible for the retention of S^- on a positively charged surface: one is ion exchange of S^- for co-ions (e.g. Cl^-) in the diffuse layer and the other is surface adsorption onto the charged-surface. The latter is dependent on the electrical potential of the surface which can be calculated from SGC theory. For a given sample ion, the relative contributions of the processes to the total retention is dependent on

the ion exchange capacity of the stationary phase and on the ionic strength of the mobile phase. The above studies were performed with the reverse-phase sorbent Amberlite XAD-2, which is a macroporous styrene-divinylbenzene copolymer. In the first paper on the subject, Cantwell and Puon suggested that the electrical double-layer model could explain the sorption of sample ions under ion pair chromatography conditions on a C18 bonded phase, and more recently Cantwell proposed a detailed electrical double-layer sorption model for "ion-pair" retention on C18 sorbent [95,96]. According to the model, pairing-ion P^+ can be adsorbed onto the surface of stationary phase, and creates a positive surface charge. Because electroneutrality must be maintained in the region of the sorbent/solution interface, there must exist in the solution near the interface a surface excess of negative charge (e.g. Cl^-) that is stoichiometrically equivalent to the surface charge density of P^+ . This region of negative charge is called the diffuse part of the electrical double-layer. S^- can be sorbed in two ways: ion exchange with Cl^- in the diffuse layer and adsorption onto the charged surface. In the model, the surface adsorption is dependent on the electrical potential of the surface, while the ion exchange is not. Quantitative equations have been developed for the capacity factor (k'_s) of S^- on a reversed-phase column.

The concept of electrical double-layer has been applied to the "dynamic" ion-exchange model. By assuming that the counter ion (Cl^-) can penetrate into the Stern layer ("the zone between the charge plane and the phase boundary"), Deelder et al [50] suggested that S^- can be sorbed into not only the diffuse layer but also into the Stern layer by ion exchange with X^- , and the counterions (S^- and X^-) in the Stern layer could "specifically" interact with the primary surface charge (adsorbed P^+). Pietrzyk et al [20,100,101,139-142] developed an expression, which has three adjustable parameters, for k' of S^- by considering the effect of concentration of X^- in the mobile phase on the two equilibria, equation 4-3 and 4-4, and assuming that S^- experiences an ion-exchange with Cl^- in the

diffuse layer. Bidlingmeyer et al [135,93] used the electrical double-layer concept for clarifying their primary and secondary layer concept in the ion-interaction model.

4.2 Theory of Electrical Double-layer Sorption Model

It has been shown in Chapter 3 that when a solution contains an organic ion, either P^+ or S^- , which can be adsorbed onto the ODS surface by dispersion forces and/or hydrophobic interaction, an electrical double-layer is created at the ODS/solution interface, with an excess of its inorganic counterions (e.g. Cl^- or Na^+) in the diffuse layer. As seen in Chapter 3, this can be described quantitatively with the SGC theory. Of particular interest in this chapter is the sorption behavior of S^- at the interface when the solution contains both P^+ and S^- , with P^+ present in large excess and S^- present under "trace conditions". By "trace conditions" it is usually meant that (i) the concentration of S^- on the sorbent is much smaller than that of the total surface concentration of "sorption sites", (ii) the bulk solution concentration of S^- is much smaller than those of all other components and (iii) the isotherm of S^- is linear [143]. Under these conditions, the adsorption of P^+ onto the surface will not be disturbed to any significant extent by the presence of S^- . That is, P^+ is adsorbed on the surface just as in the absence of S^- , and creates an electrical double-layer at the interface. In contrast, the sorption of S^- at the interface will be quite different now from what was in the absence of P^+ because of the presence of the large excess of P^+ . It can still be adsorbed on the surface of ODS, but the process will now be strongly influenced by the surface potential created by the adsorbed P^+ in addition to dispersion forces and/or hydrophobic interaction. Since it is a counterion of P^+ , the ion S^- can also be "sorbed" into the diffuse layer by ion-exchange for other counterions (e.g. Cl^-) in that layer. These two processes are illustrated in Fig.4-1, and will be discussed in detail in the following section. Most of the theoretical part in this section is taken, with modifications, from references 95 and 96 by Cantwell.

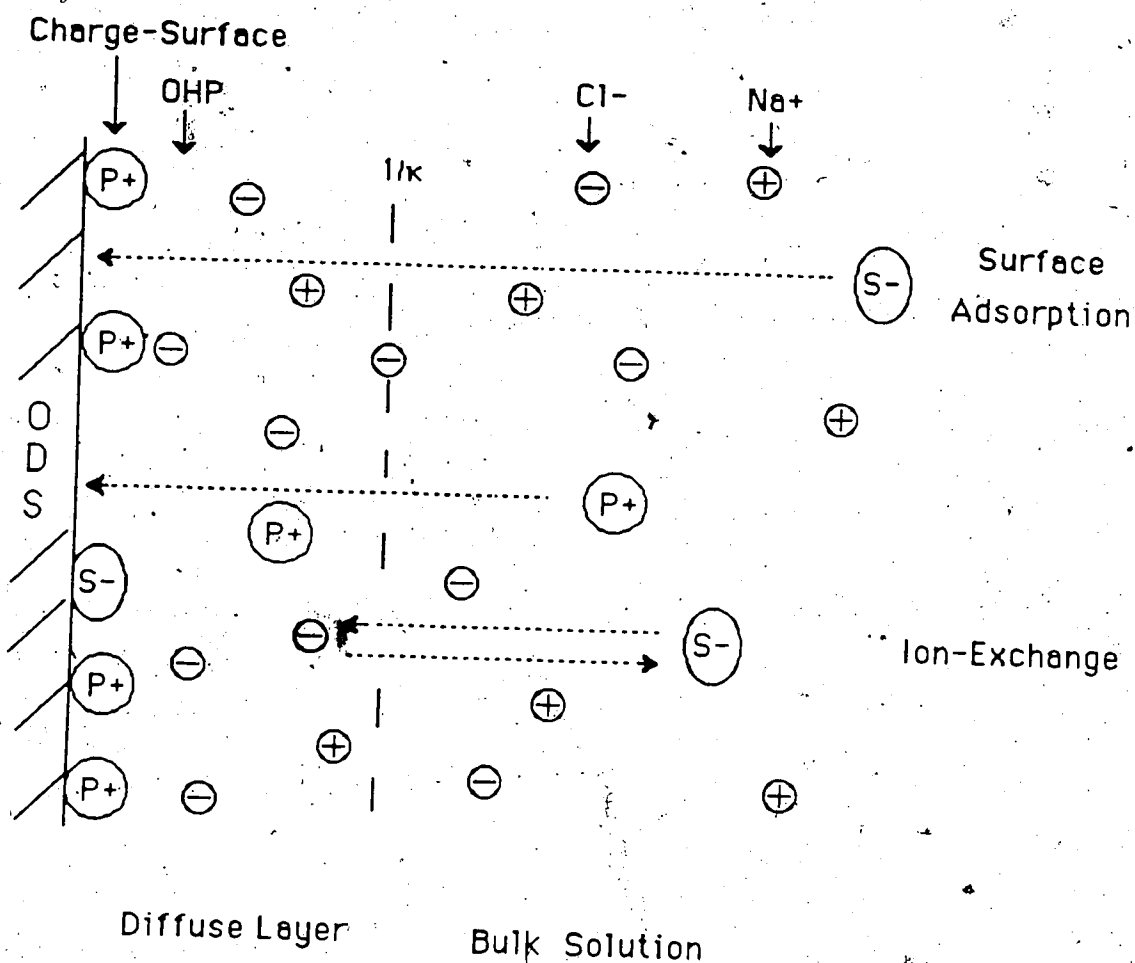
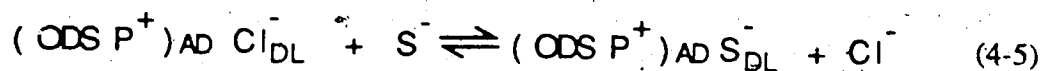


Figure 4-1 The electrical double-layer sorption model for ion pair chromatography. S^- represents the sample ion which is present at "trace conditions" and P^+ represents the pairing-ion which is in large excess. OHP represents the Outer Helmholtz Plane, which is considered as the plane of closest approach for the hydrated Cl^- to the charged surface.

4.2.1 Ion-Exchange in the Diffuse Layer

It is assumed that Cl^- is the only counterion of P^+ besides the sample ion S^- in the solution, and both Cl^- and S^- are univalent ions. The ion-exchange process between S^- and Cl^- in the diffuse layer can be represented by the equilibrium



in which P^+ with subscript AD is the adsorbed P^+ on the surface, Cl^- and S^- with subscript DL are the hydrated ions in the diffuse layer, and species without any subscripts are in the bulk solution. The ion-exchange equilibrium constant can be written as:

$$K_{\text{IEX}} = \frac{(\gamma_{\text{S}^-}^{\text{DL}} \Gamma_{\text{S}^-}^{\text{DL}}) (\gamma_{\text{Cl}^-} C_{\text{m,Cl}^-})}{(\gamma_{\text{Cl}^-}^{\text{DL}} \Gamma_{\text{Cl}^-}^{\text{DL}}) (\gamma_{\text{S}^-} C_{\text{m,S}^-})} \quad (4-6)$$

where $\Gamma_{\text{S}^-}^{\text{DL}}$ and $\Gamma_{\text{Cl}^-}^{\text{DL}}$ are the surface excesses of S^- and Cl^- in the diffuse layer; $\gamma_{\text{S}^-}^{\text{DL}}$ and $\gamma_{\text{Cl}^-}^{\text{DL}}$ are ionic activity coefficients of S^- and Cl^- in the diffuse layer; $C_{\text{m,S}^-}$ and $C_{\text{m,Cl}^-}$ are bulk solution concentrations of S^- and Cl^- ; γ_{S^-} and γ_{Cl^-} are bulk solution ionic activity coefficients of S^- and Cl^- . Since both S^- and Cl^- are univalent ions, that is $-Z^- = Z^+ = 1$, the following equations are approximately valid [139]

$$\gamma_{\text{Cl}^-} = \gamma_{\text{S}^-} \quad (4-7)$$

$$\gamma_{\text{Cl}^-}^{\text{DL}} = \gamma_{\text{S}^-}^{\text{DL}} \quad (4-8)$$

Under the specified conditions, the surface excess of Cl^- in the diffuse layer is essentially identical to that of P^+ on the surface:

$$\Gamma_{\text{Cl}^-}^{\text{DL}} = \Gamma_{\text{P}^+} \quad (4-9)$$

Since Cl^- is the only counterion of P^+ besides S^- in the solution and S^- is a trace component, the ionic strength, c , of the solution will be equal to the concentration (mol/L) of Cl^- .

$$c = C_{\text{Cl}^-} \quad (4-10)$$

By combining equation 4-7, 4-8, 4-9, 4-10 and rearranging equation 4-6, the ion-exchange distribution coefficient of S^- can be written as:

$$K_{\text{S, iex}} = K_{\text{IEX}} A_{\text{sp}} \frac{\Gamma_{\text{P}^+}}{c} \quad (4-11)$$

where A_{sp} is the specific surface area (cm^2/kg) of the packing material and Γ_{P^+} has the unit of mol/cm^2 . The "dynamic" ion-exchange capacity can be expressed as:

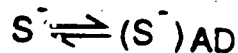
$$Q_{\text{weight}} (\text{meq/g}) = A_{\text{sp}} \Gamma_{\text{P}^+} \quad (4-12)$$

It should be pointed out that Γ_{P^+} in both equations 4-11 and 4-12 are dependent not only on the bulk concentration of P^+ , C_{m, P^+} , but also on the ionic strength c , as shown in Chapter 3. At a fixed value of c , Γ_{P^+} usually increases with increasing C_{m, P^+} , for example, in Langmuir or Freundlich fashion, or in some other fashion. The value of $K_{\text{S, iex}}$ will increase with C_{m, P^+} in the same fashion (e.g. Langmuir, Freundlich, etc). On the other hand, at a fixed value of C_{m, P^+} , Γ_{P^+} increases with increasing c (see Fig. 3-14),

but this increase is usually much slower than that of c itself. Therefore, $K_{S,iex}$ will decrease with increasing c but not as a function of $1/c$. Instead, the decrease will be at a slower rate. The consequence for $K_{S,iex}$ of the "dynamic" nature of this ion-exchanger is made evident by comparing with the situation in a conventional ion-exchanger, where $K_{S,iex}$ is inversely proportional to c [143].

4.2.2 Surface Adsorption of S^-

The adsorption of S^- onto the surface, on which a lot of P^+ has already been adsorbed, is illustrated in Fig. 4-1. Two kinds of interactions, responsible for the adsorption, can be identified: the coulombic interaction between the negatively-charged S^- and the positively-charged-surface, and the non-coulombic interaction (e.g. dispersion and/or hydrophobic effect). When an S^- ion is adsorbed from the bulk solution onto the surface, a simultaneous transfer of either its co-ion (e.g. Cl^-) from the diffuse layer to the bulk solution or of its counterion (Na^+) from the bulk solution to the diffuse layer must occur in order to maintain electroneutrality in the double-layer region. The relative extent to which each of these two charge-balancing processes occurs depends on the magnitude of Ψ_{OHP} [115,144]. At low (positive) Ψ_{OHP} , charge balancing is accomplished by the transfer of both Na^+ and Cl^- , while at large (positive) Ψ_{OHP} , only Cl^- transfer is involved because its counter-ion Na^+ is excluded from the diffuse layer by the positive potential. The energetics of the transfer of Cl^- and Na^+ contribute to the overall chemical potential change involved in the adsorption of S^- . When the ions involved are small inorganic ions like Na^+ and Cl^- , it can be assumed that this contribution is negligible compared to that from S^- . Thus the surface adsorption of S^- under "trace condition" can be represented by the process



(4-13)

along with one, or some combination of both, of the following processes:



with the processes in equation(4-14) and (4-15) assumed to be energetically equivalent.

Any S^- closer to the surface than a certain distance (arbitrarily chosen as the thickness of the compact layer, d) is considered to be adsorbed onto the surface and centered at the charged-surface, and, therefore, to experience the surface potential Ψ_0 . The equilibrium constant for the adsorption in equation 4-13 can be written as:

$$K_{ADS} = 10^3 \times \frac{\gamma_{S^-,AD} \Gamma_{S^-,ADS}}{d \gamma_{S^-} C_{S^-}} = \exp \left[- \frac{Z_- F \Psi_0 + \mu_{S^-,ADS}^0}{RT} \right] \quad (4-16)$$

in which $\Gamma_{S^-,ADS}$ is the surface excess due to the surface-adsorbed S^- , $\gamma_{S^-,AD}$ is the activity coefficient of S^- adsorbed on the surface, Z_- is the charge number on S^- , $\mu_{S^-,ADS}^0$ is the standard chemical potential for the transfer of S^- from the bulk solution to the surface when $\Psi_0 = 0$.

By rearranging equation 4-11, the surface adsorption distribution coefficient for S^- can be written as:

$$K_{S,ads} = 10^{-3} A_{sp} d \frac{\gamma_{S^-}}{\gamma_{S^-,AD}} \exp \left(- \frac{Z_- F \Psi_0 + \mu_{S^-,ADS}^0}{RT} \right) \quad (4-17)$$

And the equation can be further simplified to:

$$K_{S,ads} = 10^{-3} A_{sp} d \gamma_{S^-} \exp\left(-\frac{Z_- F \Psi_0 + \mu_{S^-,ADS}}{RT}\right) \quad (4-18)$$

$$\text{where } \mu_{S^-,ADS} = \mu_{S^-,ADS}^0 + RT \ln \gamma_{S^-,AD} \quad (4-19)$$

in which A_{sp} has the units of cm^2/kg , d is in cm , Ψ_0 is in volt, $F = 96487 \text{ coul/mol}$, $\mu_{S^-,ADS}$ is in joul/mol , $R = 8.314 \text{ joul/mol}\cdot\text{k}$, and $T = 298\text{k}$. The thermodynamic reference state for equation 4-15, at which $\gamma_{S^-,AD} = 1$, is defined as a hypothetical surface which is free of any ions (e.g. P^+ or S^-); that is, "infinite dilution" on the surface.

The surface activity coefficient, $\gamma_{S^-,AD}$, is quite different from the ionic activity coefficients. It is not related to ionic effect or electrical potential at all. It is a "correction" term to take into account the fact that the value of $\mu_{S^-,AD}$ may change due to the change in character of the surface. Changes in surface character can be from different degrees of coverage by P^+ . The best analogy in solution chemistry is the "transfer activity coefficient" which is usually used when dealing with solutes dissolved in different solvents while taking infinite dilution in aqueous as the reference state [145].

Ψ_0 is related to a_{P^+} ($= \gamma_{P^+} C_{m,P^+}$), perhaps by the Nernst equation, while the solution activity coefficient, γ_{S^-} , can be approximately related to c (when c is low) by the Debye-Huckel limiting law [145] (see Appendix III), which at 25°C is

$$\gamma_{S^-} = 10^{-0.509 c^{-1/2}} \quad (4-20)$$

Thus at a fixed c , at which γ_{P^+} and γ_{S^-} are constants, increasing C_{m,P^+} will increase Ψ_0 in equation 4-18 and therefore increase $K_{S,ads}$. In contrast, if C_{m,P^+} is fixed then increasing c will decrease γ_{S^-} , a_{P^+} and Ψ_0 , and therefore decrease $K_{S,ads}$.

The overall distribution coefficient of S^- , K_S , is the sum of the two distribution coefficients:

$$K_S = K_{S, \text{dex}} + K_{S, \text{ads}} \quad (4-21)$$

where $K_{S, \text{dex}}$ is given by equation 4-11 and $K_{S, \text{ads}}$ is given by 4-18. The retention capacity factor of S^- on the column is related to K_S by the equation

$$k'_S = \frac{W_s}{V_m} K_S \quad (4-22)$$

in which $W_s(\text{kg})$ is the weight of the stationary phase in the column and $V_m(\text{L})$ is the void volume of the column.

As discussed above, the ionic strength and the concentration of the pairing-ion in the mobile phase are the two most important parameters affecting the retention of S^- on a column under "ion-pair" conditions. When C_{m, P^+} is held constant, both $K_{S, \text{dex}}$ and $K_{S, \text{ads}}$ decrease with increasing c , and when c is held constant both $K_{S, \text{dex}}$ and $K_{S, \text{ads}}$ increase with increasing C_{m, P^+} .

As an aside, it may be noted that, if the sample ion (S^+) bears the same sign of charge as that of the pairing-ion (P^+), it is obvious that S^+ will experience a repulsion from the positively charged surface in the diffuse layer and have a negative surface excess in that layer. Consequently, S^+ will have a negative "ion-exchange" distribution coefficient (i.e. it experiences co-ion exclusion from the diffuse layer). The positive surface potential will also decrease the surface adsorption of S^+ . Thus the retention of a sample ion is dramatically reduced when it has the same sign of charge as the pairing-ion.

Experimentally testing the model presented above obviously requires measuring not only the retention of S^- at various conditions (e.g. various c and C_{m,P^+}) but also the sorption of P^+ as a function of c and C_{m,P^+} . In the present study an experimental strategy, which has been discussed in section 2-4, capable of simultaneously measuring the two has been developed.

4.3. Results And Discussions

In the present work, NBS^- is chosen as the sample ion and TBA^+ as the pairing-ion. Using the column equilibration technique, the retention of NBS^- under "trace condition" onto an ODS column was studied by measuring its distribution coefficient (K_S) as a function of the concentration of TBA^+ (ranging from 0.0017 M to 0.020 M) and ionic strength (ranging from 0.050 to 0.500). The adsorption isotherms of TBA^+ on the column were simultaneously measured. The adsorption isotherms of TBA^+ and their interpretation in terms of the SGC theory have been given in section 3.3.2. In this chapter, the electrical double-layer ion-exchange and sorption model will be quantitatively tested by fitting the experimental measured data to equation 4-21.

4.3.1 Optimizing Conditions for the Column Equilibration Technique

With the column equilibration technique, the measurements of K_S for NBS^- on the ODS column (C1 in Fig. 2-5) involves measuring the void volume (V_m) of the system, determining the total number of moles of NBS^- in the column (n_{T,NBS^-}) and calculating the value of K_S using equation 2-2 and 3-16. The value of V_m was found to be $(65.21 \pm 1.18) \mu l$ at the 95% confidence level as discussed in section 3.3.2.2. The determination of n_{T,NBS^-} involves two steps: (i) equilibrating the ODS column with a sample solution which usually contained $1.488 \times 10^{-6} M$ NBS^- and a certain concentration of TBA^+ at a particular ionic strength; (ii) eluting the NBS^- from the ODS column through an analytical column and UV detector to give the peak area for its quantitative determination.

In the equilibration step, the establishment of equilibrium between NBS^- in the sample solution and on the ODS column was verified by measuring the loading curves of NBS^- . A typical loading curve for NBS^- from a sample solution containing 0.0120M TBA^+ and ionic strength of 0.05 is presented in Fig.4-2. The complete-breakthrough volume for NBS^- is around 100ml. Loading curves measured at several other concentrations of TBA^+ and ionic strengths all showed that equilibrium for NBS^- was reached in 100 ml. Based on the results, in all the future studies a volume of 125ml of sample solution was pumped through the ODS column during the equilibration (loading) step in order to ensure that complete-breakthrough (equilibration) was reached.

It is worthwhile to point out that the complete breakthrough volume of NBS^- here is more than 10 times larger than that when no TBA^+ is present, although the amount of ODS packing used for this study (~15mg) is only about one tenth of that (~170mg) used for studying NBS^- with no TBA^+ present. This is because K_S increases dramatically under the "ion-pair" conditions.

In the elution step the NBS^- eluted from the ODS column is measured as it passes through the UV-absorbance detector. A typical signal from the UV detector is given in Fig.4-3, in which peak A is due to the absorbance of NBS^- and peak B is a "refractive index" peak due to water from column C_1 . The retention of NBS^- in this chromatogram (~8.0 min) is due to the analytical column C_2 . The area of peak A was used to obtain the total number of moles of NBS^- eluted from the ODS column by comparing it with a calibration curve of peak area vs. number of moles of NBS^- . The calibration curve, obtained by injecting standard NBS^- solutions, is shown in Fig.4-4.

The effect of TBA^+ concentration in the NBS^- standard solutions on the calibration curve has been investigated by injecting 200 μ l of a series of standard solutions which contain 9.920×10^{-5} M NBS^- and various concentration of TBA^+ with ionic strength of 0.5.

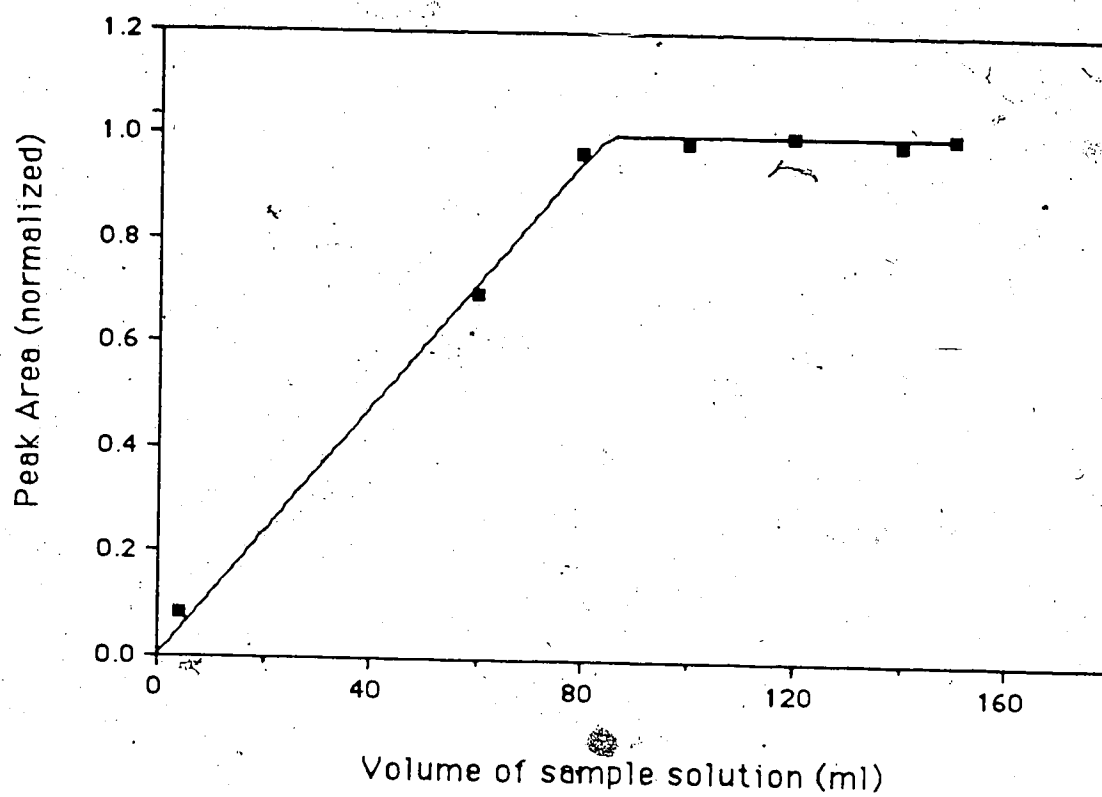


Figure 4-2 Loading curve of NBS^- on the ODS column. The sample solution contains 0.012M TBA^+ and $1.488 \times 10^{-6}\text{M NBS}^-$ with an ionic strength of 0.050.

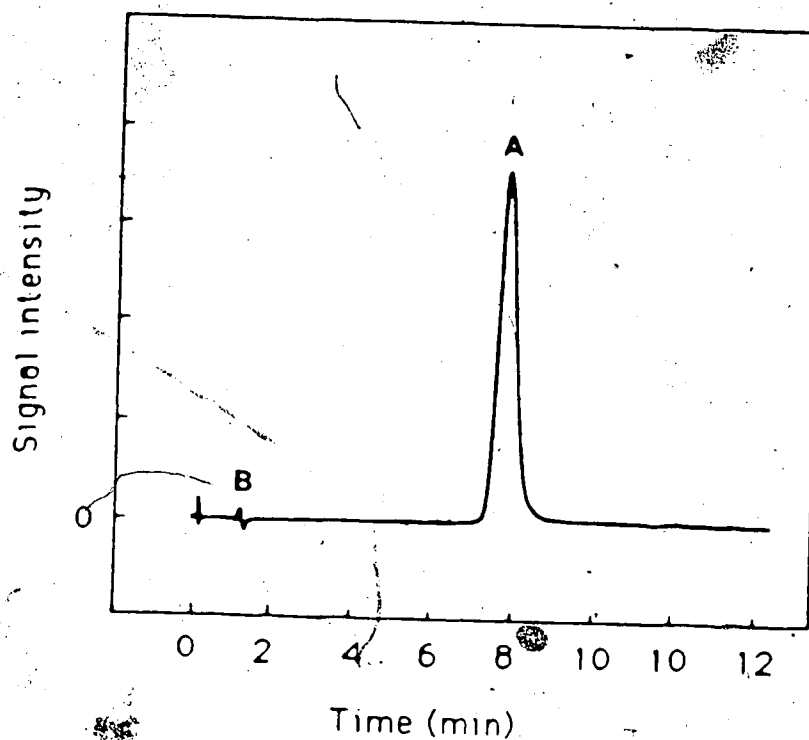


Figure 4-3 Typical signals from the UV detector D (see Fig. 2-2) for the determination of the total number of moles of NBS^- in the ODS column ($n_{\text{T},\text{NBS}^-}$). Peak A is due to NBS^- and peak B is a refractive index peak due to the water from the column C1. The retention of NBS^- in the chromatogram arises mainly from the analytical column C2. Flow rate of the eluent is 1.00 ml/min.

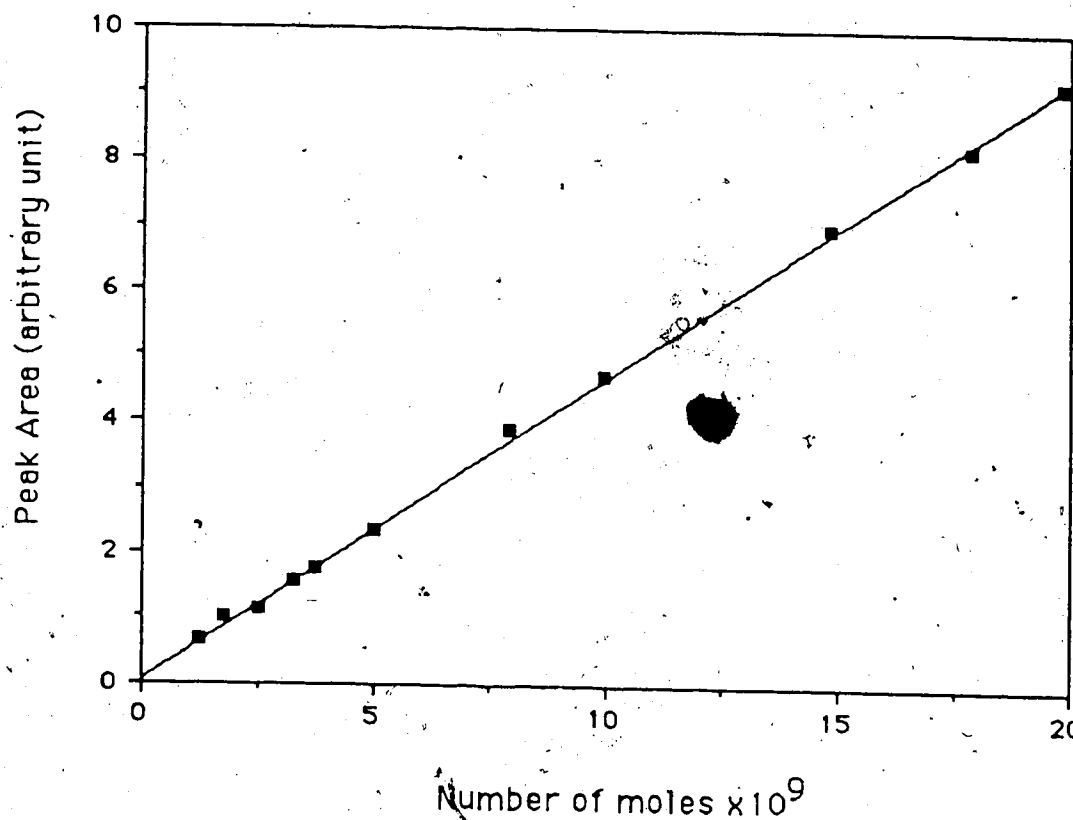


Figure 4-4 The column equilibration liquid chromatographic system calibration curve of NBS⁻ at 266nm. Two standard NBS⁻ solutions were used: one has 0.01933 M TBA⁺ and 2.480×10^{-5} M NBS⁻, and the other has 0.01933M TBA⁺ and 9.920×10^{-5} M NBS⁻. Injection volumes ranges from 50 to 200 μ l. Flow rate is 1.0 ml/min.

Shown in Fig.4-5 are the superimposed elution curves for NBS^- and TBA^+ obtained in a typical experiment. The NBS^- solute zone is overlapped by the TBA^+ zone as it migrates down column C2. In Table 4-1 is shown the influence of concentration of TBA^+ on the retention time and peak area of NBS^- . Firstly, the retention of NBS^- on the analytical column C2 was enhanced by the presence of TBA^+ in the standard solution, which is obviously due to the "ion-pair" effect. Secondly, the peak area was about 10% larger when no TBA^+ is present in the standard solution, and it becomes constant for TBA^+ concentration above at least 0.007 M. The reason for the small decrease in the peak area of NBS^- in the presence of a large excess of TBA^+ with methanol/water/NaCl eluent is not known.

In the subsequent experiments, in which TBA^+ and NBS^- were co-adsorbed on column C1, the retention time of NBS^- upon elution through column C2 was always about 8.0 min. Thus a suitable NBS^- calibration curve was prepared from standard solutions to contain 0.020 M TBA^+ , which gives an NBS^- retention time of 8.0 min (see Table 4-1).

4.3.2 Establishing Trace Conditions for NBS^- On ODS

The concentration range within which NBS^- is sorbed under "trace conditions" onto ODS was found by locating the linear range of its isotherm. The sorption isotherms of NBS^- from sample solutions which contain 0.02M of TBA^+ at ionic strengths of both 0.05 and 0.5, have been measured. This concentration of TBA^+ was chosen for study because, at a given ionic strength, K_S for NBS^- was expected to have its maximum value at this concentration. The two ionic strengths represent the highest and lowest used in all experiments. The sorption isotherms are presented in Fig.4-6. They are both linear within the concentration range of 0.0 to 2.5×10^{-6} M. Based upon this, an NBS^- concentration of 1.488×10^{-6} M was chosen for use in all subsequent experiments. The concentration was high enough to produce an accurately measurable peak area. The linearity of the isotherms

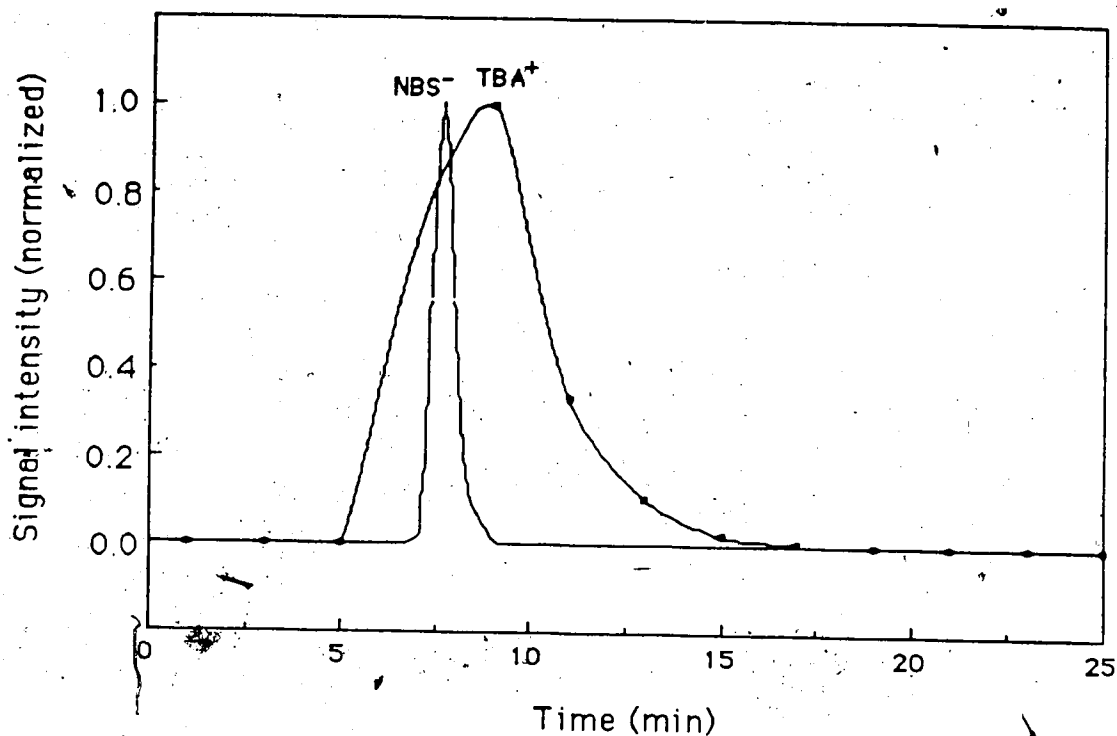


Figure 4-5 Elution curves of NBS^- and TBA^+ at the end of analytical column C_2 for a typical experiment. After the ODS column (C_1) was equilibrated with 125 ml of a sample solution (e.g. 0.012M TBA^+ and $1.488 \times 10^{-6}\text{M}$ NBS^- with an ionic strength of 0.050), the eluent was pumped at a flow rate of 1.00 ml/min through the ODS column, the analytical column C_2 and the UV detector. The NBS^- peak was given by the UV-absorbance detector at 266 nm and TBA^+ peak was obtained by collecting the eluate in a series of 2 ml portions and determining the amount of TBA^+ in each of the portions using SE/FIA.

Table 4-1 Effect of the concentration of TBA^+ in a standard NBS^- solution ($9.920 \times 10^{-5} \text{M}$) with ionic strength of 0.50 on the eluted peak area of NBS^- .

$[\text{TBA}^+]$ (mol/L)	0.0	0.0067	0.0201	0.0400	0.0500
NBS^- retention time(min)	4.06	7.32	8.03	8.11	8.19
NBS^- peak area $\times 10^{-7}$ (arbitrary unit) *	10.3 ± 0.30	9.1 ± 0.3	9.1 ± 0.4	8.9 ± 0.2	9.6 ± 0.2

* Uncertainties are standard deviations from triplicate measurements.

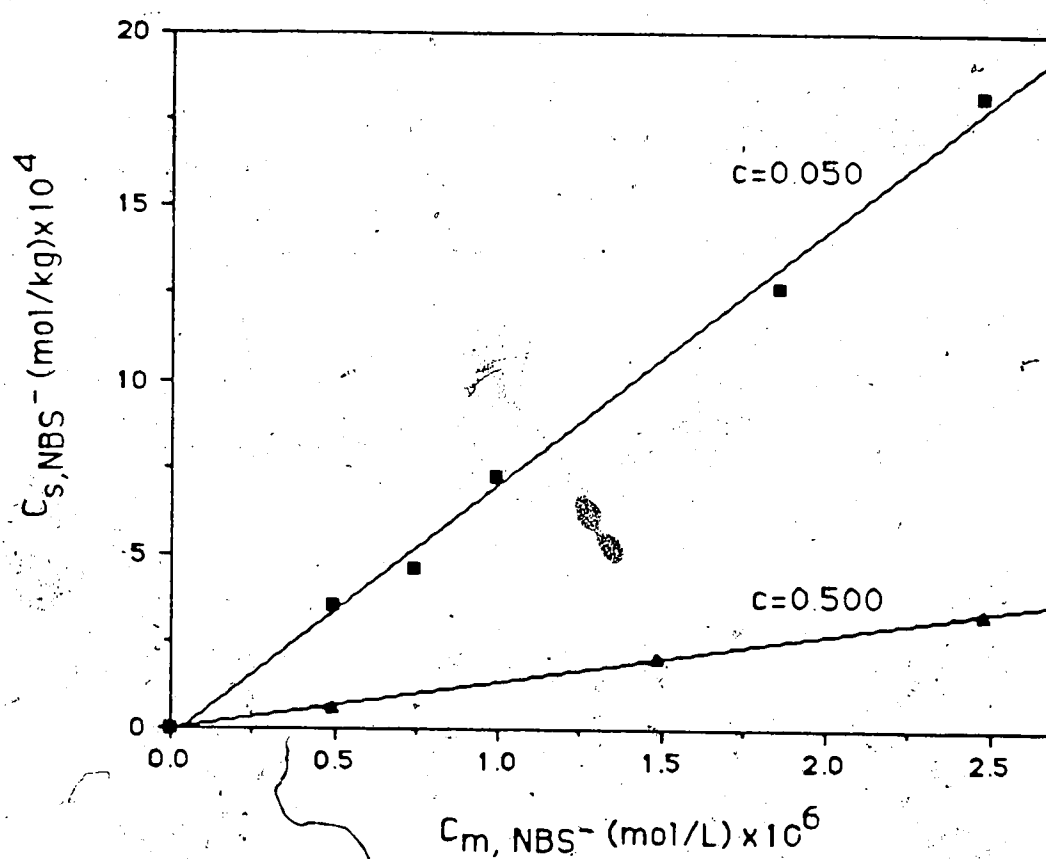


Figure 4-6 Sorption isotherms of NBS^- onto ODS packing from solution in the presence of 0.020M TBA^+ at 25°C. c is the ionic strength of the sample solution.

in Fig.4-6 shows that the concentration of NBS^- meets the "trace conditions" requirement when a large amount of TBA^+ is adsorbed onto the ODS surface. Examination of Fig.3-4 reveals that it is certainly also in the linear region of the sorption isotherm for NBS^- in the absence of TBA^+ . Therefore, it was concluded that $1.488 \times 10^{-6} \text{M}$ NBS^- in the sample solution would meet the "trace conditions" for all experimental conditions employed in this study.

4.3.3 Sorption of NBS^- Under "Ion-Pair" Conditions

The experimental data for the sorption of both NBS^- and TBA^+ as a function of the concentration of TBA^+ at five different ionic strengths are given in Table 4-2. The values of K_S for NBS^- are also given in the Table, and they are plotted as a function of the concentration of TBA^+ at various ionic strengths in Fig.4-7. The adsorption isotherms of TBA^+ have already been plotted in Fig.3-14. As can be seen from Fig.4-7, K_S increases with increasing concentration of TBA^+ at a fixed ionic strength. The increase is more pronounced at low ionic strength (e.g. 0.05) than at high ionic strength (e.g. 0.5). K_S tends to "flatten-out" at high values of C_{m,TBA^+} when ionic strength is relatively high (i.e. 0.5). At a fixed concentration of TBA^+ , K_S decreases quickly with increasing ionic strength. The decrease is more pronounced when ionic strength is low.

In this section the electrical double-layer sorption model will be used to describe these experimental results. For the $\text{NBS}^-/\text{TBA}^+$ system, equations 4-21, 4-11 and 4-18 have the forms

$$K_S = K_{S,\text{lex}} + K_{S,\text{ads}}$$

(4-23a)

Table 4-2 Experimental data on the sorption of NBS⁺ in the presence of TBA⁺ and on the adsorption isotherms of TBA⁺ at five different ionic strengths at 25°C^{*}

ionic strength	C_{m,TBA^+} mol/L	Γ_{T,TBA^+} mol $\times 10^6$	C_{s,TBA^+} mol/kg	Γ_{T,NBS^+} mol $\times 10^9$	C_{s,NBS^+} (mol/kg) $\times 10^4$	K_S (L/kg)
0.050	0.00171	1.548 \pm 0.022	0.0908 \pm 0.0013	9.811 \pm 0.116	6.148 \pm 0.072	413.2 \pm 4.9
0.050	0.004575	2.068 \pm 0.033	0.1120 \pm 0.0018	11.80 \pm 0.088	7.011 \pm 0.052	471.3 \pm 3.5
0.050	0.009155	2.557 \pm 0.010	0.1241 \pm 0.0005	13.54 \pm 0.098	8.506 \pm 0.062	571.6 \pm 4.1
0.050	0.01435	3.085 \pm 0.033	0.1361 \pm 0.0015			
0.050	0.01452			15.97 \pm 0.075	10.04 \pm 0.047	646.6 \pm 3.1
0.050	0.02022	3.560 \pm 0.047	0.1418 \pm 0.0019	17.65 \pm 0.112	11.11 \pm 0.071	746.6 \pm 4.8
0.070	0.001933	1.722 \pm 0.004	0.1010 \pm 0.0002	6.879 \pm 0.08	4.292 \pm 0.050	288.4 \pm 3.3
0.070	0.005154	2.253 \pm 0.009	0.1213 \pm 0.0005	10.31 \pm 0.03	6.462 \pm 0.019	434.2 \pm 1.3
0.070	0.007730	2.571 \pm 0.015	0.1308 \pm 0.0008	11.10 \pm 0.15	6.962 \pm 0.094	467.9 \pm 6.3
0.070	0.01031	2.845 \pm 0.011	0.1375 \pm 0.0005	11.33 \pm 0.13	7.108 \pm 0.081	477.7 \pm 5.5
0.070	0.01417	3.230 \pm 0.024	0.1459 \pm 0.0018	12.31 \pm 0.07	7.727 \pm 0.044	519.3 \pm 3.0
0.070	0.01933	3.651 \pm 0.015	0.1513 \pm 0.0006	13.02 \pm 0.15	8.177 \pm 0.094	549.5 \pm 6.3
0.100	0.001740	1.705 \pm 0.008	0.1008 \pm 0.0005	4.095 \pm 0.011	2.530 \pm 0.007	170.0 \pm 0.5
0.100	0.004579	2.244 \pm 0.021	0.1231 \pm 0.0011	5.868 \pm 0.058	3.652 \pm 0.036	245.4 \pm 2.4
0.100	0.009143	2.783 \pm 0.047	0.1384 \pm 0.0023	7.197 \pm 0.018	4.494 \pm 0.011	302.0 \pm 0.8
0.100	0.01454	3.348 \pm 0.042	0.1519 \pm 0.0019	8.879 \pm 0.060	5.558 \pm 0.038	373.5 \pm 2.5
0.100	0.02047	3.873 \pm 0.080	0.1606 \pm 0.0033	9.177 \pm 0.055	5.747 \pm 0.034	386.2 \pm 2.3
0.300	0.001721	2.026 \pm 0.022	0.1211 \pm 0.0013	1.961 \pm 0.002	1.180 \pm 0.002	79.3 \pm 0.1
0.300	0.004641	2.603 \pm 0.030	0.1456 \pm 0.0016	2.860 \pm 0.022	1.749 \pm 0.013	117.5 \pm 0.9
0.300	0.009804	3.110 \pm 0.028	0.1564 \pm 0.0014	3.452 \pm 0.018	2.123 \pm 0.011	142.7 \pm 0.7
0.300	0.01436	3.658 \pm 0.043	0.1723 \pm 0.0020	3.886 \pm 0.060	2.398 \pm 0.037	161.2 \pm 2.5
0.300	0.02011	4.170 \pm 0.037	0.1809 \pm 0.0016	4.108 \pm 0.055	2.539 \pm 0.034	170.6 \pm 2.3
0.500	0.001933	2.289 \pm 0.041	0.1369 \pm 0.0024	1.442 \pm 0.010	0.913 \pm 0.006	61.3 \pm 0.4
0.500	0.005154	2.918 \pm 0.012	0.1634 \pm 0.0007	2.086 \pm 0.017	1.320 \pm 0.011	88.71 \pm 1.0
0.500	0.009019	3.405 \pm 0.012	0.1783 \pm 0.0008	2.301 \pm 0.005	1.425 \pm 0.003	95.8 \pm 0.2
0.500	0.01417	3.928 \pm 0.012	0.1901 \pm 0.0006	2.921 \pm 0.005	1.849 \pm 0.003	124.3 \pm 0.2
0.500	0.01870	4.319 \pm 0.013	0.1962 \pm 0.0006	3.149 \pm 0.009	1.993 \pm 0.006	133.9 \pm 0.4
0.500	0.02290	4.686 \pm 0.016	0.2021 \pm 0.0007	3.257 \pm 0.019	2.061 \pm 0.012	138.5 \pm 0.8

* Uncertainties are standard deviations of triplicate measurements.

** Γ_{TBA^+} (mol/cm²) can be obtained by multiplying C_{s,TBA^+} (mol/kg) by 3.236×10^{-10} kg/cm².

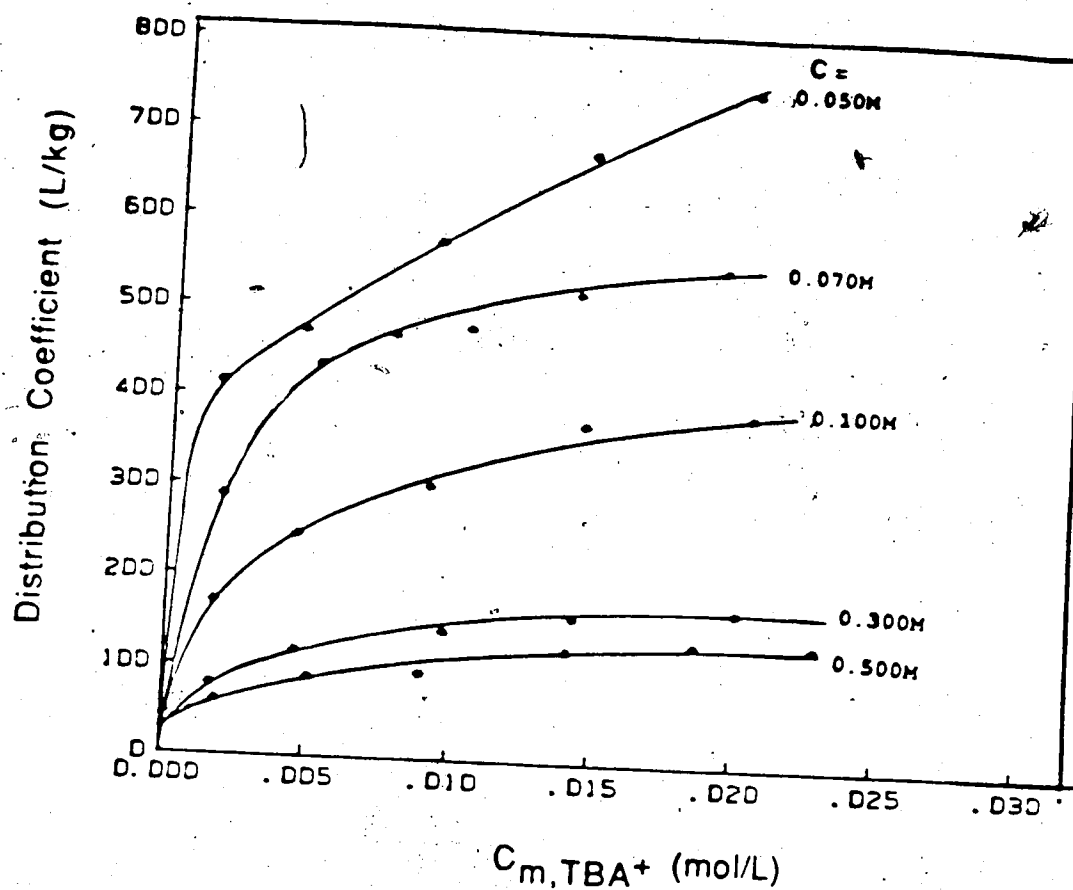


Figure 4-7 Distribution coefficient of NBS⁻ (ks) on the ODS packing vs. the concentration of TBA⁺ at five different ionic strengths. The concentration of NBS⁻ in the solutions was fixed at $1.488 \times 10^{-6}M$.

where

$$K_{S, \text{IEX}} = K_{\text{IEX}} A_{\text{sp}} \frac{\Gamma_{\text{TBA}^+}}{c} \quad (4-23b)$$

$$K_{S, \text{ads}} = 10^{-3} A_{\text{sp}} d \gamma_{\text{NBS}^-} \exp\left(-\frac{Z_- F \Psi_0 + \mu_{\text{NBS}^-, \text{ADS}}}{RT}\right) \quad (4-23c)$$

in which K_{IEX} is the equilibrium constant for the ion exchange of NBS^- for Cl^- in the diffuse layer; d is the thickness of the compact part of the electrical double-layer, which has been evaluated in section 3.3.2.5 to be $10.3 \times 10^{-8} \text{ cm}$; γ_{NBS^-} is the bulk solution activity coefficient of NBS^- ; and $\mu_{\text{NBS}^-, \text{ADS}}$ (joule/mol) is the chemical potential for transfer one mole of NBS^- from the bulk solution to the surface of the ODS.

The model evaluation is based on the following principle: At a fixed activity of TBA^+ (e.g. $a_{\text{TBA}^+} = 4 \times 10^{-3} \text{ M}$), equations 4-23 a-c contain the following:

- (i) four variables: K_S (L/kg), Γ_{TBA^+} (mol/cm²), γ_{NBS^-} and c ;
- (ii) three known constants: $A_{\text{sp}} = 3.09 \times 10^{-9} \text{ cm}^2/\text{kg}$, $d = 10.3 \times 10^{-8} \text{ cm}$ and Ψ_0 whose values at several different a_{TBA^+} have been given in Table 3-13;
- (iii) two unknown constants: K_{IEX} and $\mu_{\text{NBS}^-, \text{ADS}}$ (joule/mol).

Of the four variables only c is an independent variable. The values of K_S and Γ_{TBA^+} at various c can be obtained from Fig.4-7 and Fig.3-15 respectively, while those of γ_{NBS^-} can be obtained from the literature (see below). Of all the variables and constants in equation 4-23 a-c, only K_{IEX} and $\mu_{\text{NBS}^-, \text{ADS}}$ are unknown. Thus it is possible to

perform a non-linear least-squares fit of equation 4-23 a-c to the experimental data and to evaluate the two adjustable parameters K_{IEX} and $\mu_{\text{NBS}^-, \text{ADS}}$. How well the equation fits the data is an indication of how well the model agrees with the experiment.

The values of γ_{NBS^-} at high ionic strength (>0.1) were assumed to be the same as those of p-toluenesulfonate and can be obtained from the literature [146]. While those at low ionic strength were obtained from the extended Debye-Huckel equation [120] by assuming its ionic size parameter to be 3.5×10^{-8} cm (see Appendix III). The values of γ_{NBS^-} are given in Tables 4-3 to 4-9.

The values of Γ_{TBA^+} and K_S at various c can be obtained in the following way: The solution activity coefficients of TBA^+ (given in Table 3-8) were used to convert the molar concentration (the x-axis in both Fig. 3-15 and 4-7) into activities. Then at a fixed value of activity of TBA^+ (a_{TBA^+}), the values of Γ_{TBA^+} at each of the five different c were obtained from the plots in Fig. 3-15 as described in section 3.3.2.5. Likewise, at the same fixed value of a_{TBA^+} , the values of K_S for NBS^- at each of the five different c were obtained from the plots in Fig. 4-7. These operations to obtain the values of Γ_{TBA^+} and K_S at the five different c were repeated for several different values of a_{TBA^+} . The values of Γ_{TBA^+} and K_S thus obtained, at various c and different a_{TBA^+} , are listed in the 2nd and 4th columns in Table 4-3 to 4-9.

Equations 4-23 a-c were fitted to the values of Γ_{TBA^+} , K_S and γ_{NBS^-} at various c for each of the seven a_{TBA^+} with a nonlinear least-squares curve-fitting program KINET [147] (see Appendix V). The values of K_{IEX} and $\mu_{\text{NBS}^-, \text{ADS}}$ with which equation 4-23a-c can best be fit to these experimental data, along with their standard deviations are listed in Table 4-10. Also listed in Table 4-10 are the computed values of $Z \cdot F \Psi_0$ and the "electrochemical potential" ($Z \cdot F \Psi_0 + \mu_{\text{NBS}^-, \text{ADS}}$) for the numerator of the

Table 4-3 Experimental and calculated values of the distribution coefficient of NBS^- , and experimental values of surface excess of TBA^+ at five different ionic strengths when $a_{\text{TBA}^+} = 2.0 \times 10^{-3} \text{ M}$ and $\Psi_0 = 0.106 \text{ volt}$.

c	Γ_{TBA^+} (mol/cm^2) $\times 10^{12}$	γ_{NBS^-}	K_S (exp.)	K_S^* (calc.)	$K_{S,\text{ads}}^*$ (calc.)	$K_{S,\text{iex}}^*$ (calc.)
0.050	32.5	0.810	440	432	12.3	420
0.070	35.0	0.785	324	335	11.9	323
0.100	36.3	0.759	206	246	11.5	235
0.300	43.9	0.660	100	105	10.0	94.5
0.500	48.9	0.608	80.6	72.4	9.2	93.2

* calculated values from equation 4-23a-c.

Table 4-4: Experimental and calculated values of the distribution coefficient of NBS^- , and experimental values of surface excess of TBA^+ at five different ionic strengths when $a_{\text{TBA}^+} = 4.0 \times 10^{-3} \text{ M}$ and $\Psi_0 = 0.107 \text{ volt}$.

c	Γ_{TBA^+} (mol/cm ²) $\times 10^{12}$	γ_{NBS^-}	K_S (exp.)	K_S^* (calc.)	$K_{S,\text{ads}}^*$ (calc.)	$K_{S,\text{lex}}^*$ (calc.)
0.050	34.4	0.810	492	490	11.8	478
0.070	39.3	0.785	420	403	11.5	392
0.100	40.9	0.759	263	296	11.0	285
0.300	48.9	0.660	128	123	9.60	114
0.500	54.4	0.608	95.0	85.0	8.90	75.9

* calculated values from equation 4-23a-c.

Table 4-5 Experimental and calculated values of the distribution coefficient of NBS^- , and experimental values of surface excess of TBA^+ at five different ionic strengths when $a_{\text{TBA}^+} = 6.0 \times 10^{-3} \text{ M}$ and $\Psi_0 = 0.125 \text{ volt}$.

c	Γ_{TBA^+} (mol/cm^2) $\times 10^{12}$	γ_{NBS^-}	K_S (exp.)	K_S^* (calc.)	$K_{S,\text{ads}}^*$ (calc.)	$K_{S,\text{iex}}^*$ (calc.)
0.050	38.0	0.810	542	547	34.8	512
0.070	42.4	0.785	460	442	33.7	408
0.100	44.0	0.759	311	329	32.6	296
0.300	52.1	0.660	145	145	28.4	117
0.500	58.0	0.608	111	104	26.1	78.0

* calculated values from equation 4-23a-c.

Table 4-6 Experimental and calculated values of the distribution coefficient of NBS^- , and experimental values of surface excess of TBA^+ at five different ionic strengths when $a_{\text{TBA}^+} = 8.0 \times 10^{-3} \text{ M}$ and $\Psi_0 = 0.140 \text{ volt}$.

c	Γ_{TBA^+} (mol/cm ²) $\times 10^{12}$	γ_{NBS^-}	K_S (exp.)	K_S^* (calc.)	$K_{S,\text{ads}}^*$ (calc.)	$K_{S,\text{iex}}^*$ (calc.)
0.050	40.8	0.810	585	592	47.4	544
0.070	44.6	0.785	487	471	45.9	425
0.100	46.3	0.759	345	353	44.4	309
0.300	54.4	0.660	155	160	38.6	121
0.500	60.5	0.608	121	116	35.5	80.6

* calculated values from equation 4-23a-c.

Table 4-7 Experimental and calculated values of the distribution coefficient of NBS^- , and experimental values of surface excess of TBA^+ at five different ionic strengths when $a_{\text{TBA}^+} = 10.0 \times 10^{-3} \text{ M}$ and $\Psi_0 = 0.154 \text{ volt}$.

c	Γ_{TBA^+} (mol/cm^2) $\times 10^{12}$	γ_{NBS^-}	K_S (exp.)	K_S^* (calc.)	$K_{S,\text{ads}}^*$ (calc.)	$K_{S,\text{iex}}^*$ (calc.)
0.050	44.0	0.810	625	631	49.7	581
0.070	46.2	0.785	509	494	48.2	446
0.100	48.3	0.759	366	373	46.6	326
0.300	56.2	0.660	161	167	40.5	127
0.500	64.7	0.608	127	122	37.3	84.4

* calculated values from equation 4-23a-c.

Table 4-8 Experimental and calculated values of the distribution coefficient of NBS^- , and experimental values of surface excess of TBA^+ at five different ionic strengths when $a_{\text{TBA}^+} = 12.0 \times 10^{-3} \text{ M}$ and $\Psi_0 = 0.163 \text{ volt}$.

c	Γ_{TBA^+} (mol/cm ²) $\times 10^{12}$	γ_{NBS^-}	K_S (exp.)	K_S^* (calc.)	$K_{S,\text{ads}}^*$ (calc.)	$K_{S,\text{iex}}^*$ (calc.)
0.050	44.3	0.810	663	663	45.7	618
0.070	47.5	0.785	528	528	44.2	474
0.100	49.8	0.759	379	391	43.3	348
0.300	57.5	0.660	168	172	37.7	134
0.500	64.0	0.608	132	124	34.7	89.3

* calculated values from equation 4-23a-c.

Table 4-9 Experimental and calculated values of the distribution coefficient of NBS^- , and experimental values of surface excess of TBA^+ at five different ionic strengths when $a_{\text{TBA}^+} = 14.0 \times 10^{-3} \text{ M}$ and $\Psi_0 = 0.169 \text{ volt}$.

c	Γ_{TBA^+} (mol/cm^2) $\times 10^{12}$	γ_{NBS^-}	K_S (exp.)	K_S^* (calc.)	$K_{S,\text{ads}}^*$ (calc.)	$K_{S,\text{iex}}^*$ (calc.)
0.050	45.0	0.810	700	692	37.0	655
0.070	48.5	0.785	541	540	35.8	504
0.100	51.1	0.759	388	406	34.6	372
0.300	58.6	0.660	171	172	30.1	142
0.500	65.1	0.608	134	123	27.8	84.8

* calculated values from equation 4-23a-c.

Table 4-10 Results of the non-linear least-squares fitting of the experimental data to equation 4-23a-c.

μ_{TBA}^+ (mol/L)	K_{IEX}^*	$\mu_{NBS^-,ADS}^*$ (kJ/mol)	$Z.F\psi_0$ (kJ/mol)	$(Z.F\psi_0 + \mu_{NBS^-,ADS})$ (kJ/mol)
0.002	209 ± 10	0.64 ± 2.9	-10.2 ± 0.6	-9.56 ± 2.96
0.004	226 ± 18	0.86 ± 5.8	-10.3 ± 0.8	-9.44 ± 5.85
0.006	218 ± 11	0.13 ± 1.3	-12.0 ± 0.8	-12.1 ± 1.53
0.008	216 ± 8	0.60 ± 0.70	-13.5 ± 0.9	-12.9 ± 0.8
0.010	219 ± 7	1.8 ± 0.6	-14.9 ± 1.0	-13.1 ± 1.2
0.012	226 ± 6	2.9 ± 0.6	-15.7 ± 1.1	-12.8 ± 1.3
0.014	236 ± 8	4.0 ± 1.1	-16.4 ± 1.1	-12.4 ± 1.6
mean	$221 \pm 10^{**}$			

* Uncertainties for K_{IEX} and $\mu_{NBS^-,ADS}$ are standard deviations.

** Uncertainty in the mean value of K_{IEX} is a "pooled" value of the individual standard deviations.

exponential term in equation 4-23c. The electrochemical potential is, in fact, a free-energy for the adsorption.

Using the values of K_{IEX} and $\mu_{\text{NBS}^-, \text{ADS}}$ it is now possible to calculate the values of K_{S} , $K_{\text{S, iex}}$ and $K_{\text{S, ads}}$ for a fixed value of a_{TBA^+} at each of the five ionic strengths using equation 4-23a-c, respectively. These calculated values are given in the last three columns in Tables 4-3 to 4-9 for the seven different a_{TBA^+} . They are plotted in Fig. 4-8 to 4-11 as a function of ionic strength for four of the values of a_{TBA^+} (0.004, 0.008, 0.010 and 0.014M). In the figures the points are the experimentally measured values of K_{S} ; the solid line shows the theoretical values calculated from equation 4-23 a-c using the values of K_{IEX} and $\mu_{\text{NBS}^-, \text{ADS}}$ from Table 4-10. The dashed line labelled IEX, showing the contribution of the ion-exchange process ($K_{\text{S, iex}}$), was calculated from equations 4-23b using the value of K_{IEX} from Table 4-10 and the dotted line labelled ADS, showing the contribution of surface adsorption ($K_{\text{S, ads}}$), was calculated from equation 4-23c using the value of $\mu_{\text{NBS}^-, \text{ADS}}$ from Table 4-10.

Fig. 4-8 to 4-11 clearly indicate that ion-exchange is the main mechanism for the sorption of NBS^- at the interface. The surface adsorption process is not important in most of the cases, and only becomes significant when ionic strength is high. This is not surprising considering the finding of Hux and Cantwell [41] regarding the sorption of an organic cation (m-nitrobenzyltrimethylammonium) onto the surface of sulfonated ion-exchangers of low capacity. They found that as the ion-exchange capacity was increased from 0.01 to 0.05 meq/g the contribution of ion-exchange became relatively more important than that of surface adsorption. Since the ODS packing in the present study has a "dynamic" ion-exchange capacity ranging from 0.09 to 0.20 meq/g, which is even larger than the capacities studied by Hux and Cantwell, one might expect that ion-exchange would be the dominant sorption process. It can be seen from Fig. 4-8 to 4-11 and Tables 4-3 to

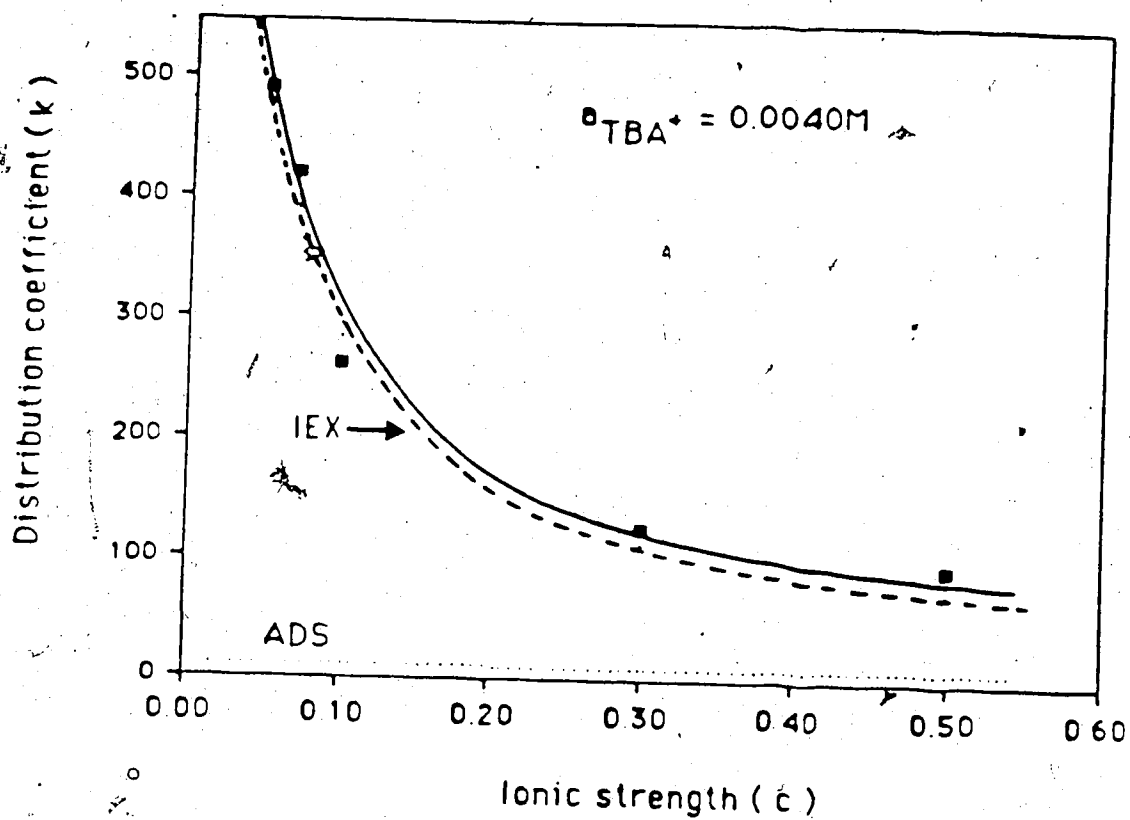


Figure 4-8 Distribution coefficient of NBS⁻ on the ODS packing vs. ionic strength at $TBA^+ = 0.0040M$. Points are experimental. The solid line through points is from the least-squares fit of equation 4-23a-c.

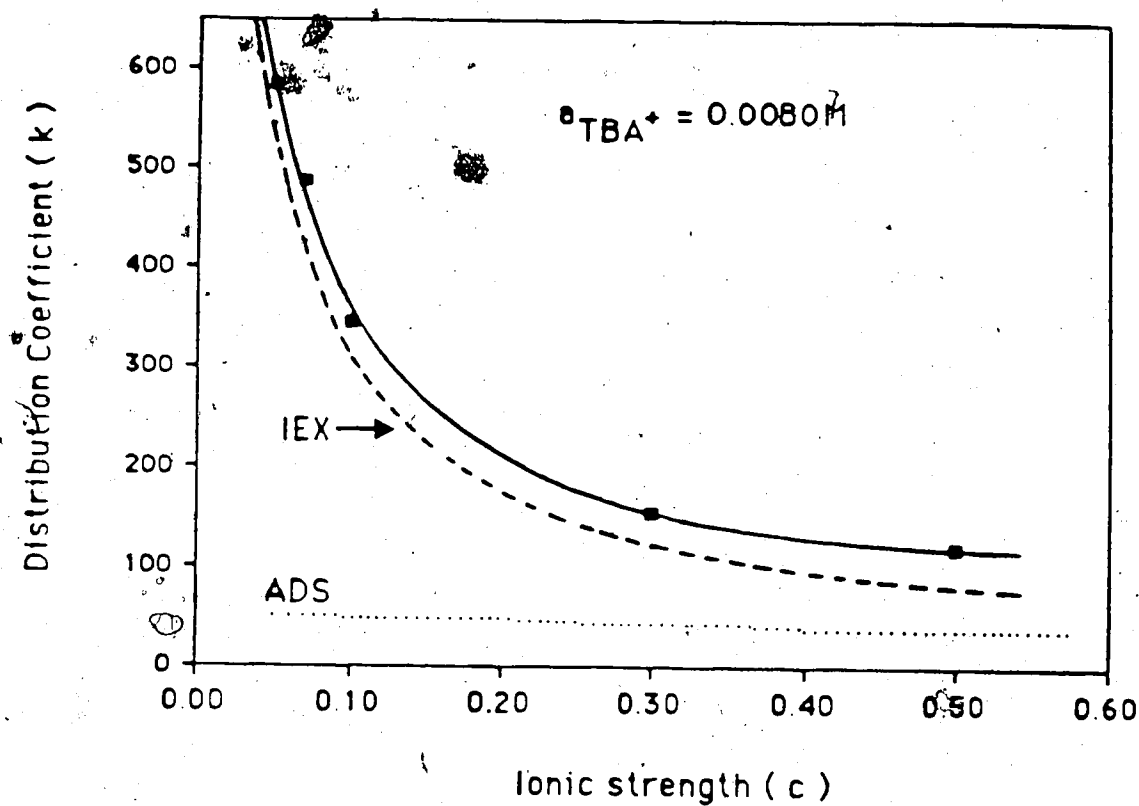


Figure 4-9 Distribution coefficient of NBS^- on the ODS packing vs. ionic strength at $a_{\text{TBA}^+} = 0.0080\text{M}$. Points are experimental. The solid line through points is from the least-squares fit of equation 4-23a-c.

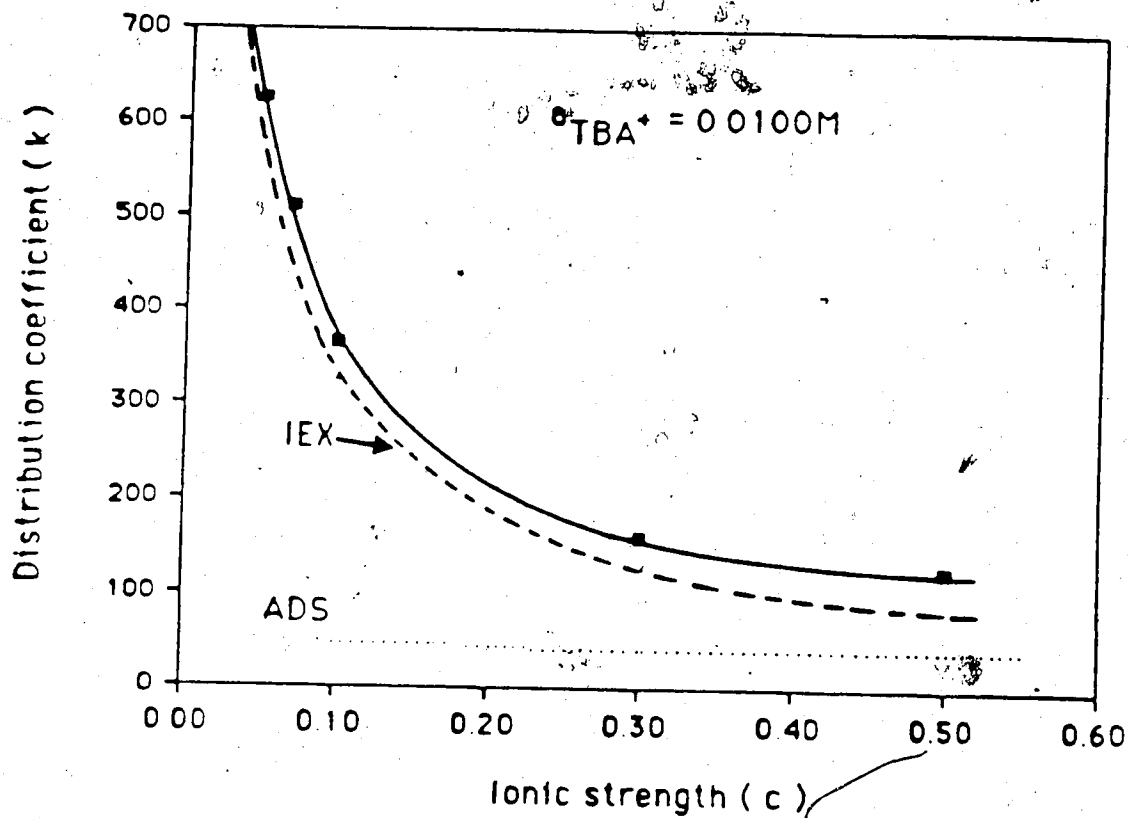


Figure 4-10 Distribution coefficient of NBS⁻ on the ODS packing vs. ionic strength at $a_{TBA^+} = 0.010M$. Points are experimental. The solid line through points is from the least-squares fit of equation 4-23a-c.

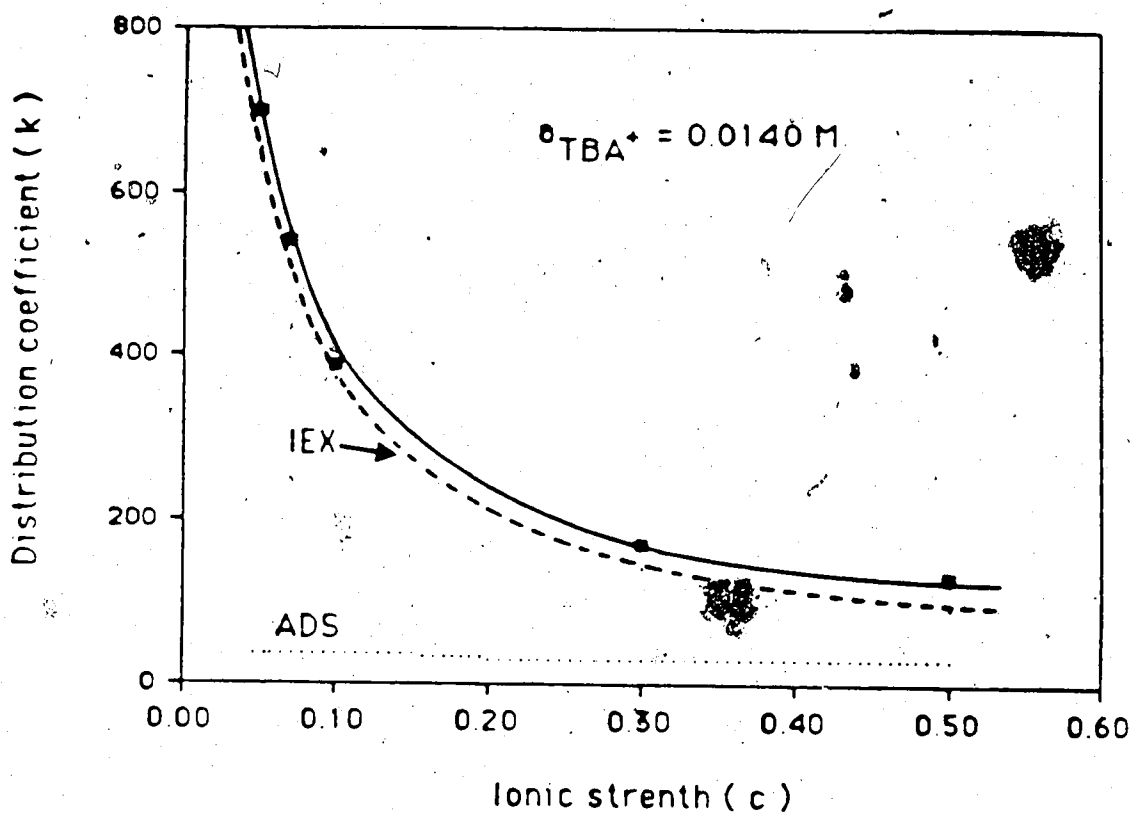


Figure 4-11 Distribution coefficient of NBS⁻ on the ODS packing vs. ionic strength at $a_{TBA^+} = 0.014 M$. Points are experimental. The solid line through points is from the least-squares fit of equation 4-23a-c.

4-9 that at a constant $a_{TBA^+} + K_{S, \text{icx}}$ decreases markedly with c . The reason for this, as discussed in section 4.2, is the decrease of (Γ_{TBA^+}/c) in equation 4-23b with increasing c . In contrast, the value of $K_{S, \text{ads}}$ at constant a_{TBA^+} decreases only slightly with increasing c . This is because, at constant a_{TBA^+} , Ψ_0 is constant and γ_{NBS^-} is the only parameter in equation 4-23 c which changes with c . Obviously, since $K_{S, \text{icx}}$ decreases rapidly with c while $K_{S, \text{ads}}$ decreases only slightly, the relative contribution of $K_{S, \text{icx}}$ to the overall K_S increases at higher c . This is also consistent with the finding of Hux and Cantwell [41].

Some comments on the observed values of the two "adjustable parameters", K_{IEX} and $\mu_{NBS^-, \text{ADS}}$, in Tables 4-10 are in order. Over the small range of ion-exchange capacity (0.091-0.200 meq/g) the value of K_{IEX} is essentially constant, independent of a_{TBA^+} and c (this can be shown by t-testing for the largest and smallest values at the 99% confidence level using three degrees of freedom).

The values of the chemical potential term $\mu_{NBS^-, \text{ADS}}$ listed in Table 4-10 have relatively large standard deviations. This is due to the fact that $\mu_{NBS^-, \text{ADS}}$ is the only adjustable parameter of $K_{S, \text{ads}}$ (see equation 4-23c) and it is much smaller than $Z_F \Psi_0$, to which it is added. This can be seen in the last three columns in Table 4-10. Therefore, any small "noise" in $K_{S, \text{icx}}$ will be reflected by large relative standard deviations of $\mu_{NBS^-, \text{ADS}}$. The large standard deviation of $\mu_{NBS^-, \text{ADS}}$ has very little effect on the overall goodness of fit of equations 4-23a-c to the experimental data because it is usually much smaller than $Z_F \Psi_0$ and does not have much "weight" in the fitting process. The uncertainties in the values of $\mu_{NBS^-, \text{ADS}}$ in Table 4-10 are too large to allow any interpretation of a trend toward increasing or decreasing with a change in a_{TBA^+} . It might be noted, however, that in situations where the ion exchange capacity (Q_{weight} or Γ_{TBA^+}) varies greatly with experimental conditions, which is not the case here, it would not be surprising to find that μ_{ADS} changes. The effect could arise in the following way: as the ODS surface is covered to a larger degree by TBA^+ ion, the hydrophobic character of the

surface would change and the surface activity coefficient, $\gamma_{S,AD}$, changes. This would cause $\mu_{S,ADS}$ to change. The meaning of $\mu_{NBS^-,ADS}$ can be further clarified by imagining a neutral compound S (whose structure is the same as S-) being adsorbed onto the surface in the presence of a large excess of TBA^+ in the solution. For a neutral solute there is no ion-exchange, so that $\mu_{S,ADS}$ is the only term in the numerator of the exponent of equation 4-23c. The change in $\mu_{S,ADS}$ is another way of saying that S is adsorbed on the surface to a different extent. It has been reported that the adsorption of neutral organic compounds onto the ODS surface decreases with increasing concentration of another charged organic ion in the solution and, thus, on the ODS surface [18,22,65]. In the context of their models, Hung and Taylor [47,48] suggested that the decrease is due to the decrease in available surface area as more of the pairing-ions are adsorbed onto the surface, and Knox and co-worker [65] suggested that the decrease is caused by "a slight lessening of the interaction with the stationary phase as this becomes progressively more polar through adsorption of the hetaeron".

4.4. Conclusion

A good agreement between the experimentally measured values for K_S of NBS^- and those calculated from equation 4-23 a-c at various ionic strengths and different activities of TBA^+ is obvious from both Tables 4-3 to 4-8 and the Fig.4-8 to 4-11. This ability to quantitatively describe the experimental facts is considered to be direct experimental support for the electrical double-layer sorption model. Under the present experimental conditions, for which the "dynamic" ion-exchange capacity is relatively large, ion-exchange is the more important sorption process; surface adsorption becomes significant only when the ionic strength is very high.

Chapter 5

Future Studies

The electrical double-layer sorption model for ion pair chromatography has been successfully used to describe the retention behavior of a sample ion (NBS^-) in the presence of large excess of a pairing-ion (TBA^+) and an inert electrolyte (NaCl). It was shown that the sample ion can be retained on an ODS column by two separate processes: ion-exchange for other co-ions (Cl^-) in the diffuse layer and surface adsorption onto the "charged surface". In this chapter, additional studies designed to understand how the concentration of organic modifiers (e.g. methanol, acetonitrile etc) in the mobile phase and the size or hydrophobicity of the sample ion influence the relative contribution of the two retention processes to the overall are discussed.

5.1. Mobile Phases with Organic Modifiers

This study would involve investigating the retention of NBS^- onto an ODS column as a function of the concentration of an organic modifier (e.g. methanol) in the mobile phase. In a typical system of ion pair chromatography on bonded C18 phases, the mobile phase is usually an aqueous buffer solution with a certain percentage of an organic modifier (e.g. 40% methanol). It is well known that the addition of an organic modifier to the mobile phase causes decreases both in the overall sorption of sample ions [12,15,49, 129 130,153,154] and in the sorption of pairing-ions on the ODS surface [47,48,49,129]. In this experiment, the influence of organic modifier concentration on the sorption of the pairing-ion and on the two separate retention processes of the sample ion, namely ion-exchange and the surface adsorption, will be studied.

The experimental strategy and procedures for measuring the distribution coefficients of NBS^- , under "trace conditions" in the presence of large excess of TBA^+ , and the sorption isotherms of TBA^+ onto the ODS packing would be essentially the same as those described in section 2.4 except that the sample solution would be prepared from an water/methanol mixed solution containing a fixed percentage (e.g. 40%) of methanol. Two families of curves, similar to those in Fig.3-14 (sorption isotherms of TBA^+) and Fig.4-7, would be simultaneously obtained from the experiment for this mobile phase. The experiment would be repeated using mobile phases containing different percentages (e.g. 60%, 80% and 90% v/v) of methanol. The contributions of ion-exchange and surface adsorption to the overall retention of NBS^- would be evaluated using the electrical double-layer sorption model for each of the mobile phase compositions. The effect of methanol in the mobile phase on the two retention processes could then be quantified.

In this experiment, the measurement of the void volume, V_m , might be a potential problem. A number of workers reported that the void volume of an ODS column decreases with increasing concentration of organic modifiers in the mobile phases [45, 81, 107, 155]. It is generally agreed that the decrease is caused by the sorption of the organic modifiers onto or into the ODS surface. Sorption isotherms of methanol and acetonitrile onto ODS packings from their aqueous solutions have been measured by Scott et al [81] and by Karger et al [155]. One way to determine V_m in this experiment was described by Karger et al [155]: The ODS column is first equilibrated with water and then is eluted with ethanol into a volumetric flask. The volume of water, V_{max} , in the collected eluate is determined (see section 2.3.5). Next, the column is equilibrated with a solution containing methanol at a percentage, C_m , (e.g. 60% v/v) of interest, and is then eluted with ethanol into a volumetric flask. The total volume, V_t , (including all the methanol in the voids and "extracted" into the surface) in the collected eluate is determined by a GC method (see

section 2.3.5). The void volume of the column, V_m , for the solution containing methanol at the specified concentration can be calculated by the following iterative processes:

(i) assuming $V_m = V_{max}$ (5-1)

(ii) then the volume of methanol "extracted" into the surface can be calculated from the equation

$$V_x = V_t - C \cdot V_m \quad (5-2)$$

(iii) a better estimate of V_m is obtained by equation

$$V_m = V_{max} - V_x \quad (5-3)$$

The value of V_m thus obtained is then used in equation 5-2 to get a new value of V_x . This procedure is repeated until V_m has an essentially constant value.

5.2 Retention Mechanism of Large Organic Sample Ions

It seems, from both the present thesis and the literature, that ion-exchange in the diffuse layer is likely to be the dominant retention process for inorganic and small organic sample ions in ion pair chromatography when pairing-ions are relatively large organic ions (e.g. TBA^+). If the sample ion is a large organic sample ion or a biomolecule, the situation might be different. Since the separation of large organic ions and biomolecules by ion pair chromatography has become increasingly important in the recent years [8,156,157,158], it is of both practical and theoretical interest to study the retention "mechanism" of these ions.

It is well known that the adsorption of organic ions onto a chemically bonded reverse-phase increases with increasing number of hydrocarbon groups in the molecules due to the increase of dispersion forces and/or hydrophobic interaction [25]. So it is

expected that the surface adsorption process will increase with increasing number of hydrocarbon groups in the sample ions. It is also known that the ion-exchange of organic ions onto conventional ion-exchangers increases with increasing number of hydrocarbon groups in the organic ions [143]. Therefore, sorption due to ion-exchange process is also expected to increase with increasing size of the sample ions. The relative contributions of the two retention processes for large organic sample ions will be the concern of the study.

While the experimental strategy and apparatus setup are basically the same as those described in the thesis, this study would involve measuring the retention of sample ions on an ODS column as a function of the number of carbon atoms in the sample ions in a homologous series, such as $C_nH_{2n+1}-C_6H_4-SO_3^-$, and with TBA^+ as the pairing-ion. The mobile phase could be neat-aqueous or water/methanol mixed solution but its composition must be fixed. With one of the homologous series as a sample ion, its retention behavior, under "trace conditions" in the presence of large excess of the pairing-ion TBA^+ , and the surface concentration of TBA^+ on the ODS packing are measured as a function of the concentration of TBA^+ and ionic strength in the solution. When several members ($n=2, 4, 6, 8$ and 12) of the homologous series have been studied, the electrical double-layer sorption model is applied to the experimental data for each of them to evaluate the two retention processes. Then a trend (either increase or decrease) of the relative contributions of surface adsorption or ion-exchange with increasing size of the sample ions would be observed.

Bibliography

1. K.G. Wahlund and K. Groningsson, *Acta Pharm. Suecica*. 7, 615 (1970)
2. S. Eksborg, P.O. Lagerstrom, R. Modin and G. Schill, *J.Chromatogr.* 83, 99 (1973).
3. S. Eksborg and G. Schill, *Anal. Chem.* 45, 2092 (1973).
4. B.A. Persson and B.L.Karger, *J.Chromatogr.Sci.* 12, 521(1974).
5. B.L. Karger, S.G. Su, S. Marchese and B.A. Persson, *J.Chromatogr.Sci.* 12, 678 (1974).
6. K.G. Wahlund, *J.Chromatogr.* 115, 411 (1975).
7. D.P. Wittmer, N.O. Nuessle and W.G. Haney, Jr., *Anal.Chem.* 47, 1422 (1975).
8. M.T.W. Hearn, "Ion-pair chromatography", Marcel Dekker Inc., New York, 1985.
9. R.H.A. Sorel and A. Hulshoff in "Advances in Chromatography", ed. J.C. Giddings et al, Marcel Dekker, Inc., New York, Vol. 21, Chapter 3, 1983.
10. M.T.W. Hearn in "Advances in Chromatography", ed. J.C. Giddings et al, Marcel Dekker, Inc., New York, Vol. 18, Chapter 2, 1980.
11. L.R. Snyder and J.J. Kirkland, "Introduction to Liquid Chromatography", 2nd ed., John Wiley&Sons, New York, Chapter 11, 1979.
12. C. Horvath, W. Melander, I. Molnar and P. Molnar, *Anal.Chem.* 49, 2295 (1977).
13. B. Fransson, K.G. Wahlund, I.M. Johnsson and G.Schill, *J.Chromatogr.* 125, 327 (1976).
14. E. Tomlinson, T.M. Jeffries and C.M. Riley, *J.Chromatogr.* 159, 315 (1978).
15. J.H. Knox and J. Jurand, *J.Chromatogr.* 125, 89 (1976).
16. J.H. Knox and J. Jurand, *J.Chromatogr.* 149, 297 (1978).
17. J.C. Kraak, K.M. Jonker and J.F.K. Huber, *J.Chromatogr.* 142, 671 (1977).

18. B.A. Bidlingmeyer, S.N. Deming, W.P. Price, Jr., B. Sachok and M. Petrusek, *J. Chromatogr.* 186, 419 (1979).
19. T.D. Rotsch and D.J. Pietrzyk, *J. Chromatogr. Sci.* 19, 88 (1981).
20. T.D. Rotsch and D.J. Pietrzyk, *Anal. Chem.* 52, 1323 (1980).
21. A. Kasturi and R.K. Gilpin, *J. Chromatogr. Sci.* 25, 29 (1987).
22. J.J. Stranahan and S.N. Deming, *Anal. Chem.* 54, 2251 (1982).
23. R.E. Majors, *Liq. Chromatogr. Mag.* 3, 774 (1985).
24. E. Grushka and E.J. Kikta, Jr., *Anal. Chem.* 49, 1004A (1977).
25. W.R. Melander and C. Horvath in "High-Performance Liquid Chromatography: Advances and Perspectives", ed. C. Horvath, Vol. 2, Academic Press, New York, 1980.
26. L.R. Snyder and J.J. Kirkland, "Introduction to Modern Liquid Chromatography", 2nd ed., John Wiley & Sons, Inc., New York, 1979.
27. L.C. Sander and S.A. Wise, "CRC Critical Reviews in Anal. Chem." 18, 299 (1987).
28. P. Roumeliotis and K.K. Unger, *J. Chromatogr.* 149, 211 (1978).
29. G.E. Berendsen, K.A. Pikaart and L. de Galan, *J. Liq. Chromatogr.* 3, 1437 (1980).
30. H. Englehardt and G. Ahr, *Chromatographia* 14, 227 (1981).
31. A. Sokolowski and K.G. Wahlund, *J. Chromatogr.* 189, 299 (1980).
32. M. Ryba, *Chromatographia* 15, 227 (1982).
33. W.S. Hancock, C.A. Bishop, R.C. Prestidge, D.R.K. Harding and M.T.W. Hearn, *Science* 200, 1168 (1978).
34. A. Nahum and C. Horvath, *J. Chromatogr.* 203, 53 (1981).
35. K.E. Bij, W.R. Melander, A. Nahum and C. Horvath, *J. Chromatogr.* 203, 65 (1981).
36. P.C. Sadek and P.W. Carr, *J. Chromatogr. Sci.* 21, 314 (1983).

37. K. Karch, I. Sebestian and I. Halasz, *J. Chromatogr.* 122, 3 (1976).
38. J.J. Kipling, "Adsorption from Solutions of Non-electrolytes", Academic Press, New York, 1965.
39. G.D. Parfitt and C.H. Rochester, "Adsorption from Solution at The Solid/Liquid Interface", Academic Press, New York, 1983.
40. R. Hux, Ph.D. Desertation, Univ. of Alberta, 1983.
41. R.A. Hux and F.F. Cantwell, *Anal. Chem.* 56, 1258 (1984).
42. S. May, R.A. Hux and F.F. Cantwell, *Anal. Chem.* 54, 1279 (1982).
43. F.F. Cantwell, J.S. Nielsen and S.E. Hrudey, *Anal. Chem.* 54, 1498 (1982).
44. A. Tilly-Melin, M. Ljungcrantz and G. Schill, *J. Chromatogr.* 185, 225 (1979).
45. A. Tilly-Melin, Y. Askemark, K.G. Wahlund and G. Schill, *Anal. Chem.* 51, 976 (1979).
46. O.A.G.J. van der Houwen, R.H.A. Sorel, A. Hulshoff, J. Teeuwsen and A.W.M. Indemans, *J. Chromatogr.* 209, 393 (1981).
47. C.T. Hung and R.B. Taylor, *J. Chromatogr.* 202, 333 (1980).
48. C.T. Hung and R.B. Taylor, *J. Chromatogr.* 209, 175 (1981).
49. R.S. Deelder, H.A.J. Linssen, P. Konijnendijk and J.L.M. Van De Venne, *J. Chromatogr.* 185, 241 (1979).
50. R.S. Deelder and J.H.M. Van Den Berg, *J. Chromatogr.* 218, 327 (1981).
51. L.R. Snyder and J.J. Kirkland, "Introduction to Liquid Chromatography", 2nd ed., Wiley, New York, pp296, 1979.
52. J. Kawase, *Anal. Chem.* 52, 2123 (1980).
53. Z. Marzenko and H. Kalowska, *Anal. Chim. Acta* 123, 279 (1981).
54. K. Toei, S. Motomizu and T. Umano, *Tanata* 29, 103 (1982).
55. K. Gustavii and G. Schill, *Acta Pharm. Suecica* 3, 241 (1966).
56. B. Karlberg and S. Thelander, *Anal. Chim. Acta* 98, 1 (1978).

57. F.H. Bergamin, J.X. Medeiros, B.F. Reis and E.A.G. Zagatto, *Anal. Chim. Acta* 101, 9 (1978).
58. L.Fossey and F.F. Cantwell, *Anal. Chem.* 54, 1693 (1982).
59. C.A. Lucy and F.F. Cantwell, *Anal. Chem.* 58, 2727 (1986).
60. J. Kawase, Y. Takao and K. Tsuji, *J. Chromatogr.* 262, 293 (1983).
61. F. Smedes, J.C. Kraak, C.F. Werkhoven-Goewie, U.A. Th. Brinkman and R.W. Frei, *J. Chromatogr.* 247, 123 (1982).
62. P.C. Hiemenz, "Principle of Colloid and Surface Chemistry", 2nd ed., Marcel Dekker Inc., New York, 1986.
63. M.J. Rosen, "Surfactants and Interfacial Phenomena", John Wiley & Sons, New York, pp104-105, 1978.
64. "CRC Handbook of Physical Chemistry", CRC Press, Cleveland, OH, 48th ed., 1967.
65. J.H. Knox and R.A. Hartwick, *J. Chromatogr.* 204, 3 (1981).
66. J.H. Knox and J. Jurand, *J. Chromatogr.* 149, 297 (1978).
67. R.H.A. Sorel and A. Hulshoff, *J. Liq. Chromatogr.* 4, 1961 (1981).
68. E. Tomlinson, C.M. Riley and T.M. Jefferies, *J. Chromatogr.* 173, 89 (1979).
69. M. Deux, M. Lafosse, P. Agbo-Hazoume, B. Chaabane-Doumandji, M. Gibert and Y. Levi, *J. Chromatogr.* 354, 119 (1986).
70. J.D. Barnhurst, *J. Org. Chem.* 26, 4520 (1961).
71. H.H. Bauer, G.D. Christian and J.E. O'Reilly, "Instrumental Analysis", Allyn and Bacon Inc., Boston, 1978.
72. C. Horvath, W. Melander and I. Molnar, *J. Chromatogr.* 125, 129 (1976).
73. I. Molnar and C. Horvath, *Clin. Chem.* 22, 1497 (1976).
74. L.R. Snyder, "Principles of Adsorption Chromatography", Marcel Dekker Inc., New York, 1968.
75. J.J. Kirkland, *J. Chromatogr. Sci.* 9, 206 (1971).

76. C.H. Lochmuller and D.R. Wilder, J. Chromatogr. Sci. 17, 574 (1979).
77. D.E. Martire and R.E. Boehm, J. Phys. Chem. 87, 1045 (1983).
78. H. Colin and G. Guiochon, J. Chromatogr. Sci. 158, 183 (1978).
79. S.A. Wise, W.J. Bonnet, F.R. Guenther and W.E. May, J. Chromatogr. Sci. 19, 457 (1981).
80. H. Hemetsberger, W. Maasfeld and H. Ricken, Chromatographia 1, 303 (1976).
81. R.P.W. Scott and P. Kucera, J. Chromatogr. 175, 51 (1979).
82. R.P.W. Scott and P. Kucera, J. Chromatogr. 142, 231 (1977).
83. C. Horvath and W. Melander, J. Chromatogr. Sci. 15, 393 (1977).
84. W.E. Rudzinski, D. Bennett and V. Garcia, J. Liq. Chromatogr. 5, 1295 (1982).
85. W.E. Rudzinski, D. Bennett, V. Garcia and M. Seymour, J. Chromatogr. Sci. 21, 57 (1983).
86. C.F. Gelijkens and A.P. De Leenheer, J. Chromatogr. 194, 305 (1980).
87. A. Sokolowski, Chromatographia 22, 168 (1986).
88. D.J. Pietryzk and C.H. Chu, Anal. Chem. 49, 757 (1977).
89. D.J. Pietryzk and C.H. Chu, Anal. Chem. 49, 860 (1977).
90. M.A. Curtis and L.B. Rogers, Anal. Chem. 53, 2347 (1981).
91. Z. Varga-Puchmay and J. Inczedy, J. Liq. Chromatogr. 3, 1669 (1980).
92. M.J.M. Wells and C.R. Clark, Anal. Chem. 53, 1341 (1981).
93. B.A. Bidlingmeyer and F.V. Warren, Jr., Anal. Chem. 54, 2351 (1982).
94. F.F. Cantwell and S. Puon, Anal. Chem. 51, 623 (1979).
95. F.F. Cantwell in "Ion Exchange And Solvent Extraction", ed. J.A. Marinsky and Y. Marcus, Marcel Dekker Inc., New York, Vol. 9, pp339-372, 1985.
96. F.F. Cantwell, J. Pharmaceutical & Biomedical Analysis 2, 153 (1984).
97. P.G. Rigas and D.J. Pietrzyk, Anal. Chem. 58, 2226 (1986).
98. S.G. Weber and J.D. Orr, J. Chromatogr. 322, 433 (1985).

99. J.M. Rosenfield, M. Mureika-Russell and A. Phatuk, J. Chromatogr. 283, 127 (1984).
100. Z. Iskandarani and D.J. Pietrzyk, Anal. Chem. 54, 1065 (1982).
101. Z. Iskandarani and D.J. Pietrzyk, Anal. Chem. 54, 2427 (1982).
102. R.L. Smith and D.J. Pietrzyk, Anal. Chem. 56, 1572 (1984).
103. P.G. Rigas and D.J. Pietrzyk, Anal. Chem. 59, 1388 (1987).
104. P.G. Rigas and D.J. Pietrzyk, Anal. Chem. 60, 454 (1988).
105. T.D. Rotsch, W.R. Cahill, Jr., D.J. Pietrzyk and F.F. Cantwell, Can. J. Chem. 59, 2179 (1981).
106. W.E. Hammers, C.N.M. Aussems and M. Janssen, J. Chromatogr. 360, 1 (1986).
107. M.E. Del Rey and L.E. Vera-Avila, J. Liq. Chromatogr. 10, 2911 (1987).
108. P.R. Berdard and W.C. Purdy, J. Liq. Chromatogr. 8, 2417 (1985).
109. S.L. Bafna, M.B. Patel, M.C. Doshi and S.S. Kazi, J. Chromatogr. 201, 131 (1980).
110. W.E. Barber and P. Carr, J. Chromatogr. 301, 25 (1984).
111. J. Stahlberg, J. Chromatogr. 356, 231 (1986).
112. J.S. Fritz, D.L. DuVal and R.E. Barron, Anal. Chem. 56, 1177 (1984).
113. D.P. Lee, Anal. Chem. 52, 2425 (1980).
114. J.O'M. Bockris and A.K.N. Reddy, "Modern Electrochemistry", Vol. 2, Plenum, New York, 1970.
115. D.C. Grahame, Chem. Rev. 41, 441 (1947).
116. O. Jansson, I. Andersson and B.A. Persson, J. Chromatogr. 203, 93 (1981).
117. J-X. Huang and C. Horvath, J. Chromatogr. 406, 275 (1987).
118. J.H. Knox and G.R. Laird, J. Chromatogr. 122, 17 (1976).
119. P.K. Nandi, J. Phy. Chem. 78, 1197 (1974).
120. J. Kielland, J. Am. Chem. Soc. 59, 1675 (1937).

121. A. Bartha and Gy. Vigh, *J. Chromatogr.* 260, 337 (1983).
122. S. Lindenbaum and G.E. Boyd, *J. Phy. Chem.* 68, 911 (1964).
123. H.E. Wirth, *J. Phy. Chem.* 71, 2922 (1967).
124. E.M. Arnett, M. Ho and L.L. Schaleger, *J. Am. Chem. Soc.* 92, 7039 (1970).
125. Kunio Tamaki, *Bull. Chem. Soc. Japan* 40, 38 (1967).
126. W. Jost, K. Unger and G. Schill, *Anal. Biochem.* 119, 214 (1982).
127. P.T. Kissinger, *Anal. Chem.* 49, 883 (1977).
128. J.P. Crombeen, J.C. Kraak and H. Poppe, *J. Chromatogr.* 167, 297 (1978).
129. C.P. Terweij-Groen, S. Heemstra and J.C. Kraak, *J. Chromatogr.* 161, 69 (1978).
130. J.L.M. Van De Venne, J.L.H.M. Hendrikx and R.S. Deelder, *J. Chromatogr.* 167, 1 (1978).
131. A. Bartha and Gy. Vigh, *J. Chromatogr.* 265, 171 (1983).
132. A. Bartha, H.A.H. Billiet, L.De. Galan and Gy. Vigh, *J. Chromatogr.* 291, 91 (1984).
133. A. Bartha, Gy. Vigh, H.A.H. Billiet and L.De. Galan, *J. Chromatogr.* 303, 29 (1984).
134. A. Bartha, Gy. Vigh, H.A.H. Billiet and L.De. Galan, *Chromatographia* 20, 587 (1985).
135. B.A. Bidlingmeyer, *J. Chromatogr. Sci.* 18, 525 (1980).
136. R.C. Kong, B. Sachok and S.N. Deming, *J. Chromatogr.* 199, 307 (1980).
137. S.N. Deming, J.J. Stranahan, W. Lin and M. Tang, *Anal. Chem.* 55, 1872 (1983).
138. S. Afrashtehfar and F.F. Cantwell, *Anal. Chem.* 54, 2422 (1982).
139. P.G. Rigas and D.J. Pietrzyk, *Anal. Chem.* 60, 454 (1988).
140. P.G. Rigas and D.J. Pietrzyk, *Anal. Chem.* 59, 1388 (1987).
141. P.G. Rigas and D.J. Pietrzyk, *Anal. Chem.* 58, 2226 (1986).

142. R.L. Smith and D.J. Pietrzyk, *Anal. Chem.* **56**, 1572 (1984).
143. F. Helfferich, "Ion Exchange", McGraw-Hill, New York, 1962.
144. K.M. Van Dolsen and M.J. Vold in "Adsorption from Aqueous Solution", ed. W.J. Webber and E. Matijevic, American Chemical Society, Washington, D.C., Chapter 12, 1968.
145. H.A. Laitinen and W.E. Harris, "Chemical Analysis", 2nd edn., McGraw-Hill, New York, 1975.
146. O.D. Bonner, G.D. Easterling, D.L. West and V.F. Holland, *J. Am. Chem. Soc.* **77**, 242 (1955).
147. J.L. Dye and V.A. Nicely, *J. Chem. Educ.* **48**, 443 (1971).
148. C.H. Giles, D. Smith and A. Huitson, *J. Colloid. Interface Sci.* **47**, 755 (1974).
149. J.Th. Overbeek in "Colloid Science", ed., H.R. Kruyt, Elsevier, New York, Vol. 1, Chapter 4, 1952.
150. "Standard Mathematical Tables", CRC Press, Cleveland, OH, 19th ed., 1971.
151. G.N. Lewis and M. Randall, "Thermodynamics", 2nd ed., (rev. K.S. Pitzer and L. Brewer), McGraw-Hill, New York, 1961, pp320-323.
152. R.A. Robinson and R.H. Stokes, "Electrolyte Solutions", 2nd ed., Academic Press, New York, 1959.
153. C.M. Riley, E. Tomlinson and T.M. Jefferies, *J. Chromatogr.* **185**, 197 (1979).
154. J. Fekete, P. Del Castilho and J.C. Kraak, *J. Chromatogr.* **204**, 319 (1981).
155. R.M. McCormic and B.L. Karger, *Anal. Chem.* **52**, 2249 (1980).
156. B. Fransson, *J. Chromatogr.* **361**, 161 (1986).
157. B. Fransson, U. Ragnarsson and O. Zetterqvist, *J. Chromatogr.* **240**, 165 (1982).
158. W.S. Hancock, "Handbook of HPLC for The Separation of Amino Acids, Peptides And Proteins", CRC Press, Boca Raton, 1984.
159. W.R. Melander, K. Kalghatgi and C. Horvath, *J. Chromatogr.* **201**, 201 (1980).
160. W.R. Melander and C. Horvath, *J. Chromatogr.* **201**, 211 (1980).

161. E. Arvidsson, L. Hackzell, G. Schill and D. Westerlund, *Chromatographia* 25, 430 (1988)
162. R.K. Iler, "The Chemistry of Silica", John Wiley & Sons, New York, 1979, pp660-661.
163. R.J. Hunter, "Zeta Potential in Colloid Science", Academic Press, New York, 1981, pp40-42
164. A.W. Adamson, "Physical Chemistry of Surfaces", 2nd ed., Interscience, New York, 1967, Chapter 4.

Appendix I

Microsoft Basic Program For Calculating The Surface Charge Density On ODS Packing From The Experimentally Measured Surface Excess of NBS⁻

```
10 REM * This program based on the SGC theory is for anion (NBS-)
20 REM * it is to calculate the charge density & potential at OHP
30 REM * from the experimentally measured data (i.e. solution concentration,
32 REM * surface concentration and ionic strength)

35 REM * input data

40 PRINT "[NBS-]m =? mol/L"
50 INPUT pm
60 LPRINT "[NBS-]m = " pm; " mol/L"

70 PRINT "concentration on adsorbent =? mol/kg"
80 INPUT s
90 LPRINT "concentration on ODS ="; s;"mol/kg"

100 PRINT "ion strength = ?"
120 INPUT c
130 LPRINT "ionic strenth = ";c

140 REM * calculating

150 a=pm/c
```



```
160 b=s/3.09E+09
180 x=-96487!*b
190 LPRINT "surface excess(exp.measured)"; b;"mol/cm2"

200 REM * iterative process

210 FOR i=1 TO 10
220 y=85300!*x*c^-.5
230 LET d=-LOG((-y)+((-y)^2+1)^.5)

235 REM *  $\sinh^{-1}x = \ln[x + (x^2 + 1)^{1/2}]$  only when  $x > 0$  [ref.150]
240 REM *  $\sinh^{-1}(-x) = -\sinh^{-1}x$ 

247 p= 0.051355*d
250 z= (EXP(-(19.47*p))-1)/(EXP(19.47*p)-1)
260 LET r=(1/z)*a
270 x=-96487!*b*(a-r)/(a-r*(1-a))
280 IF i>7 THEN 290 ELSE 300
290 LPRINT "x";i;"==";x
300 NEXT i

310 REM * iterative process finished

320 REM * calculating parameters

330 sa=x/96487!
340 LET G=2*d/(EXP(d)-EXP(-d))
```

-7

350 REM * printing out results

360 LPRINT "surface excess(AD)";sa;"mol/cm2"

370 LPRINT "the surface charge density ==";x;"coul/cm2"

380 LPRINT "potential at OHP ==";p;"volt"

390 LPRINT "u factor=";G

400 END

500 REM * meaning of symbols

510 REM *pm = solution concentration of NBS- (mol/L)

520 REM *s = concentration of NBS- on ODS (mol/kg)

530 REM *c = ionic strength

540 REM *b = measured surface excess of NBS- (mol/cm2)

550 REM *specific surface area = 3.09×10^9 cm²/kg.

560 REM * sa = surface excess of NBS- (only those adsorbed on the surface)

570 REM *x=charge density

580 REM *z=(excess of NBS-)/(excess of CL-) in the diffuse layer

590 REM *p=potential at OHP

600 REM * u factor=the correction parametor for SGC plotting

Appendix II

Microsoft Basic Program For Calculating The Surface Charge Density On ODS Packing From The Experimentally Measured Surface Excess of TBA⁺

```
10 REM * This program based on the SGC theory is for cation (TBA+)
20 REM * it is to calculate the charge density & potential at OHP
30 REM * from the experimentally measured data (i.e. solution concentration,
32 REM * surface concentration and ionic strength)

35 REM * input data

40 PRINT "[TBA+]m =? mol/L"
50 INPUT pm
60 LPRINT "[TBA+]m = " pm; " mol/L"

70 PRINT "concentration on adsorbent =? mol/kg"
80 INPUT s
90 LPRINT "concentration on ODS ="; s;"mol/kg"

100 PRINT "ion strength = ?"
120 INPUT c
130 LPRINT "ionic strenth = ";c

140 REM * calculating

150 a=pm/c
```

```
160 b=s/3.09E+09
180 x=96487!*b
190 LPRINT "surface excess(exp.measured)"; b;"mol/cm2"

200 REM * iterative process

210 FOR i=1 TO 10
220 y=85300!*x*c^-.5
230 LET d=LOG(y+(y^2+1)^.5)

235 REM *  $\sinh^{-1} x = \ln[x + (x^2 + 1)^{.5}]$  [ref.150]

247 p=.051355*d
250 z=((EXP(-(19.47*p))-1)/(EXP(19.47*p)-1))
260 LET r=z*a
270 x=96487!*b*(a-r)/(a-r*(1-a))
280 IF i>7 THEN 290 ELSE 300
290 LPRINT "x";i;"==";x
300 NEXT i

310 REM * iterative process finished

320 REM * calculating parameters

330 sa=x/96487!
340 LET G=2*d/(EXP(d)-EXP(-d))
```

350 REM * printing out results

360 LPRINT "surface excess(AD)";sa;"mol/cm2"

370 LPRINT "the surface charge density ==";x;"coul/cm2"

380 LPRINT "potential at OHP ==";p;"volt"

390 LPRINT "u factor=";G

400 END

500 REM * meaning of symbols

510 REM *pm = solution concentration of TBA+ (mol/L)

520 REM *s = concentration of TBA+ on ODS (mol/kg)

530 REM *c = ionic strength

540 REM *b = measured surface excess of TBA+ (mol/cm2)

550 REM *specific surface area = 3.09×10^9 cm²/kg

560 REM *sa = surface excess of TBA+ (only those adsorbed on the surface)

570 REM *x=charge density

580 REM *z=(excess of TBA+)/(excess of Na+) in the diffuse layer

590 REM *p=potential at OHP

600 REM * u factor=ionic strength parameter for SGC plotting

Appendix III

Activity Coefficient Of NBS^- In Aqueous

Solution At Various Ionic Strengths

It is assumed that the activity coefficient of p-nitrobenzenesulfonic (NBS^-) has the same values as that of p-toluenesulfonic ion. The values of activity coefficient for p-toluenesulfonic with ionic strength above 0.10 have been measured by Bonner et al [146] using the isopiestic method [151,152]. In their measurements, LiCl was used as the reference electrolyte. Some of the measured values are listed in Table A-3a. The values of activity coefficient at ionic strengths below 0.10 can be obtained from the tables given by Kielland[120] by choosing an appropriate value of ionic size parameter for NBS^- . The value of ionic size parameter for NBS^- is chosen to have such a value that the plot of γ_{NBS^-} vs. c has a smooth connection (no 'break') at $c=0.10$ with the data of Bonner. The ionic size parameter obtained for NBS^- in this way is 3.5×10^{-8} cm. The values of activity coefficient for NBS^- with ionic strength below 0.10 thus obtained are given in Table A-3b. The plot of g_{NBS^-} vs. c is shown in Fig.A-3.

Table A-3a Activity coefficient of NBS^- at ionic strengths above 0.10 [146]

c	0.10	0.20	0.30	0.40	0.50	0.60
γ_{NBS^-}	0.758	0.703	0.660	0.630	0.608	0.589

Table A-3b Activity coefficient of NBS^- at ionic strengths below 0.10 from reference 120 using ionic size parameter of 3.5×10^{-8} cm.

c	0.0	0.005	0.01	0.025	0.05	0.10
γ_{NBS^-}		0.926	0.900	0.855	0.810	0.760

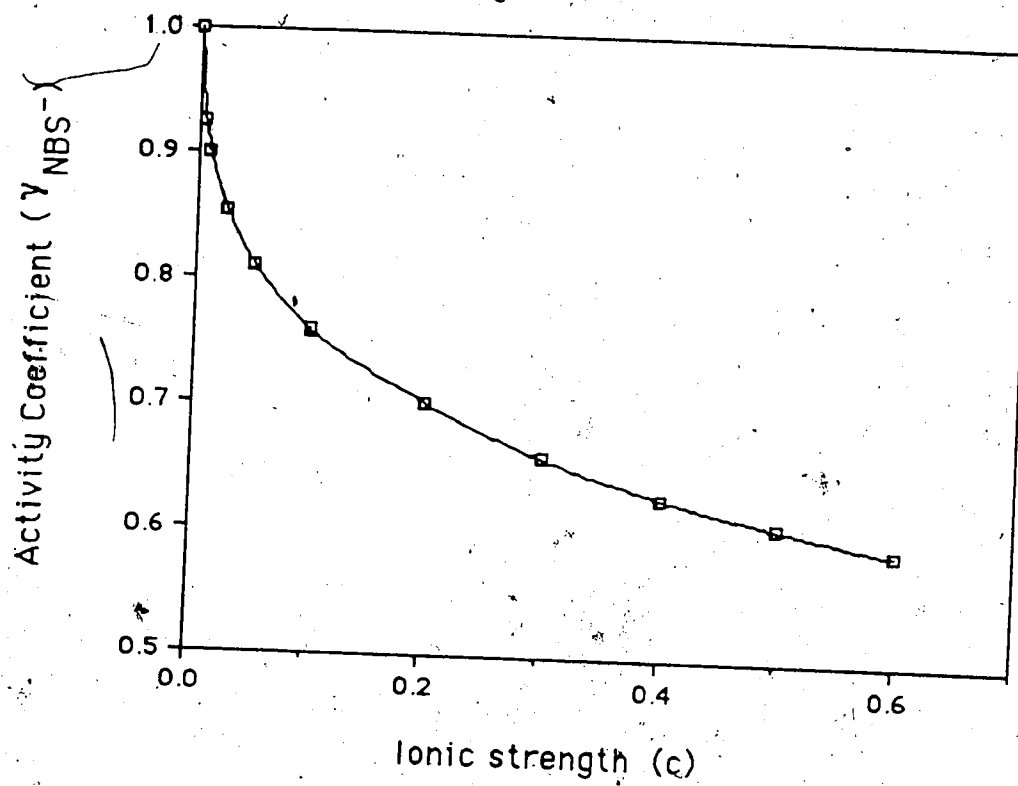


Figure A-3 Plot of activity coefficient of NBS^- in aqueous solution vs. ionic strength

Appendix IV

Activity Coefficient Of TBA^+ In Aqueous

Solution At Various Ionic Strengths

The activity coefficients, γ_{TBA^+} , of TBA^+ (Cl^- as the counterion) in aqueous solution with ionic strength above 0.10 have been measured by Lindenbaum and Boyd [12]. In their measurements, the isopiestic method [151,152] was used with NaCl solution as the reference. Some values of these measured γ_{TBA^+} are listed in Table A-4a. Values of γ_{TBA^+} with ionic strength below 0.10 can be obtained from the tables of Kielland [120] by choosing an appropriate value for the ionic size parameter for TBA^+ . The ionic size parameter is chosen to have such a value that the plot of γ_{TBA^+} vs. ionic strength (c) has a smooth connection at $c=0.10$ with the data of Lindenbaum and Boyd. The value for the ionic size parameter thus chosen is 3.0×10^{-8} cm. Values of γ_{TBA^+} with ionic strength below 0.10 are given in Table A-4b. The plot of γ_{TBA^+} vs. c is presented in Fig.A-4.

Table A-4a Activity coefficient of TBA^+ at ionic strengths above 0.10 [122]

c	0.10	0.20	0.30	0.40	0.50	0.60
γ_{TBA^+}	0.752	0.701	0.670	0.650	0.637 ^o	0.529

Table A-4b Activity coefficient of TBA^+ at ionic strengths below 0.10 from
reference 120 using an ionic size parameter of 3.0×10^{-8} cm.

c	0.0	0.005	0.01	0.025	0.05	0.10
γ_{TBA^+}	1.0	0.925	0.899	0.850	0.805	0.755

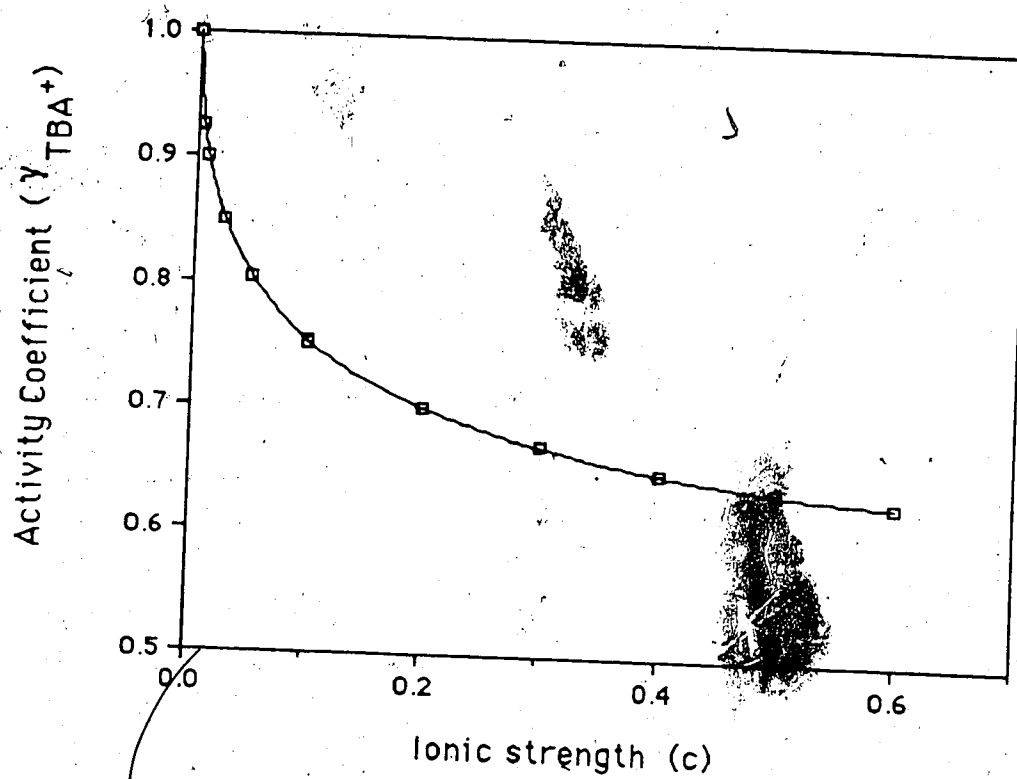


Figure A-4 Plot of activity coefficient of TBA⁺ in aqueous solution vs. ionic strength

Appendix V
The Subroutine Program (EQN) To Define
The Equation To Be Used With The Least-Square
Curvefitting KINET

EQU.LIU RP-ION PAIR CHROMATGR. MODEL EQUATION
 BY HANJIU LIU NOV.28, 1986

THIS PROGRAM CONTAINS THE EQUATION REQUIRED BY KINET TO CURVE FIT
 CHROMATOGRAPHIC RETENTION DATA FOR NEGATIVE ORGANIC IONS ON
 RP PACKING (ODS) WHEN A POSITIVE PAIR-ION IS PRESENT (TBA+)
 A DATA FILE IS ALSO REQUIRED CONTAINING ALL CONSTANTS, ESTIMATES OF
 PARAMETERS (U(1) AND U(2)) AND RETENTION DATA (XX(1),XX(2) AND XX(3))
 WITH ESTIMATES OF VARIANCES. THIS DATA FILE CAN BE CREATED WITH
 AID OF THE INTERACTIVE PROGRAM PIDEK2..

..... LIST OF VARIABLES

XX(1) = X = SURFACE EXCESS OF TBA+ (MOL/CM2) / IONIC STRENGTH = RATIO
 XX(2) = Y = ACTIVITY COEFFICIENT OF SAMPLE ION (NBS-)
 XX(3) = Z = Distribution Coefficient of NBS- (L/kg)
 U(1) = ESTIMATE OF ION EXCHANGE EQUILIBRIUM CONSTANT
 U(2) = ESTIMATE OF CHEMICAL POTENTIAL FOR ADSORPTION
 CONST(1) = POTENTIAL AT CHARGED SURFACE (VOLT)

.....
 SUBROUTINE EQN

IMPLICIT REAL*8(A-H,O-Z)
 COMMON ZZZZZ,KOUNT,1999,ITAPE,1998,JTAPE,1997,IWT,1996,LAP,
 C 1994,XINCR,NOPT,1993,NOVAR,1992,NOUNK,1991,X,U,ITMAX,1990,
 C WTX,TEST,1,1889,AV,RESID,IAR,1888,EPS,ITYP,1887,XX,RXTYP,
 C DX11,FOP,FO,FU,P,ZL,TO,EIGVAL,XST,T,DT,L,1886,M,1885,JJJ,
 C 1884,Y,DY,VECT,NCST,1880,CONST
 DIMENSION X(4,100),U(20),WTX(4,100),XX(4),FOP(100),FO(100),
 C FU(100),P(20,21),VECT(20,21),ZL(100),TO(20),EIGVAL(20),XST(100),
 C Y(10),DY(10),CONST(16)
 GOTO(2,3,4,5,1),ITYP
 1 CONTINUE
 ITAPE=5
 JTAPE=6
 C INSERT NOUNK AND NOVAR ASSIGNMENTS HERE
 NOVAR=3
 NOUNK=2
 RETURN
 2 CONTINUE
 C INSERT CALCULATION OF (YCALC) AND RESID HERE
 EXPON=DEXP(38.94*CONST(1) - 4.036E-4*U(2))
 DIEX = 1000.0*3.09E6*U(1)*XX(1)
 DADS = 3.09E6*10.3E-8*XX(2)*EXPON
 DTOT = DIEX + DADS
 RESID = DTOT - XX(3)
 RETURN
 END